HIGH TEMPERATURE OXIDATION OF LOW CARBON STEELS CONTAINING RESIDUAL COPPER

by

Dilip Kumar
B.Sc. (Engg.), Ranchi University, Ranchi, India

A Thesis submitted in partial fulfilment of the requirements for the Degree of

Master of Applied Science (M.A.Sc.)

in

The Faculty of Graduate Studies
(Department of Metals and Materials Engineering)

We accept this thesis as conforming to the required standard

The University of British Columbia
December 2001

In presenting this thesis in partial fulfilment of the requirements for an advanced degree at the University of British Columbia, I agree that the Library shall make it freely available for reference and study. I further agree that permission for extensive copying of this thesis for scholarly purposes may be granted by the head of my department or by his or her representatives. It is understood that copying or publication of this thesis for financial gain shall not be allowed without my written permission.

Department of Metals and Materials Engineering
The University of British Columbia
Vancouver, Canada

Date December 4, 2001

ABSTRACT

Oxidation studies were carried out on low carbon steels containing 0.2%, 0.39% and 0.78% (wt) Cu at temperatures 1000°, 1100°, 1200° and 1275°C for times 5 minutes to 2 hrs in air. Oxide growth curves were plotted from the weight gain data. The scale surfaces were examined under optical microscope as well as SEM. Analyses by EDX, XRD as well as XPS were also performed on a few of them. Cross-sectional examination of samples was carried out under SEM in order to study the Cu enrichment at the substrate surface. The growth curves displayed parabolic behavior in general, even during the early stages of oxidation. However, the parabolic rate constants dropped to lower values after a certain time at 1200°C as well as 1275°C. Usually, the scale was adherent in the beginning. However, it became detached from the substrate with passage of time. Decreasing Cu content and decreasing temperature enhanced the scale detachment. Oxide surfaces in the steels oxidized for times 1 hour or less exhibited growth of whiskers of $CuFe_2O_4$ spinels over the scale comprising mainly of FeO. Increasing temperature increased the diameters of whiskers marginally and decreased their lengths. Increasing Cu reduced the growth of whisker. The whiskers disappeared from scale surface when the steel was oxidized for 2 hours and what remained afterwards on the surface consisted only of Fe_2O_3 crystals. Enrichment of Cu was observed at the oxide-metal interface and the grain boundaries close to the steel surface even in the early stages of oxidation at all temperatures. However, the enriched phase at the surface was discontinuous and separated from the substrate at 1000°C. Grain boundary enrichment of Cu was very

marginal at 1000°C. At 1100°C, the size of Cu rich phase increased for lower Cu levels (e.g. 0.22% and 0.39%). However, this phase remained discontinuous and separated from substrate for these steels. On the other hand, a continuous layer of Cu was observed at the surface at most of the locations for 0.78% Cu steel. Additionally, there were locations near the interface devoid of any surface enrichment but accompanied by penetration of grain boundaries by the enriched layer. Increasing the temperature above 1100°C caused enhanced internal oxidation of Si, Mn and Fe. Increasing the time of oxidation accentuated this process. Increasing the time also increased the Cu content of the enriched layer at both 1000°C as well as 1100°C. The thickness of the enriched phase also increased with time. Increasing temperature too, had a similar effect. However, increasing the time to 2 hours at 1200°C and 1275°C caused the thickness of highly enriched layer to decrease. No penetration of grain boundaries by the enriched phase was observed at 1200°C and 1275°C.

CONTENT

LIST OF FIGURES

LIST OF TABLES

ACKNOWLEDGEMENT

I express sincere gratitude to my research supervisors, Dr. Peter Barr and Dr. Indira Samarasekera for their invaluable guidance and continuous encouragement during the course of research work. Additionally, I thank Dr. Peter Barr also for his guidance in preparation of this thesis.

I thank Ms Mary Mager for her invaluable assistance during scanning electron microscopy of specimens. I also appreciate the support provided by Dr. Rees Llewellyn for allowing me to go to UBC when needed during working hours.

Finally, I wish to thank my wife, Kiran without whose continuous dedication and support, it would have been very much impossible for me to accomplish this work.

HIGH TEMPERATURE OXIDATION OF LOW CARBON STEELS CONTAINING RESIDUAL COPPER

1. Introduction

High temperature oxidation of steels is of great interest in metallurgical, electrochemical and process industries[1]. For example, reheating furnaces are used to heat slabs prior to hot rolling in steel industries. These furnaces expose the steel to an oxidizing environment for several hours in raising the slab temperature to 1215-1300°C. More recently, tunnel furnaces are being used to heat continuously cast thin slabs to 1100°C for ~half an hour[2] prior to hot rolling. The heating process causes growth of oxide scale on the surface of slabs. Although the scale is removed prior to rolling it constitutes a loss of product, typically 1-3% of the total steel throughput for conventional reheating furnaces. Scaling of thin slabs in tunnel furnaces is also of concern due to large surface area to weight ratio, although the heating time is much smaller.

Scrap loaded electric arc furnace (EAF) steelmaking requires only $1/3^{rd}$ to $1/6^{th}$ of the energy needed in blast furnace/BOF steelmaking process where iron oxide is the starting material[3]. Additionally, EAF also generates much less amount of CO_2 in proportion to the energy consumption. Thus recycling and reusing of steel scrap is

highly desirable for global environmental protection. However, steel scrap contains significant copper levels (upto 0.35% or, more). It is also being predicted that concentration of copper in steel scrap is going to increase further, e.g. to 0.45% by the year 2020 in Japan[3] with a similar trend in other countries[4-5]. Most of copper in the scrap is transferred to the steel product as the oxidation refining process during steelmaking does not remove it[3, 6]. Additionally, copper might be alloyed intentionally in steels for improving the mechanical as well as corrosion properties[6-7].

When steels containing residual copper are heated at elevated temperatures e.g. in reheating/tunnel furnaces prior to rolling, iron is preferentially oxidized during scaling process and copper remains behind due to its nobility compared to iron[6-10]. This results into enrichment of copper at the steel surfaces. The enrichment proceeds until the solubility limit of copper in steel is reached, when a second, metallic copper-rich phase precipitates at the metal-scale interface. This causes a concentration gradient of copper to be established between the surface and the interior. As a result, diffusion of copper takes place towards the interior. The balance between enrichment and diffusion changes with temperature and above a certain temperature diffusion is so rapid that the concentration of copper at the surface remains below the solubility limit[11]. The furnace atmosphere also is important[10] as increased oxygen content in the furnace gases enhances scaling and hence copper enrichment at lower temperature, e.g. 1100°C. However, at higher temperatures, e.g. 1250°C, increased scaling due to higher oxygen content causes occlusion of copper into the scale.

If the scaling temperature is below the melting point of copper, this phase is solid and due to its low solubility of iron[7], may act as a barrier to diffusion of iron

resulting into slower rates of oxidation. If, however the scaling temperature is above the melting point of copper, the new phase is precipitated as a liquid at the scale-metal interface. When such steel is subsequently deformed, e.g. during hot rolling, the copper infiltrates the grain boundaries of austenite in the surface and sub surface regions. As these grain boundaries are unable to withstand shear and tensile stresses, they are forced open and the surface appears crazed. Further rolling results into minute surface discontinuities of an irregular nature, elongated in the direction of rolling of the strip[8]. Such slabs must be scrapped or returned for surface conditioning. This phenomenon in steelmaking is known as 'hot shortness'.

Additionally, residual copper in steels can render the scale more adherent[12] that can result into incomplete descaling prior to hot rolling. As a result, special descaling methods might be needed since residual scale rolled into steel surface causes surface defects and/ or, excessive roll wear.

2. Literature Survey

2.1 Low carbon steels - general

There is a plethora of literature available on oxidation of metals at high temperatures and many books have been written on this topic by several authors, e.g. Birks and Meier[7] and Kofstad[13]. However, few investigations were reported on high temperature oxidation of low carbon steels and those concerning steels with residual copper were fewer still. Most of these investigations were carried out at the laboratory scale. For example, the effects of water vapor and carbon dioxide on scaling rates were reported by Rahmel and Tobolski[14]. Sacks and Tuck[15] reviewed the potential impact of many variables based on previous research in the field of high temperature oxidation.

The methods of reducing the scale formation through favorable control strategies were described by Cook and Rasmussen[16-17]. They showed that scale-free heating could only be attained by burning the fuel with stoichiometric, preheated air, and that tight control of the air/fuel ratio was required throughout the operation. The presence of water vapor and carbon dioxide was found to increase the rate, with water vapor having a larger effect at higher temperatures. Sachs and Tuck[18] studied the effect of oxidizing gases on the high temperature oxidation of iron and steel in an integrated heating strategy for application to reheating furnaces. Hemsath and Vereecke[19] studied the billet reheating in a direct-fired laboratory furnace by burning the fuel at low air/fuel ratios with preheated air and demonstrated that their strategies resulted in substantial savings by minimizing the scale formation. Kuhn and Oeters[20] as well as Selenz and Oeters[21] examined the effect of several species, providing data on the coefficients of linear rate behavior occurring during initial stages of oxidation. Minaev et al[22] studied the effect of fuel type and temperature on scale formation for five grades of steel. The fuel with the lowest oxidizing potential gave the least scale at the higher temperatures, but the effect was less marked at lower temperatures. The effect of cold working on oxidation of iron was studied by Caplan and Cohen[23] and Caplan et al[24]. At temperatures upto 550°C, cold worked iron exhibited oxidation rates greater than annealed samples which was attributed partly to poor scale adhesion for the annealed specimens.

Jarl and Leden[25] were among the first few to collect oxidation data under industrial conditions. The results were incorporated into a model for on-line calculation of oxide scale formation in a walking beam reheating furnace. The experiments were conducted on carbon-manganese steels at 900-1200°C in a laboratory chamber furnace

as well as in a walking beam furnace fired by propane and heavy oil containing 0.3-6.0 vol.% O_2. It was reported that oxidation rates at 1200°C were 4 to 5 times higher than that at 900°C and that increasing oxygen content in the gas markedly increased the oxidation rate at temperatures >900°C. A combination of linear as well as parabolic models was proposed and the predicted values of linear and parabolic rate constants (k_l and k_p) were compared with those obtained from experimental results. The developed model seemed to give a good description of the experimental results. For example, it could describe a mainly parabolic oxidation rate; the influence of the oxygen content in atmosphere on the initial oxidation rate could also be accounted for. For the parabolic rate constant (k_p), the deviation between theoretically calculated and experimentally determined values was within 40% which was claimed to be good. Losses of metal heated in the chamber furnace at 3.0 vol.% O_2 were also recalculated and a good agreement with the measured values was found. Further, the model was implemented in a program for computer control system for the walking beam furnace and it was found that agreement between the amounts of measured scale formed in the furnace during various heating conditions and calculated losses was good. However, only one measurement of scale loss was undertaken in the industrial environment. Hence this agreement might not be true for all the predictions.

Experiments were conducted by Abuluwefa et al[26] by putting rider samples over the actual slabs in a furnace fueled by coke oven gas. It was found that 80% of the total scale was formed when the temperature was in excess of 1000°C. Widely differing results of scale weights for an identical grade of steel under identical conditions (except the differences in furnace operating conditions) were found. However, it was not

possible to quantify the widely differing results. Empirical expressions for oxidation rate constants were also presented and it was found that the ratio of industrial and theoretical rate constants was a strong function of temperature. A Possible explanation of this behavior was considered to lie in the fact that scaling of a slab in the industrial furnace was assumed to be, for any given time, to be occurring at the computed average temperature of the slab. In reality the effective temperature of the scale layer was higher than the temperature of the slab.

Oxidation behavior of low carbon steel samples in binary gas mixtures of oxygen and nitrogen was studied by Abuluwefa et al[27] at oxygen concentrations 1-15% and temperatures 100-1250°C. It was found that at gas flow rates lower than 4.2 cm/s, oxidation rates were increasing with increasing flow rates and at flow rates above this value, the oxidation rate became independent of the flow rate. The oxidation rate curves (Fig. 1) showed two distinct regions, namely linear for 5-10 minutes depending upon temperature and parabolic or, sometimes logarithmic afterwards. Increasing the oxygen content increased the linear rate constant (k_l) and for a fixed oxygen content, k_l was mildly dependent upon temperature. An activation energy of about 17 $\pm$ 4 kJ/mole was obtained from the $\ln(k_l) \sim 1/T$ plots which was typical for a gas phase diffusion controlled mechanism. It was also found that subsequent oxidation rate followed a parabolic law. The parabolic rate constant (k_p) was derived from straight portions of wt. gain vs. time plots and the values were in good agreement with those reported by earlier authors[27]. In addition, k_p was independent of the gas composition.

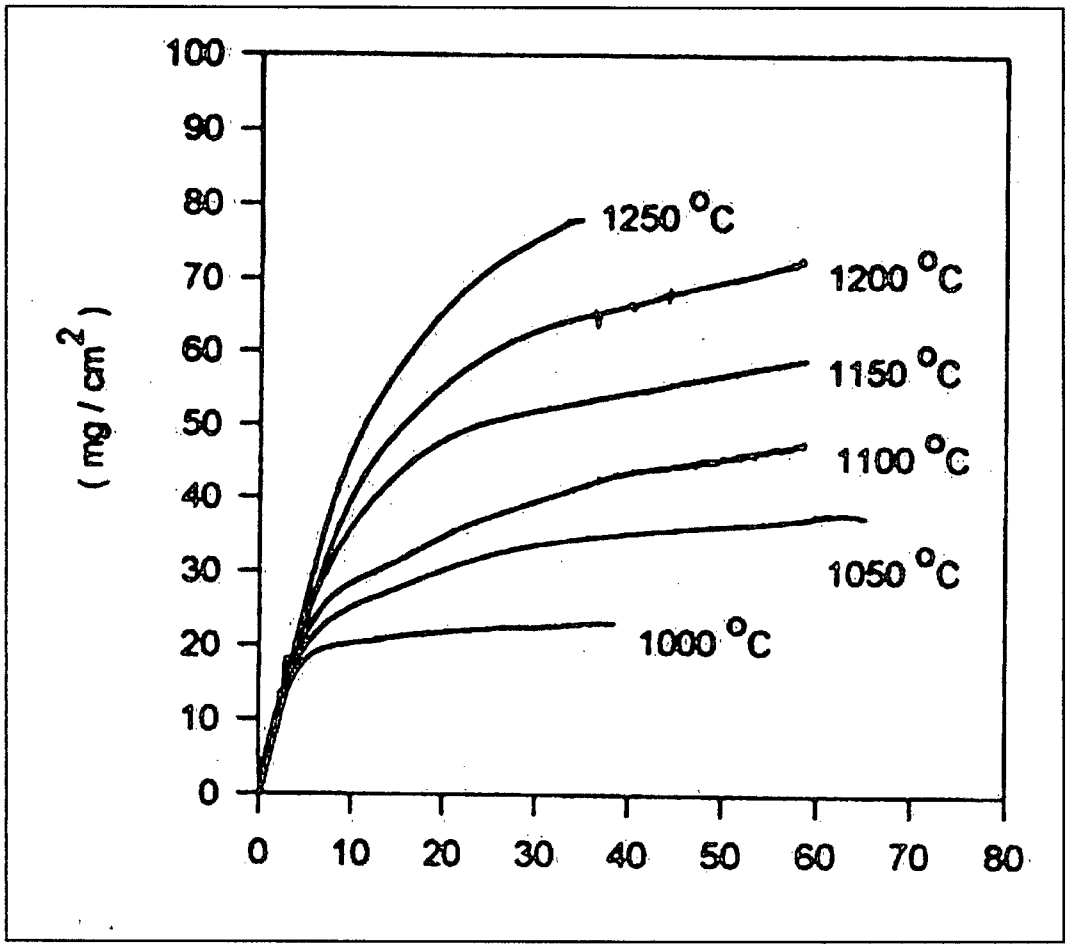

Fig. 1 Weight gain during oxidation in a gas mixture[27] containing 6% O_2 and 94% N_2.

A series of screening experiments was performed by Ormerod et al[1] to assess the effects of independent variables on the parabolic scale growth coefficient in the high temperature range. Steel grade, oxidation atmosphere, oxidation temperature, gas composition and steel surface texture were used as independent variables. It was found that effect of temperature was the greatest and for low carbon grade, the cast surface had a lower oxidation rate than the machined surface. The results generally showed

parabolic behavior and the rate constant obtained typically was comparable with the data obtained by previous authors.

Oxidation of low carbon steel in nitrogen based atmospheres of O_2, CO_2, and H_2O was studied by Abuluwefa et al[28] in the temperature range of 800~1150°C. It was found that reaction rates during oxidation in the binary atmospheres of CO_2-N_2 and H_2O-N_2 followed a linear rate law and were proportional to the partial pressures of CO_2 and H_2O. Rates of oxidation in H_2O-N_2 atmospheres were found to be higher than those of oxidation in CO_2-N_2 atmospheres. Moreover, these rates were controlled by reactions at the oxide surface and were highly dependent upon oxidation temperature. Oxidation in ternary and quaternary gases of O_2, CO_2, H_2O and N_2 showed that the magnitude of the initial linear oxidation rates depended mainly on the concentration level of free oxygen in the oxidizing atmosphere and the presence of CO_2 & H_2O, at their respective concentrations, contributed little. The oxidation process in these atmospheres followed an initial linear rate law, which then gradually transformed to a parabolic rate law. Experiments on ternary and quaternary systems indicated that the predominant oxidizing agent was free oxygen. Moreover, the combined presence of the gaseous components in furnace atmosphere behaved in an additive way with respect to initial rates of oxidation. Initial linear rates for oxidation in multi-component systems were predicted by the summation of calculated individual linear ratios for oxidation in each gaseous component. Good agreement between measured and calculated rates was obtained, particularly for higher O_2.

Microstructures of scales resulting from 1 hr of oxidation in CO_2-N_2, H_2O-N_2 and ternary/quaternary atmospheres containing O_2 were also examined. It was found

that for the samples oxidized in O_2 containing gases, scales consisted of higher oxides e.g. Fe_3O_4, Fe_2O_3 and Fe_xO and they became detached from metal substrate at early stages of oxidation. On the other hand, only Fe_xO was present as oxide phase and no pores or, scale detachment from the metal substrate was observed in the microstructure obtained from oxidation in CO_2 and H_2O atmospheres. This was attributed to formation of a layer of pores parallel to the metal substrate in the early stages of oxidation. However, the studies on microstructures were very limited. Perhaps the greatest criticism of this work will be to the size of their samples (i.e. 18X18X8 mm) which was very small for oxidation experiments due to possible edge effects.

Laboratory isothermal and non-isothermal experiments were conducted by Abuluwefa et al[29] along with plant trials on oxidation of low carbon steels in quaternary atmospheres of O_2, CO_2, H_2O and N_2 of compositions (I - 1% O_2, 10% CO_2, 3% H_2, balance N_2 and II - 6% O_2, 6% CO_2, 3% H_2, balance N_2) close to that of individual walking beam reheat furnace. It was found that the initial linear rate constants were most sensitive to O_2 concentration in the gas mixtures. For example, k_l for the low oxygen was less than half of that for high oxygen, despite the higher concentration of CO_2 in the former. Also, a slight dependence of k_l on temperature was observed. This dependence came from the fact that rates of oxidation in CO_2 and H_2O atmospheres are surface reaction controlled and hence are dependent on reaction temperature. However, as the scale thickness increased the process gradually transformed to follow a parabolic law, i.e. oxidation became controlled by diffusional transport through the oxide layer. Increasing the oxygen level enhanced the transition from linear to parabolic oxidation.

In non-isothermal experiments, it was found that initial oxidation proceeded exponentially with time. However, the oxidation rate was observed to slow down at 900°C due to metal scale separation. At this temperature, a comparatively more rigid oxide (Fe_3O_4 or, Fe_2O_3) formed preventing wustite from deforming plastically. Due to this, samples became unable to accommodate dimensional changes resulting into separation of scale from the metal surface. This hindered the outward diffusion of iron cations. It was also found that decreasing heating rate decreased the oxidation rate. However, due to metal scale separation, the effect of furnace atmosphere on the rates of oxidation was less pronounced.

In trials conducted in industrial reheat furnace in atmospheres with low (1.5%) and high (3.0%) O_2, it was found that reheating at low air/fuel ratio resulted in a reduction of steel loss of approximately 35% (Fig. 2). A general equation for prediction of weight gain due to oxidation during reheating was developed using isothermal linear and parabolic oxidation rate constants. The agreement between predicted and measured weight gain was poor due to metal scale separation that could not be quantified. Examination of weight gains obtained from oxidation in the laboratory and from industrial reheat furnace showed that much more oxidation took place during reheating in the industrial furnace. This suggested that oxidation in the industrial reheat furnace followed a linear rather than parabolic mechanism. Accordingly, weight gains for oxidation during reheating in the industrial furnace were compared with the predicted values using the isothermal linear oxidation rate constants. The predicted and measured rates during reheating with the low oxygen atmosphere were in good agreement. However, for reheating with the high oxygen atmosphere, the predicted oxygen curves

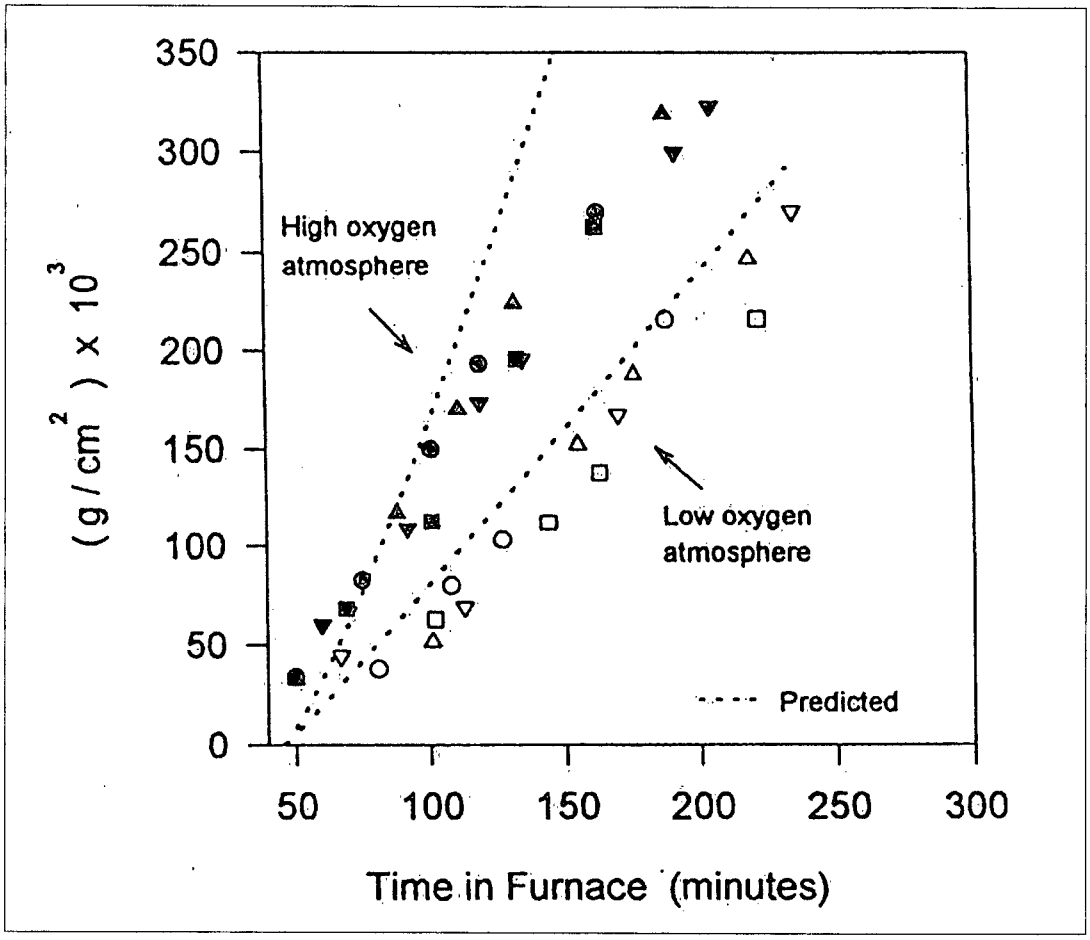

Fig.2 Weight gain curves for oxidation of low carbon steel during reheating in the industrial walking-beam furnace. Open and solid symbols represent low and high air/fuel ratio trials, respectively[29].

were found to be higher, especially at longer reheating times. This indicated that a certain degree of solid state diffusion control existed for oxidation during reheating with the high air/fuel ratio. Accordingly, it was concluded that the controlling mechanism in the oxidation of low carbon steel during reheating in the industrial reheat furnace was intermediate between linear and parabolic, whereas the linear mechanism predominated.

Limited study of scale microstructures indicated that scales consisted of all three oxides, i.e. Fe_xO, Fe_3O_4 and Fe_2O_3 in both the cases (laboratory and industrial). Scale-metal separation was observed at 900°C as discussed earlier. In industrial reheating also, scale-metal separation took place, however the phenomenon appeared to be less significant (possibly due to large dimensions of steel riders).

2.2 Low carbon steels containing residual copper

Influence of residual elements (e.g. Sn, Sb, As and Ni) on scaling and hot shortness of low carbon steels containing residual copper was studied by Melford[30] who was the first among researchers to examine high temperature oxidation of this steel. It was found that presence of Sn reduced the solubility of Cu in austenite by approximately a factor of three. Hence a molten Cu-rich phase was expected to precipitate at a much lower level of enrichment at elevated temperature in presence of Sn. Moreover, the existence of Sn in the molten phase after its precipitation extended its stability over a wider range of temperature. The effects of Sb and As were similar. The addition of Ni was found to have a beneficial effect provided no Sn was present. Ni at 1200°C was found to be no more soluble in a molten Cu-Sn rich phase than it was in austenite. Moreover, the addition of Ni in amounts equal to Cu content did not stabilize the austenite at 1200°C and hence increase the solubility of Cu in presence of Sn. It was also found that MnS inclusions in the steel fixed some Cu by forming CuS around these particles.

Based on the results, a semi-empirical expression was proposed for limiting residual content in steel for a particular soaking practice in the reheating furnace. A mechanism was also suggested for dissipation of Cu layer, i.e. that of detachment and

occlusion in the oxide scale. This was possibly because inward diffusion of oxygen atoms became more predominant than the outward transport of Fe ions once a molten Cu-rich phase appeared on the surface. This resulted into formation of FeO at the interface between the molten phase and the rest of the substrate. This in turn, it was proposed, might lead to an efficient containment of the molten material since it was often observed that molten metals frequently did not wet the oxides of other metals although they might wet their own oxides perfectly. Additionally, the rates of enrichment and dispersion of copper in austenite (Fig. 3) were compared by determining

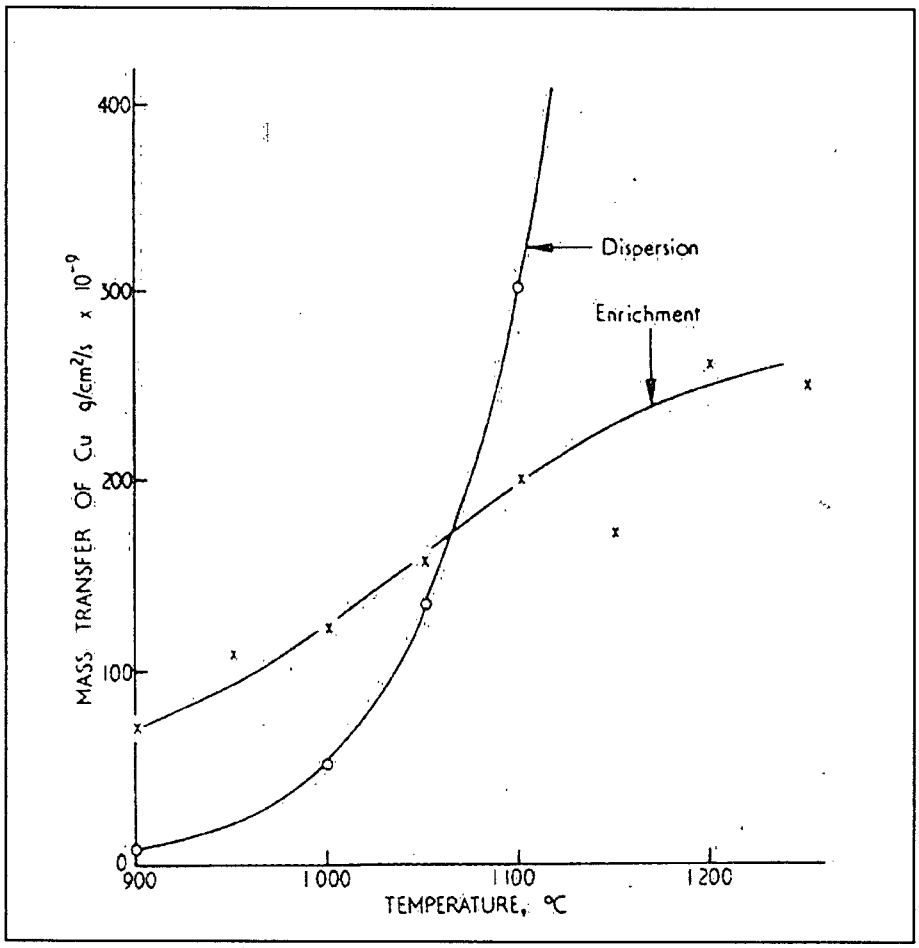

Fig. 3 Comparison of enrichment and dispersion rates for copper in iron[30].

the scaling rates for mild steel (0.23%C, 0.27%Cu) and taking the published diffusion data to calculate the rate of dispersion by diffusion. From the calculations, it would seem that dispersion of copper would be most rapid above 1080°C. However, this was in poor agreement with experience, possibly because of less accurate and relevant diffusion data.

The work done by Melford was a pioneer research on the effect of residual elements on oxidation and hot shortness of mild steel. For example, this investigation was the first to point out that the effect of Sn on reducing the solubility of Cu in austenite was much more prominent than its effect on decreasing the melting point of Cu-rich layer. Additionally, it also suggested for the first time the mechanisms of dispersion of Cu-rich layer at higher temperatures, namely diffusion and occlusion. Many researchers took lead from this and did work to elaborate further on these two mechanisms, subsequently. However, this work suffered from some pitfalls, namely

(i) It was predicted that dispersion of copper should be more predominant than enrichment at temperatures above 1080°C, however this could not be substantiated with evidence. On the other hand, it was found that Cu-enriched layer contained 70% Cu, 15% Ni, 10% Sn and 5% Fe after oxidation at 1250°C (time was not mentioned). This was a very high enrichment level at 1250°C and led credence to belief that enrichment continued and dissipation by diffusion was insignificant even at this temperature.

(ii) It was also mentioned that very high Cu enrichment (and no Ni enrichment) near the surface of an alloy (5% Cu, 5% Ni, and 2% Sn) was observed in a sample heated in a neutral atmosphere. This was an evidence that showed that Cu-enriched

phase precipitated even in absence of oxidation. No comment was made on this observation.

Hot shortness and scaling of steels containing 0.41% Cu as well as 0.35% Cu, 0.066% Sn was studied by Nicholson[31] by oxidizing them at 1100°C for two hours and carrying out hot bend tests at temperatures 725-1350°C. Deep Cu penetration along grain boundaries was observed and severe cracking was seen suddenly at 1075°C for 0.41% Cu steel. The cracking was negligible below this temperature. The other mild steel containing 0.35% Cu and 0.066% Sn began to crack at 725°C and surface break-up was seen up to a maximum of 1100°C. A third steel containing 0.35% Cu and 0.33% Ni did not crack up to the maximum temperature of 1350°C. Additionally, increased severity of cracking was found with increasing Cu content and higher soaking times. Also, there was a critical soaking temperature above which cracking did not occur. These observations were in general, in good agreement with those made by Melford[30]. It was also found by Nicholson that the effect of Cu on occlusion in the scale was relatively small at temperatures below 1100°C. However, as the temperature was increased, the percentage of Cu occluded in the scale increased significantly with increasing Cu content.

It was presented that there seemed to be three factors controlling the critical temperature of steel, namely scaling rate, diffusion of Cu into austenite and occlusion of Cu into the scale. While a lower scaling rate would be expected to reduce the rate of deposition of Cu at the metal surface, it also rendered a smaller portion of this Cu harmless by occlusion into the scale. This was the reason for increased severity of cracking with decreasing oxygen content or, decreasing scaling rate, particularly at

higher temperatures. It was argued that higher solubility of oxygen was expected in the liquid Cu that might cause oxidation to take place at the Cu/steel interface, thus enveloping Cu into the scale. It was also found that Ni was also occluded but not to the same degree as copper.

Solubility of Cu in austenite as well as dihedral angle of Cu-rich phase at austenite grain boundaries was measured by Salter[32] at various temperatures ranging from 900 to 1275°C. It was found that solubility of copper in austenite decreased near the melting point of copper (Fig. 4) resulting into an increase in the amount of undissolved Cu-rich phase. It was argued that the apparent dip in solubility at 1100°C could be explained by eutectic instead of peritectic at the Cu-rich end of the Fe-Cu phase diagram. This effect was possibly caused by the presence of C, Mn and Si. It was also discussed that there was a minimum value for the dihedral angle of the Cu-rich phase near the melting temperature of Cu (Fig. 5). Thus, the maximum amount of Cu-rich phase out of solution coupled with a minimum dihedral angle at the melting point of copper caused maximum grain boundary penetration at this temperature resulting into likelihood of maximum embrittlement at 1100°C. Above this temperature, more Cu went into the solution and at the same time dihedral angle of the Cu-rich phase also increased. This was the reason for reduction in severity of hot shortness beyond 1200°C.

The work of Salter was very interesting and significant as it threw new light on the origin of Cu penetration during scaling. The work on solubility of Cu at higher temperatures was in contrast to the published work.

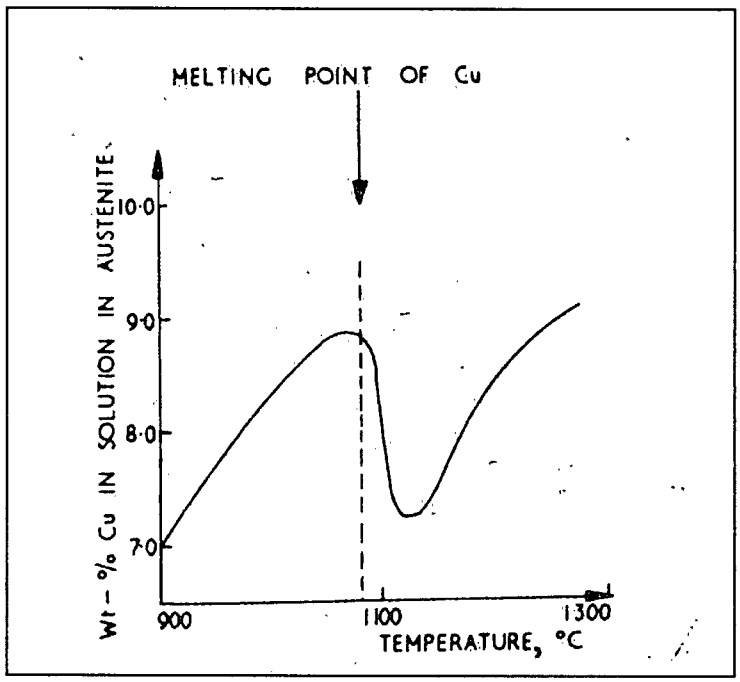

Fig. 4 Effect of temperature on the solubility of Cu in austenite[32].

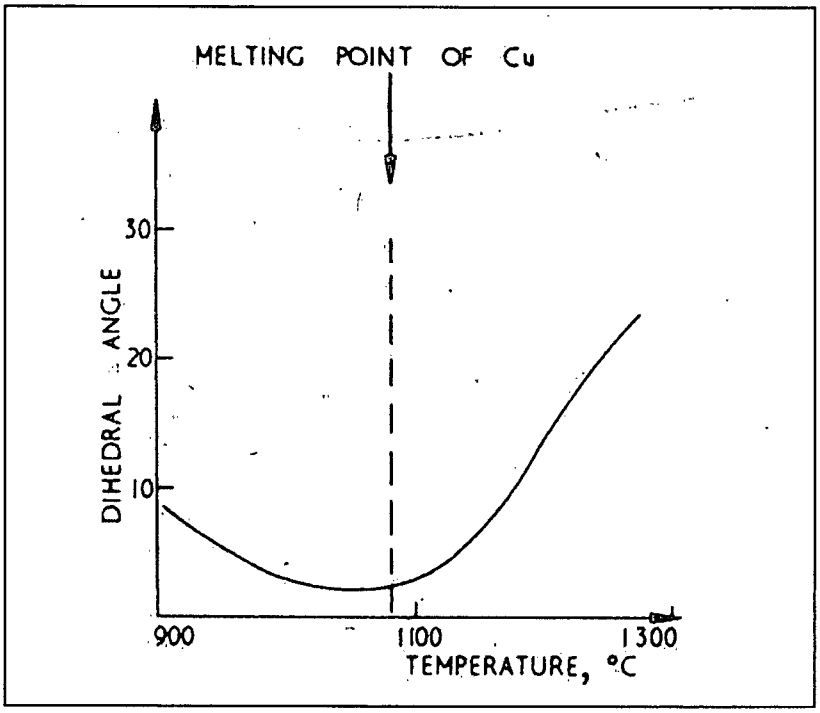

Fig. 5 Effect of temperature on the dihedral angle of Cu-rich phase[32].

Study on scaling and hot shortness of Cu-containing low carbon rimming and killed steels was undertaken by Nicholson and Murray[10] at temperatures 900-1350°C under different environments. It was found that Sn accentuated the effect of Cu primarily because of its effect in reducing the solubility of Cu in austenite. Ni reduced the effect of Cu by increasing its solubility in austenite and also by increasing the melting point of Cu-rich phase. Nickel also increased the scale adherence due partly to surface roughening occurring during oxidation and perhaps more strongly to the stabilization of austenite to room temperature by locally enhanced Ni content. This would prevent the de-scaling action caused by the shear forces set up at the interface when austenite transforms the ferrite.

The effect of oxygen content in the atmosphere was also studied and it was concluded that while hot shortness increased at lower temperatures with increasing oxygen content, at higher temperatures it passed through a peak above which increasing the oxygen content decreased the surface cracking. This was due to the balance between the scaling rate causing enrichment and diffusion of Cu in the substrate as well as occlusion causing dispersion of the enriched layer. Lowering the oxygen content at a given temperature reduced the scaling rate and hence the Cu-enrichment was reduced. However, it also reduced the copper occlusion by reducing the partial pressure at the interface (Fig. 6). At lower temperatures however, occlusion was not so important. As the temperature was increased the process of Cu occlusion into the scale became increasingly important and greatly reduced the Cu build up at the interface. The effect of deoxidizing elements was to reduce surface hot shortness due to copper particularly at high temperatures and oxygen contents. This was because the deoxidizing elements,

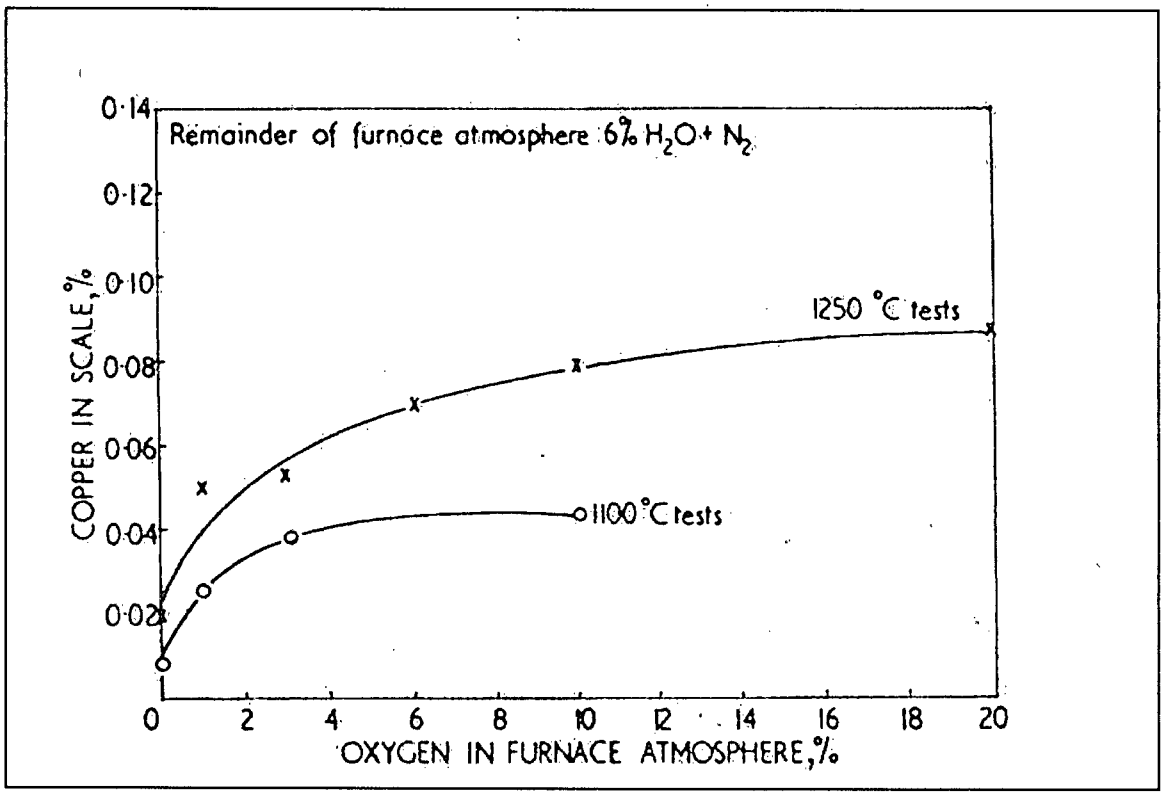

Fig. 6 Effect of furnace oxygen content on occlusion of copper into scale for 0.16% Cu steel[10].

e.g. Al, Mn and Si could oxidize readily under the low oxygen partial pressure in the region of the metal surface and thus promote the occlusion process of Cu.

Increasing the water vapor content was to increase the scaling rate without increasing the occlusion rate to the same extent as oxygen. Increasing the water vapor content therefore increased Cu-build-up and surface cracking. The reason for this was not clear.

This work covered the effects of several parameters such as temperature, deoxidizers, oxygen and moisture contents in the furnace, etc. on scaling as well as hot shortness of mild steels. The authors should also be credited for their investigation on

scale adherence due to presence of Ni. The importance of dispersion of enriched layer by occlusion at higher temperatures and oxygen contents was also highlighted.

Scaling characteristics of complex Cu-bearing steels (1.83% Cu, 1.7% Si, 1.03% Mn and 0.8% Mo) as well as plain Cu-bearing steels (3.0 wt % Cu) were investigated by Cox and Winn[33] by oxidizing at temperatures of 900-1100°C for 20 and 6 hours respectively in the air. It was found that for plain Cu steels at 900°C, Cu was present at the steel surface as almost continuous phase and in the wustite layer in the form of globules. In the Cu-Si-Mn steels oxidized at 900°C, the copper was not concentrated at the steel surface, but dispersed as small globules in the wustite layer. At 1100°C the Cu-steels contained large areas of relatively pure Cu at the interface. Discrete formations of iron silicate were also observed within the FeO grains and at some FeO grain boundaries. However, the Cu-Si-Mn steels contained an additional layer present between the steel and the wustite. This layer consisted of a two phase matrix containing Fe and Mo mixed oxide crystals and dendrites of FeO.

In Cu-steels oxidized at 1100°C, the copper phases contained 0.0-5.0% Fe and hence would be completely liquid at this temperature. In comparison, the Fe content of Cu-layer in the Cu-Si-Mn steel was 15-60%. At 1100°C, alloys in this composition range would be in a mushy state containing liquid Cu and austenite. The high Fe content of the Cu layer was attributed to the presence of the adjacent silicate layer close to the FeO layer which reduced the rate of Fe diffusion outwards through FeO and allowed the Fe content of Cu layer to build up. The reduced fluidity of Cu alloy in Cu-Si-Mn steels at 1100°C was considered to account for the improvement in hot working properties (i.e. absence of hot shortness) of these alloys.

This paper described the effect of presence of elements such as Si, Mn and Mo on the Cu-rich layer and hence on hot shortness. This work showed that these elements could reduce the fluidity of Cu-rich phase and hence prevent the hot shortness at 1100°C. However, the authors did not compare plain Cu steels and complex Cu steels containing identical amounts of Cu. Rather, complex Cu steels had much less Cu (i.e. 1.85%) in comparison to plain Cu steels with 3% Cu.

Effects of alloying elements (e.g. Ni, Mn, Sn, Sb and As) on solubility and surface energy of Cu in mild steel was studied by Salter[34] by heating for 2 hrs at temperatures between 900 and 1250°C. It was found that Ni caused an increased solubility of Cu in austenite (Fig. 7) and had little effect upon the dihedral angle in the critical temperature range (i.e. in which Cu had minimum solubility and minimum dihedral angle in austenite). However, it markedly decreased the dihedral angle at higher temperatures. Ni also caused a slight increase in the melting point of Cu-rich phase thus restricting the hot shortness range. Mn generally had little effect on dihedral angle. However, it did cause a modest decrease in the solubility of Cu. It also lowered the melting temperature of Cu-rich phase slighty. Sn, Sb and to lesser extent As caused a serious reduction in the solubility of Cu in austenite (Fig. 7). Hence increasing the content of these elements in the steel resulted in an increase in the amount of undissolved phase thus decreasing the degree of scaling necessary for causing the Cu-rich phase to be formed. All these elements in increasing order caused an overall increase in the dihedral angle, i.e. decrease in wettability, particularly in the critical

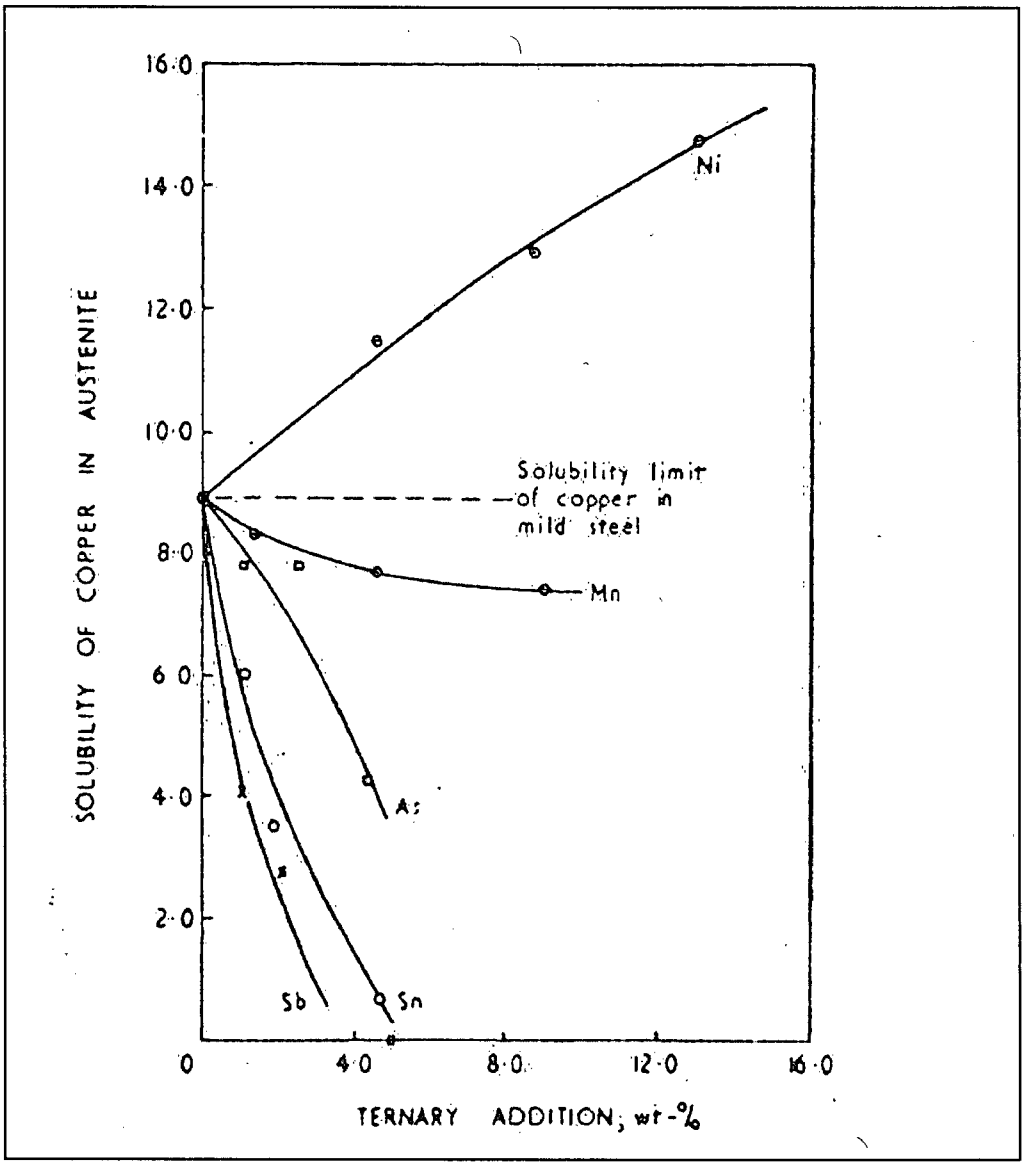

Fig. 7 Effect of ternary additions on the solubility of Cu in austenite[34] at 1250°C.

range, i.e. 1050°-1150°C. However, the effect of Sn on dihedral angle was not significant. This meant that Sn and Sb increased the amount of Cu-rich phase to the greatest extent and hence had the maximum effect on hot shortness. All these elements also caused marked reduction in the melting point of Cu-rich phase, thus tending to increase the hot shortness range.

This fundamental work is an example of detailed studies on the effect of other residuals on the solubility and dihedral angle of Cu in austenite. This investigation classified residual elements into three categories, namely beneficial (Ni), neutral (Mn) and detrimental (Sn, Sb and As). This classification agreed well with the previously observed effects of these elements upon severity of hot shortness. The results therefore offered good explanation to some of the fundamental factors affecting the problem.

Effect of Ni on high temperature oxidation characteristics of low Carbon steels containing 1.15% Cu, 0.04 -1.16% Ni and 0.40% Si (with Ni:Cu ratios varying from 0.03 to 1.0) was studied by Fisher[35] by heating them at 1150°C for 5 hrs in a gas mixture of 65% N_2, 11% O_2 and 24% H_2O (by vol.). It was observed that the oxide scale consisted of four layers, namely Fe_2O_3, Fe_3O_4, Fe_3O_4 + FeO and FeO + patches of Fe_2SiO_4. The first two layers were fairly compact, however part of the third layer and all of the fourth layer was very porous. The pores possibly formed when the space created by the outward diffusion of Fe ions was not filled by plastic shrinkage of the scale. The inner layer also contained occluded metallic particles. The number of these occluded metallic particles increased with increasing content of Ni in the steel. Additionally, increasing Ni content caused the average Cu content of the occluded phase to decrease while both the average Ni and Fe contents increased. In steels containing Ni:Cu ratio of 0.35 or greater, the composition of the scale varied with distance from the scale/metal interface. This was mainly due to selective oxidation of the particles after they got occluded into the scale.

Additionally, a zone of very fine oxide particles was also noticed ~ 40 μm deep in the metal. These particles were ≤1 μm in diameter and were apparently formed by

internal oxidation of Si in steels. Steels containing low Ni:Cu ratios also exhibited large (several microns) wustite particles and fayalite particles in the internally oxidized zone.The scale/metal interface and internally oxidized zones of steels with Ni-Cu ratios of 0.1-0.35 were similar in appearance. Cu-rich phase was in the form of a continuous film adjacent to the scale/metal interface. This phase could also be observed in some of the austenite grain boundaries in steels with Ni:Cu ratio of 0.03. Increasing Ni:Cu ratio to 0.4 caused the disappearance of very fine SiO_2 particles. Also, there were large areas devoid of any Cu-rich phase. There were areas in the internally oxidized zones where some enrichment of Cu had occurred apparently without forming a molten phase. In the steel with Ni:Cu ratio of 1.0, no Cu-rich phase at the interface and in the internally oxidized zone was observed. This reduction of Cu concentration at the interface resulted from occlusion of Cu into the oxide enhanced by higher Ni content. The presence of Ni caused enrichment of Ni with Cu at the scale/metal interface and increased the oxygen solubility in the enriched layer enabling oxygen to diffuse inward to the matrix where it formed FeO. Additionally, the ability of Ni to increase the solubility of copper in austenite was also important. These two phenomena prevented a molten Cu-rich phase from forming before occlusion by internal oxidation and intrusion of wustite could separate the enriched region into the scale.

This work established why Ni is so effective in controlling the build up of Cu-rich layer at the interface. However, the effects of varying amounts of Cu as well as oxidation time were not examined.

Effects of Sn and Ni on the solubility and surface energy of copper in mild steel was studied by Salter[36] by varying Cu content from 1% to 15% and adding 5-15% Ni

as well as 1-5% Sn to them. It was observed that effect of Sn on the solubility of Cu in austenite predominated over that of Ni. The solubility of Cu decreased drastically with increasing Sn content (Fig. 8) and of all the steels examined, only that with 14.8% Ni exhibited noticeable level of solubility of Cu in the austenite. It was also noticed that

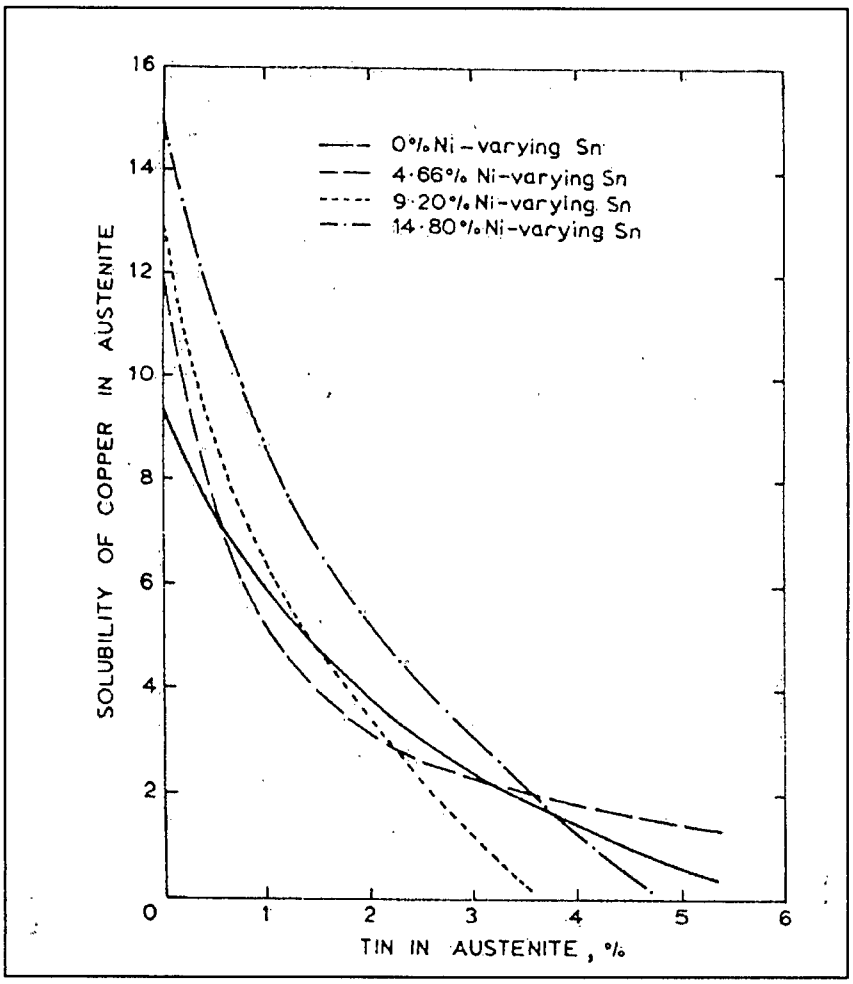

Fig. 8 Effects of mutual additions of Sn and Ni on the solubility of Cu in mild steel[36] at 1250°C.

relatively little Sn was needed to counteract the beneficial effect of a significant amount of Ni. Additionally, for a given Ni and Sn content a maximum amount of undissolved Cu-rich phase was expected between 1000-1050 °C. Increasing Sn content clearly showed a marked increase in the volume fraction of Cu-rich phase but increasing Ni content only had a marginal effect.

Dihedral angle measurements indicated a minimum at 950°C. Also, Ni tended to cause an overall lowering of the dihedral angle value, particularly at temperatures above 950°C. However, Sn content did not have clear effect.

This work clearly showed that presence of Sn would rapidly counteract any beneficial effects gained from the presence of Ni. However, this study was not done under oxidizing environments. Also, the results showed a dip in dihedral angle at 950°C. This was different from the earlier work done by the author that mentioned this minimum at 1050°C. No comment was made on the reasons of this variation. Moreover, there was too much scatter in some of the data.

Enrichment of Cu during scaling of cold rolled low carbon steels was discussed by Mayland et al[11]. It was proposed that the degree of enrichment was determined by the balance between the build up of the phase due to oxidation and its dispersion by diffusion as a result of the concentration gradient existing between the surface and the interior of the steel. Rate of formation of Cu layer was also reported as a function of reheating temperature for different Cu contents of steel (Fig. 9). It was predicted that there existed a critical temperature for each Cu level above which enrichment ceased and dispersion by diffusion predominated. The bend test results[10] for a number of low

Cu (1.8-3.04 wt%) and Ni (1.35-3.06 wt%) and other elements such as Al, Cr, Si, etc. (1-3 wt%). Additionally, experiments were also conducted on high purity steel containing 2.19-2.37 wt% Cu and 0.01-1.1% Ni. It was found that temperature was one of the main parameters governing oxidation and the rate appeared to increase drastically when the temperature increased from 900° to 1100°. However, the rate of increase was much lower when the temperature was increased further to 1200°C. It was also noticed that a metallic phase (95% Cu + 5% Fe) appeared in the inner oxide layer (FeO) which remained dispersed in the oxide at low temperatures (e.g. 900°C). However, this enriched layer became nearly continuous at higher temperatures (1050°-1200°C), and the detrimental penetration within the austenite grains occurred.

It was further observed that of the elements less oxidizable than Fe (e.g. Ni and Co), Ni modified the mechanism and gave rise to internal oxidation. The austenite grain boundaries were internally oxidized, while at the scale/metal interface a two phased zone composed of oxide and metallic globules (Fe + Ni + Cu) could be detected. The distribution of these elements varied with temperature. In fact, the behavior of steels containing Ni oxidized at 1200°C was similar to that of a Ni-free steels oxidized at 900°C. In both cases the Cu-containing metallic phase was not molten due to the presence of Ni at the operating temperature and eventually became entrapped within the oxide scale, with a discontinuous distribution. The internal oxidation was thought to be due to the liberation of oxygen by dissociation of Fe and Ni oxides at the interface and migration of oxygen through cracks and pores in the oxide layer. The element Co had only small solubility in Cu-rich phase and hence it gave a separate Fe-Co phase which concentrated along the Cu-rich phase and did not modify the phenomenon. However, by

addition of Co and Ni, one could enhance the solubility of Fe in the Cu-enriched phase and certainly increase its melting point.

On the other hand, Si and other alloying elements more oxidizeable than Cu (e.g. Al, Mn, Mo, P, Ti, Cr, Zr) did not modify the general behavior of Cu-rich phase. These elements usually appeared as occlusions in the oxide scale. At low temperatures (900°C) the effect on the scale was not marked (FeO zone often entrapped some particles such as silicates and special spinels). However, Si additions seemed to affect the oxidation process to some extent as it gave rise to a fine distribution of metallic phase into the oxide scale. At higher temperatures (1100-1200°C), however the inner oxide scale was viscous or, perhaps liquid and as a result the oxidation rate increased rapidly. Hence the beneficial effect of Si did not exist at higher temperatures.

This report presented a good work on the effect of Ni as well as other alloying elements on scaling characteristics of mild steels. It provided some excellent photographs of Cu-enriched phases at the interface. It also presented a review of the previous work on oxidation and hot shortness of Cu containing steels. However, the presentation about the effects of other elements such as Co, Al, Mn, P, etc. was not in detail. Although it was mentioned that detrimental penetration of grain boundaries occurred during oxidation, evidence for this was given only for high Cu (e.g. > 3.0 wt%) steels. Grain boundary penetration for low Cu (< 1.0 wt%) steels was not exhibited.

A mathematical model for copper enrichment during reheating was presented by Bergman and West[8]. Their model assumed that (i) there was uniform concentration of Cu initially (ii) enrichment did not extend to the center of the specimen (iii) diffusion

coefficient of Cu in austenite was independent of composition and (iv) there was no enhanced diffusion down grain boundaries. The model predicted that the enriched copper layer thickness was continuously increasing with temperature (Fig. 10). This was

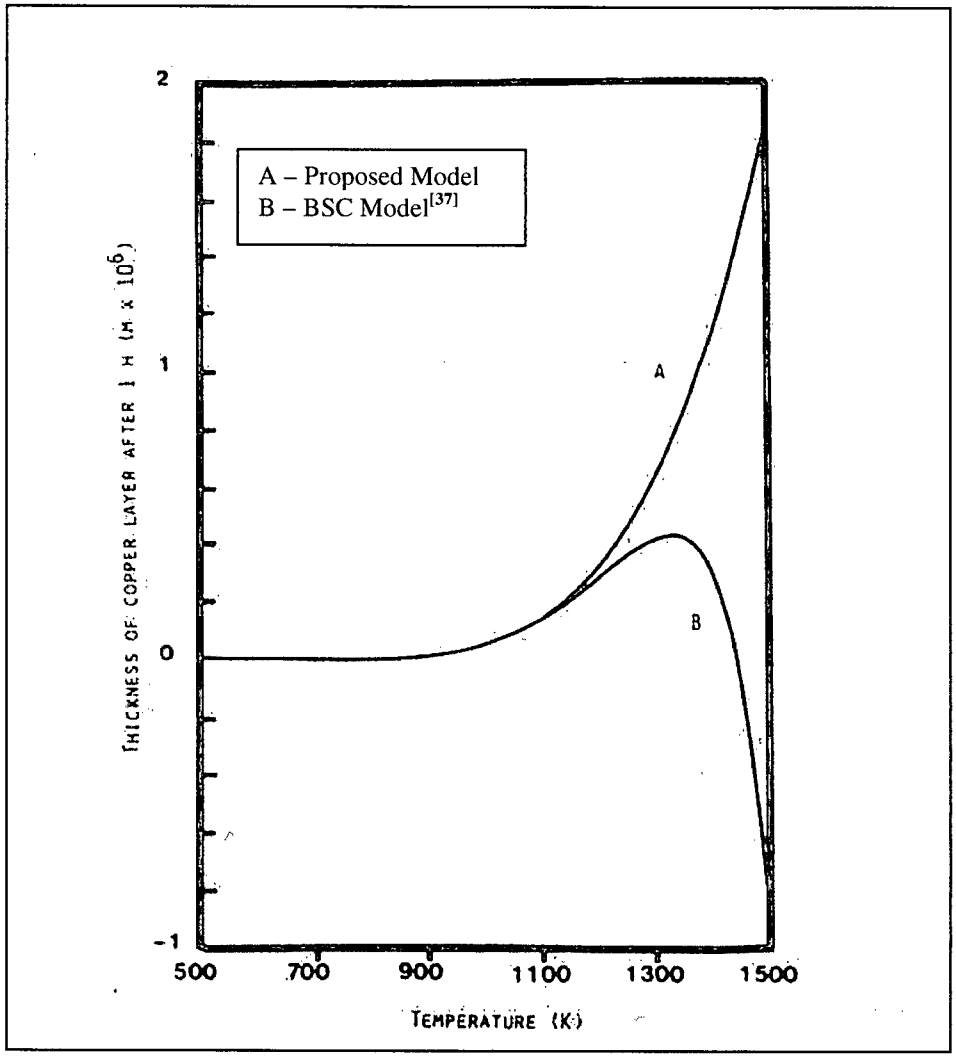

Fig. 10 Calculated thickness of Cu layer after one hour isothermal treatment[8].

in sharp contrast to earlier models[37] that envisaged a maximum in enriched layer thickness at around 1100°C. It was argued that prediction of their model was supported

by the work of Kohsaka and Ouchi[38] that found increased severity of cracking due to reheating at 1250°C.

This was an important although brief paper on Cu enrichment during reheating and questioned the existing theory that predicted a maximum in Cu layer thickness at around 1100°C due to predominance of dispersion process by back diffusion at temperatures above this.

Scaling and cracking due to residual Cu was studied by Kajitani et al[39] in steels containing 0.2% C, 0.01-0.25% Si, 0.5% Mn and 0.2-1.5% Cu. It was found that cracking occurred at and above 1050°C and the upper temperature limit for cracking increased with increasing Cu concentration as well as decreased with increasing Si content of steel. Investigations on the morphology of Cu precipitates after oxidation revealed that in the sample oxidized at 1000°C, Cu which was solid at this temperature existed in the porous layer of FeO adjacent to the metal surface. Studies by EPMA showed high Si content in this layer. At 1100°C, however liquid Cu precipitated in contact with steel. This Cu penetrated into austenite grain boundaries and resulted in crack formation. At 1300°C where crack did not occur, liquid Cu existed at the grain boundary in the FeO layer, and it was not observed at the steel surface. Cracking therefore did not occur at this temperature.

It was proposed that morphology of Cu precipitates was largely dependent upon oxidation of Si in steel. Using the phase diagram of FeO and SiO_2 system, it was argued that composition of Si-rich grain boundary phase in the scale lied on the liquidus line of FeO (Fig. 11). This means that the boundary phase was liquid at 1300°C. In contrast, below the eutectic temperature of 1177°C, FeO and $2FeO.SiO_2$ were stable. Hence the

porous layer produced at 1100°C was solid and composed of FeO and $2FeO.SiO_2$. The change in the morphology of scale by changing temperatures influenced the Cu precipitation (Fig. 12). For example, at 1300°C liquid Cu precipitated at the steel surface and then it was trapped into the grain boundary phase in scale which was liquid at this temperature. On the other hand, at 1100°C where the scale was solid, Cu continued to precipitate at the steel surface.

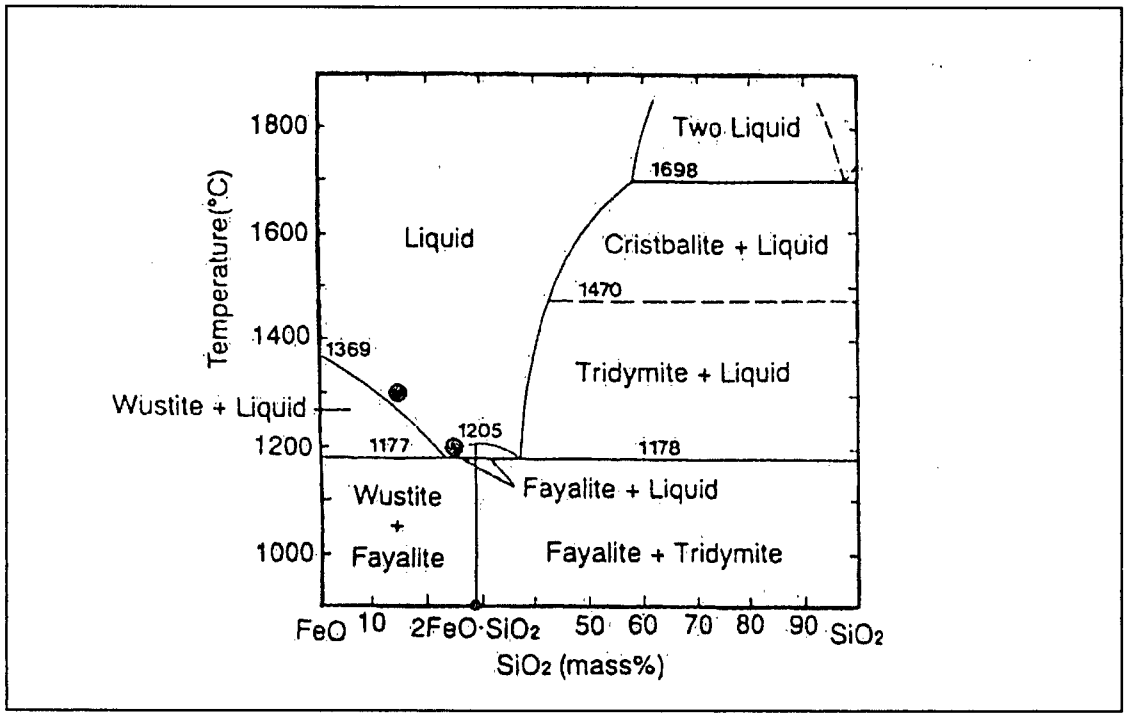

Fig. 11 Phase diagram of FeO and SiO2 system (solid marks show the composition of Si-rich boundary phase analysed by EPMA[39].

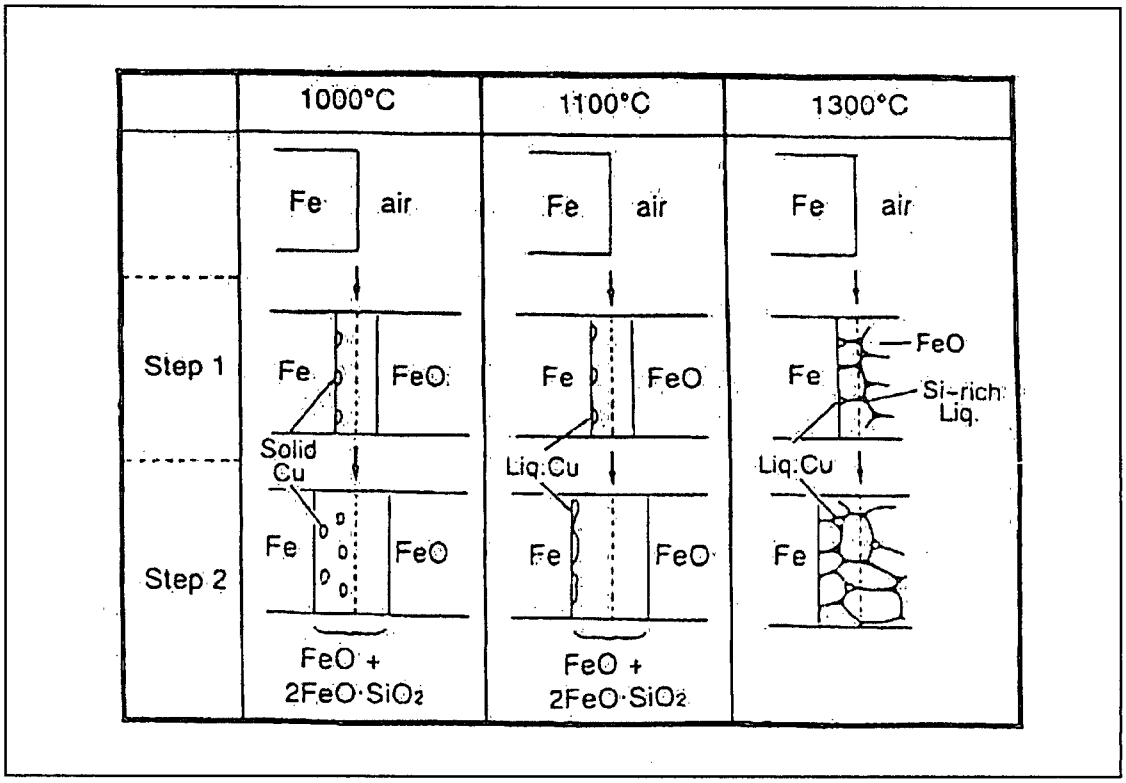

Fig. 12 Mechanism of Cu precipitation during oxidation of steel[39].

The decrease in upper limit temperature for crack formation was possibly due to increased Si-rich liquid boundary phase for higher Si-steels that helped in entrapping liquid Cu precipitates.

The issue of whether Cu was trapped into the scale or not, was related to the interfacial energy between liquid Cu and scale ($\gamma_{Cu\text{-}scale}$). If $\gamma_{Cu\text{-}scale}$ was smaller the liquid Cu was trapped into the scale, otherwise it was in contact with the steel surface. It was mentioned that $\gamma_{Cu\text{-}scale}$ decreased at 1300°C because of the liquid scale formation and hence Cu was trapped into the liquid grain boundary in the scale. They suggested that Cu continued to exist at the steel surface at 1100°C because interfacial energy between liquid Cu and steel was small. On the other hand, at 1000°C, interfacial energy between solid Cu and steel became large, and Cu was absorbed into the porous layer of

scale.This work discussed the effect of temperature and Si on the morphology of Cu precipitates at the interface. Enrichment of Cu based on interfacial energies and phase diagram of $FeO-SiO_2$ system was also explained. However, the effect of Cu on the morphology was not described as only cases of enrichment in the highest Cu content (1.5 wt %) were mentioned.

Effect of alloying elements (Cu, Sn, Ni) on hot workability of low carbon steels (0.05% C, 0.01-0.02% Si, 0.3% Mn, 0.0-0.3% Cu and 0.0-0.04% Sn) was studied by Imai et al[40] by oxidizing them in air at temperatures between 1000-1300°C for 2 to 3 hours and deforming the samples (40%) under tensile load. It was found that Sn enhanced cracking induced by Cu-enriched liquid phase and that presence of only Sn (i.e. no Cu) in the steel did not cause any cracking at all. Additionally, enrichment of Cu but no enrichment of Sn at the surface was found. A higher content of Cu (> 5%) and low or negligible content of Sn (< 1%) was observed at a distance of 10-20 μm below the surface (interface). It was speculated that Sn diffused back into the steel and was not enriched at the scale/ steel interface. However, Cu did not diffuse so rapidly as Sn and hence was enriched. This was supported by the evidence of an order of magnitude higher diffusivity of Sn in austenite as compared to that of Cu. It was concluded that as Sn had an order of magnitude higher diffusivity in the austenite as compared to Cu and also had greater solubility limit (e.g. 16% at 1100°C), even if Sn was enriched under the steel surface, liquid Sn-Fe alloys would not form and hence no surface cracking in Sn bearing steels would result.

Increasing the Ni content affected the surface cracking and 0.3% Ni could suppress the cracking almost completely. This was due to formation of a solid layer

(confirmed from phase diagrams) of 12% Cu- 19% Ni - Fe at the steel surface which separated the liquid layer having 63% Cu- 12% Sn - Fe. The solid Ni enriched layer prevented the Cu rich liquid layer from coming into contact with the steel surface. The amount of Cu-enriched liquid phase also got reduced due to presence of Ni. It was proposed that Cu concentration in the austenite at steel surface became higher as the ratio of Ni to Cu in the steel was increased. This resulted into higher value of Cu atoms' flux, i.e. J_{Cu} (= $-D.\partial C/\partial x$) back into the steel and resulted into smaller amount of liquid Cu-Sn phase and suppressed the surface cracking.

Sn reduced the solubility of Cu in the austenite and hence increased the amount of liquid Cu rich alloy at the surface. In addition, Sn also decreased the solidus temperature in Cu-Fe alloy, e.g. 10% Sn lowered the solidus temperature of Cu from 1083° to 835°C. These two factors accounted for observance of more severe cracking in Sn-bearing steels at 1100°C. Additionally, cracking occurred at a temperature as low as 1000°C in Cu-Sn bearing steels.

Effect of Sn and Ni on precipitation of Cu-rich phase in low carbon steels was studied in this investigation. It was tried to correlate the findings with solubility data from phase diagrams (calculated using the computer program Thermo-Calc). However, the concept of occlusion of Cu-rich phase due to Ni-rich layer was not discussed although, something similar did appear to happen in the samples.

High temperature oxidation and hot workability of low carbon (0.05% C) steels containing 0-0.3% Cu and 0.02-0.15% Ni was studied by Imai et al[41]. Microstructures and composition of phases formed at the scale/steel interface were investigated and they were correlated with surface cracking. It was found that 0.3% Cu steel exhibited

cracking when oxidized only at 1100°C. Oxidation at 1000°C and 1200°C did not cause any cracking. Also, this cracking phenomenon was absent in the case of 0.3% Cu - 0.15% Ni steel as well as Cu-free steels.

Microstructural examination revealed that scale/metal interface of 0.3% Cu steels was smooth at 1000-1100°C. At higher temperatures however, the interface became uneven as metallic phases were occluded into the scale. Also, internal oxidation occurred noticeably. There was much less copper in the layer at the interface at 1200°C as it was largely occluded into the scale. At lower temperatures the enriched layer had higher content because of no occlusion into the scale. Microstructural investigation further showed that Cu enriched phase formed at the interface in 0.3% Cu steels oxidized at 1000° as well as 1100°C. However, at 1100°C Cu enriched layer had penetrated some of the grain boundaries near the interface. Whereas at 1000°C, no penetration was observed. Also, at 1000°C the enriched phase appeared blocky whereas that at 1100°C was elongated and continuously spread over a layer distance. At 1200°C, however the unevenness of the interface was noticeable and metallic phase was occluded into the scale at 1200°C. Cu was enriched in the occluded phase and also in to steel near the scale/steel interface.

Presence of Ni (0.3% Cu - 0.15% Ni steel) was found to increase the unevenness of the scale/metal interface as it caused more occlusion of the metallic phase into the scale at 110°C. Both Cu and Ni were enriched in the scale as well as at the interface. At 1200°C, the metallic phases were more occluded and finely distributed in the scale. The ratio of Cu to Ni contents in the metallic phases lowered with distance in the scale from

the scale/steel interface, although there were increasing amounts of Cu and Ni as one moved away from the interface in the scale.

It was proposed that at 1100°C, in 0.3% Cu - 0.15% Ni bearing steels, high Cu (i.e. 66% Cu - 15% Ni - Fe) phase got equilibrated with low Cu (i.e. 16% Cu - 16% Ni - Fe) phase at the interface. As the oxidation progressed the high Cu phase got detached and hence occluded in scale. However, at 1200°C diffusion of Cu back into the steel became more predominant. Also, the steel was more heavily oxidized resulting into earlier occlusion of Cu rich phase in the oxide. Due to these two factors, the concentrations of Cu at the steel surface as well as in the occluded phases were relatively low (i.e. 16% Cu, 27% Ni).

Effect of Ni on the scaling of low Cu containing steels was examined in this work. and a theory was proposed behind occlusion of Cu-rich phases in the oxide. However, results were reported only for low Cu steels and no study was attempted on the effect of Ni on high Cu steels.

Distribution of alloying elements near the oxide/metal interface was studied by Geneve et al[42] for low carbon steels (0.04-0.06% C, 0.05-0.09% Ni and 0.02-0.26% Cu) oxidized at 900°C in air. A peak in concentration of all the elements except iron was found near the interface. It was argued that enrichment of elements depended upon oxidation kinetics of the alloy, the concentration and diffusion rates of elements and whether they were more or, less oxidizable than iron. For the elements that were more oxidizable than iron, e.g. Si, the reaction could lead to internal oxidation, i.e. precipitation of SiO_2 just below the interface. Some of these precipitates were incorporated into the scale during its growth. This was the reason for increased

concentration of Si in the scale side of the interface compared to the metal side. Elements less oxidizable than iron did not participate in internal oxidation and remained enriched at the metal surface as iron transferred into the scale. This was the case with Ni that exhibited greater concentration on the metal side than on the scale side of the interface. However, an element such as copper reached its solubility threshold and hence precipitated and some of the precipitates ended up into the scale when its growth took place. This gave rise to increased concentration on the scale side as compared to the metal side of the interface.

It was found that increasing Cu content caused large amounts of Ni to appear into the scale, instead of remaining in the interface on the metal side. Also, Ni atoms in the scale were located primarily in the Cu precipitates in which Ni had a high solubility. lower scale thickness in general, was observed for steels higher in residual elements such as Cu. This was because these elements accumulated near the metal/oxide interface and provided a diffusion barrier for iron atoms, inducing a decrease in the oxidation rate.

This investigation described the study of enriched layer using Auger Electron Spectroscopy. This work more or, less confirmed the findings reported by earlier workers[30-33]. However, the observation that increasing Cu caused Ni to appear in the scale rather than concentrate on the steel surface was contrary to what previous authors had reported. Earlier investigations had revealed that it was Ni that caused Cu to get incorporated into the scale by the process of occlusion.

3. Scope and Objectives

It is evident from literature survey that oxidation of steel has been the subject of several studies and the present understanding of mechanisms of scaling, enrichment and dispersion of copper layer is well advanced. However, the literature is deficient in many important areas, e.g. characterization of oxide microstructures, particularly evolution of microstructures during early stages of oxidation. Also, much remains to be done in terms of kinetics of oxidation in particular, the effect of copper on the kinetics. Since the focus has been on oxidation for longer times, the process of enrichment during the initial stages of oxidation (e.g. for times less than 2 hours) remained virtually untouched. Similar is the case of modeling the Cu-enrichment process during scaling. Although a small number of work was reported, a few simplifying assumptions as well as non-incorporation of dispersion by occlusion of Cu into the models made them inaccurate.

There is also disagreement on the enrichment and dispersion of copper. While the majority of investigators indicate that diffusion of copper away from the surface into the bulk becomes predominant after a certain temperature (depending upon copper content of the steel) which results in the disappearance of copper enriched layer, some others suggest that enrichment continues even beyond 1300°C.

The objectives of the present work, therefore were:-

(i) To examine the evolution of scale microstructures for oxidation times < 2 hours.

(ii) To determine the effects of copper content and temperature on the microstructural features of the scale.

(iii) To characterize the development and morphology of copper enriched precipitates at the interface.

(iv) To determine the kinetics of oxidation in presence of Cu.

(v) To obtain insight into the competing processes of Cu-enrichment and dispersion during scaling.

4. Methodology and experimental details

4.1 Experimental set-up

The experimental set-up (Fig. 13) was the same as that used by Ren[43] for conducting experiments on oxidation of IF steels. It consisted of a cylindrical chamber (of 55 mm diameter and 495 mm hot zone length) housed in a furnace heated by resistance coils around the chamber. The bottom of the cylindrical chamber was connected to air/argon supply for providing the required atmosphere during experiments. A thermocouple (K-type) inserted horizontally near the centre of the furnace, provided actual temperature to the control system which then adjusted current to maintain the set temperature. The sample was hung through a suspension wire from a microbalance (Denver Instruments' Model M310). The microbalance was kept on a platform that could be moved up and down on a vertical frame with the help of an electronic control. It was also possible to adjust the position of the microbalance on the platform along the horizontal direction. The microbalance was connected to a personal computer with a data acquisition software (COLLECT from Labtronics Inc.) for collecting the weights and storing them onto the hard drive periodically. A dummy sample of inconel to which a thermocouple (K-type) was connected was also kept

hanging very close to the actual sample for monitoring the exact temperature near it. The other end of the thermocouple was connected to a temperature recorder.

4.2 Experimental details

Samples of low carbon steels containing 0.22%, 0.39% and 0.78% Cu (Table I) were selected for undertaking the studies. They were cut into rectangular pieces of approximately 37 mm X 25 mm X 3.5 mm dimension. Just before beginning the experiments, each sample was ground using SiC grinding papers of 120, 240 and 320

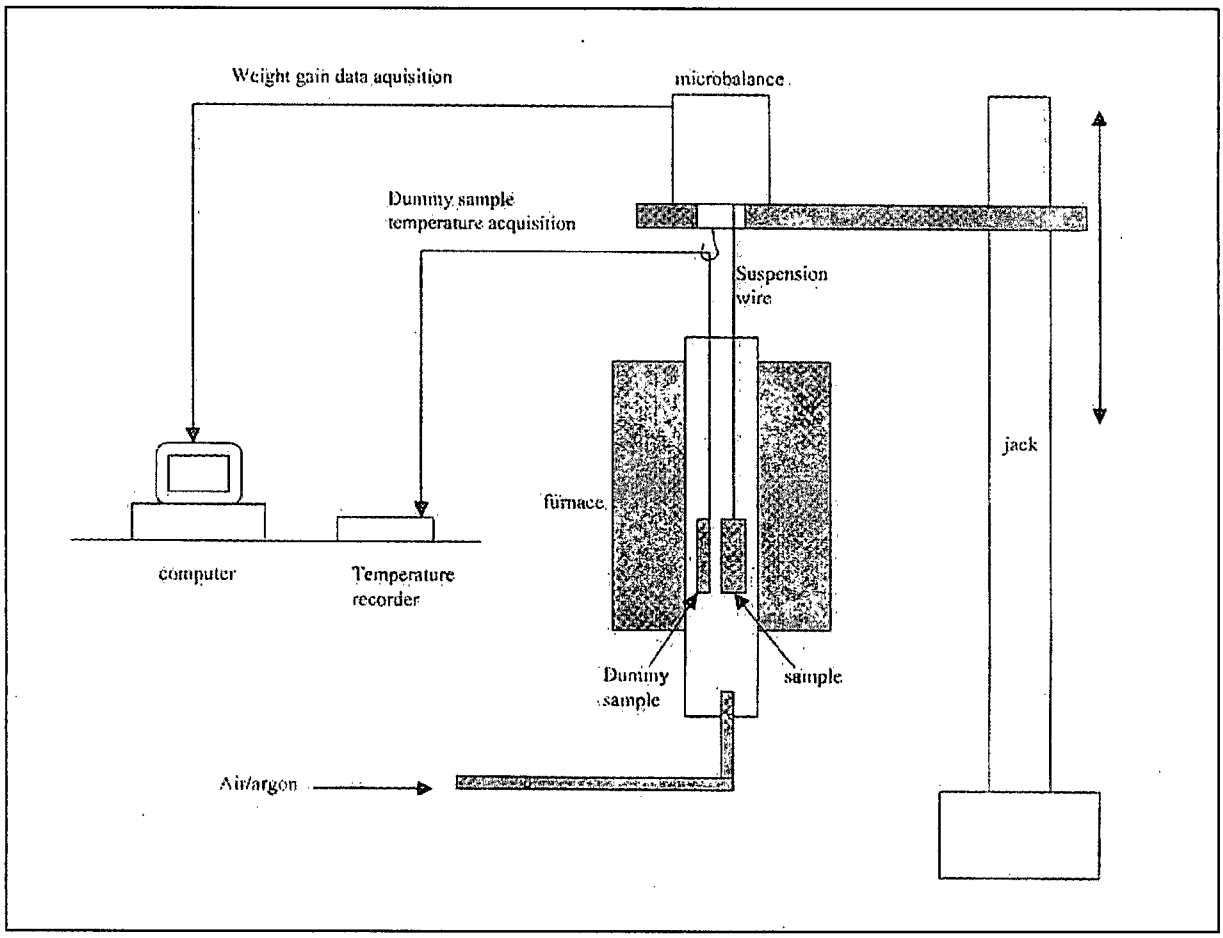

Fig. 13 Details of the experimental set-up[43]

Table I Composition of steel samples investigated							
Cu (% wt)	**C (% wt)**	**Mn (% wt)**	**S (% wt)**	**Ni (% wt)**	**Sn (% wt)**	**Al (% wt)**	**N (% wt)**
0.221	0.065	0.281	0.005	0.099	0.010	0.056	0.0036
0.393	0.065	0.307	0.006	0.098	0.010	0.035	0.0037
0.780	0.065	0.350	0.006	0.095	0.009	0.057	0.0050

grit so that the pre-exiting oxide layer was removed from the surface. The sample was then ultrasonically cleaned in acetone, dried and then lowered into the furnace chamber (that was already set at the experimental temperature) under inert argon atmosphere. The argon was kept flowing into the chamber till the sample acquired the requisite temperature (i.e. for approximately 3 minutes). Air (dried and frozen) flow was then started and the argon flow was stopped. The supply of air was maintained at the rate of 6.0 m/minute (calculated from actual flow rate). This flow speed was chosen based upon the work done by earlier workers who demonstrated that weight gain during high temperature oxidation became independent of the flow rate beyond a value corresponding to the speed of 3.0 m/minute.

Samples were oxidized at temperatures of 1000°, 1100°, 1200° and 1275°C for 5 minutes, 1/2 hr, 1 hr and 2 hrs. These temperatures were chosen as they are close to those used for heating/reheating of steel slabs prior to hot rolling. Weights were periodically recorded using the microbalance every 80 seconds. During the process, the whole system was continuously monitored for any fluctuations in temperature and the furnace was held at the appropriate temperature. After the desired time the argon flow

was restarted and air flow was put off. The sample was then raised from the hot zone and held in a cooler zone (~ 400°C) until it equilibrated. It was then removed from the furnace and sealed in a bag for future examination.

4.3 Characterization of oxides

The oxidized samples were inspected visually. Examinations of oxide surfaces were carried out under scanning electron microscope (SEM) for studying the evolution of microstructures. Energy dispersive X-Ray (EDX) analysis was performed on many of them for knowing the compositions of the microstructural constituents. X-Ray diffraction as well as X-Ray photoelectron spectroscopy (XPS) were also carried out on some of the samples in order to determine the phases present on the surfaces. Additionally, several samples were cut and their cross-sections were mounted and metallographically prepared. These were etched with 2.0% Nital and then examined under SEM for studying the development of microstructures and morphology of copper-rich precipitates at the interface.

5. Results

5.1 The Oxidation Rate Curves

The raw data allowed weight gain (mg/cm^2) to be determined as a function of oxidation time at a particular temperature. These weight gains (mg/cm^2) were plotted against time (minutes) as shown in Figs.14-16.

In general, all the weight gain ~ time curves exhibited parabolic behavior at lower temperatures, i.e. 1000°C and 1100°C (Fig. 14, 15 & 16). The parabolic nature of growth curves at these temperatures was further evidenced by plotting squares of weight gain (W^2) ~ time (t) which were straight lines for all the steels tested at 1000°C and

1100°C (Fig. 17, 18 & 19). At higher temperatures (i.e. 1200°C and 1275°C), however the growth curves for all the three steels appeared to exhibit non-parabolic behavior (Fig. 14, 15 & 16). Observing the $W^2 \sim t$ curves at these temperatures (Fig. 17, 18 & 19), it was found that they consisted of two straight lines indicating that the growth curves were still parabolic but the slopes of these curves changed to lower values after a certain time showing the evidence of reduction in the oxidation rate.

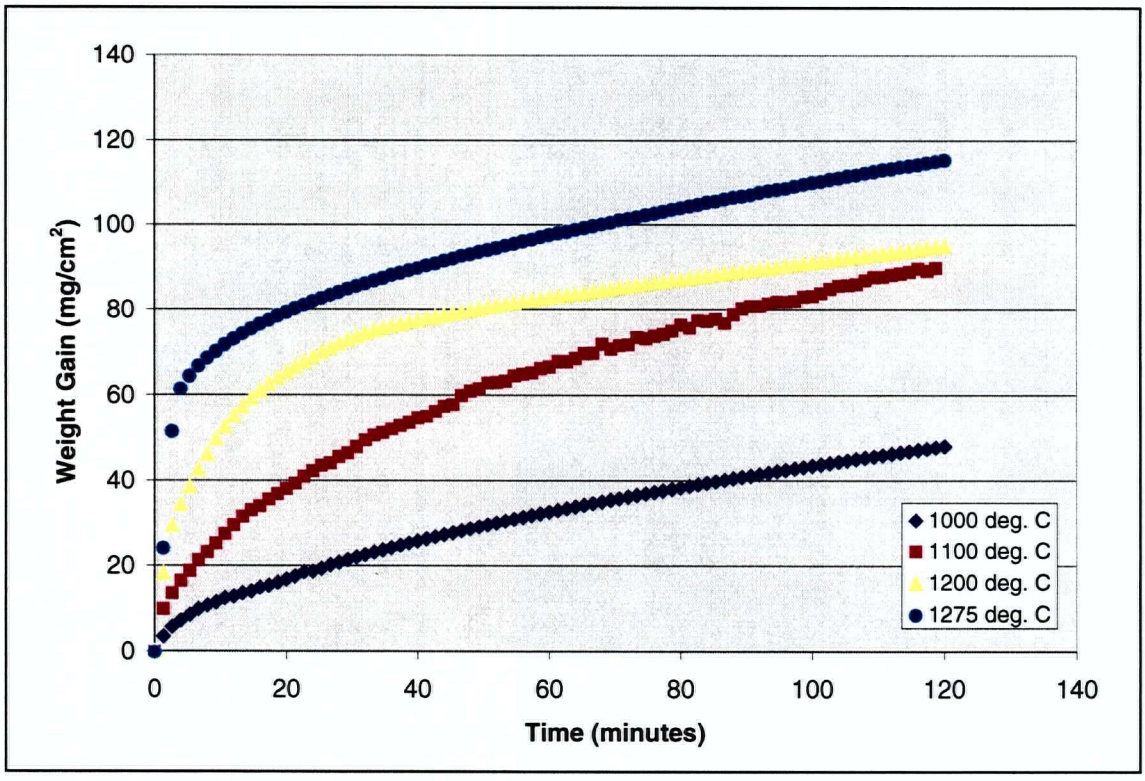

Fig. 14 Effect of Temperature on Oxide Growth for 0.22% Cu Steel

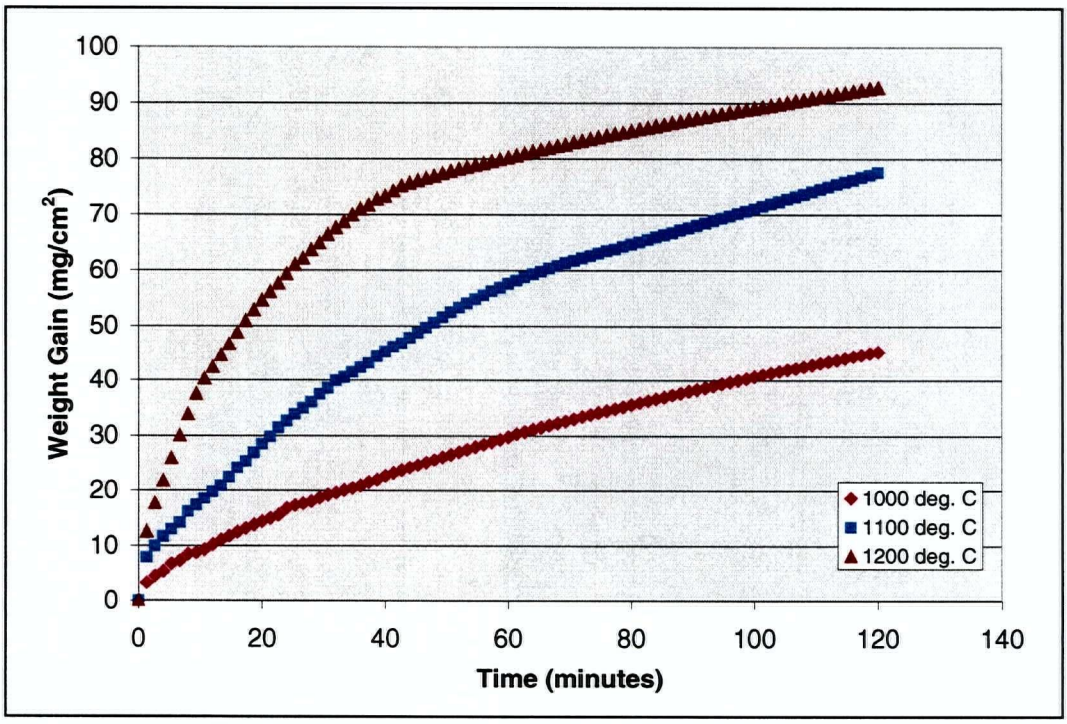

Fig. 15 Effect of Temperature on Oxide Growth for 0.39% Cu Steel

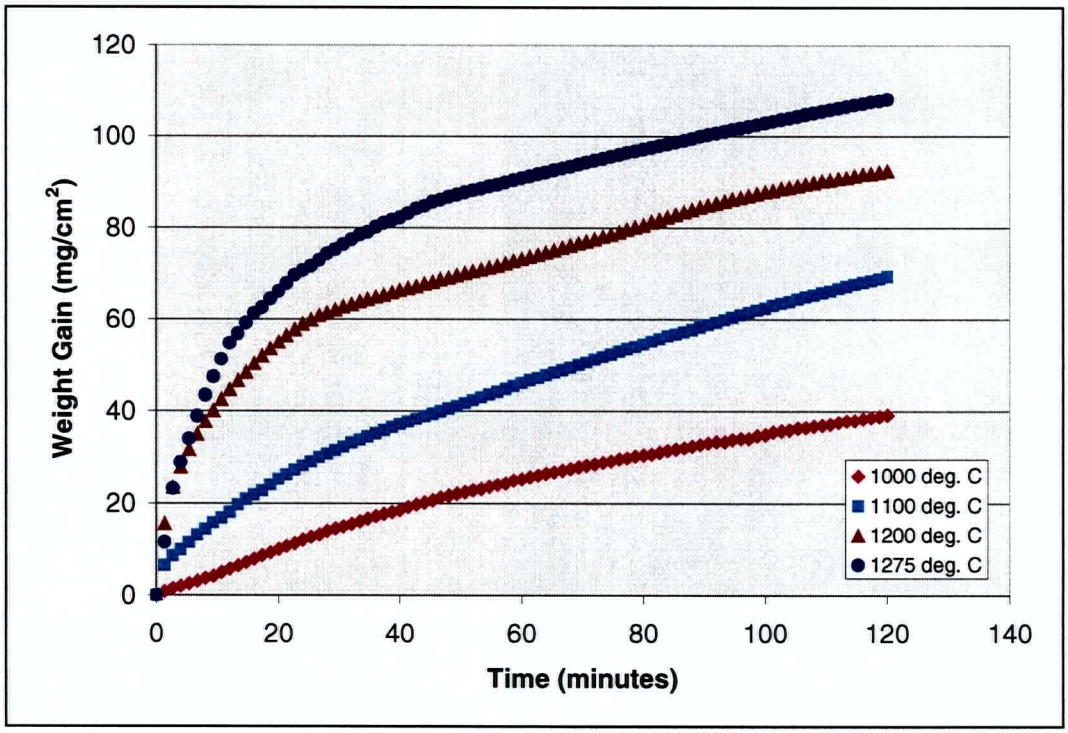

Fig. 16 Effect of Temperature on Oxide Growth for 0.78% Cu Steel

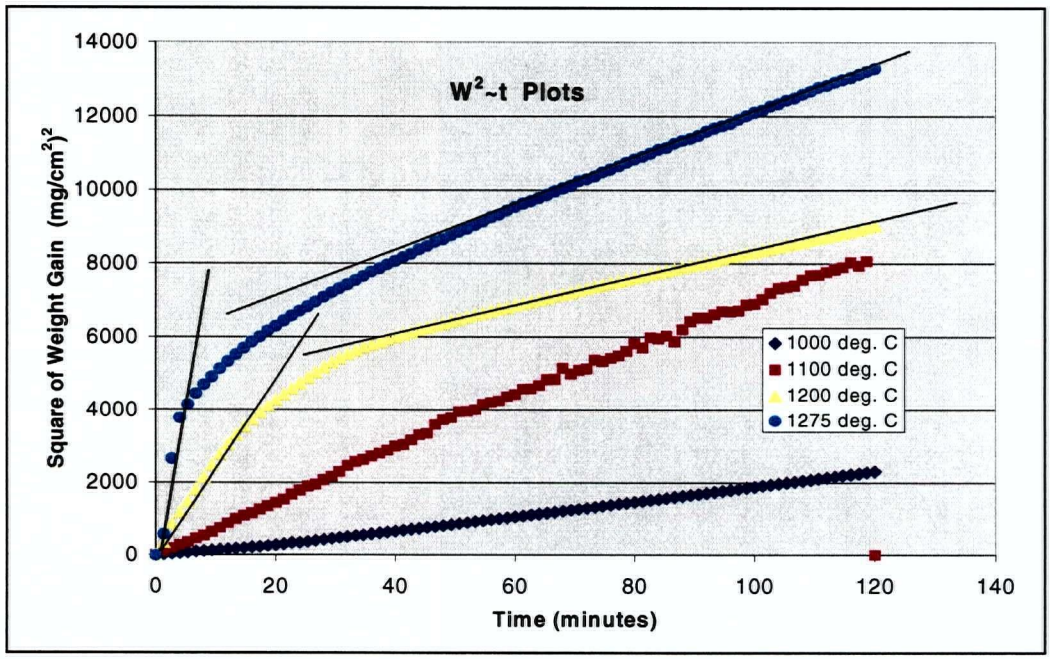

Fig. 17 Effect of Temperature on Oxide Growth for 0.22% Cu Steel

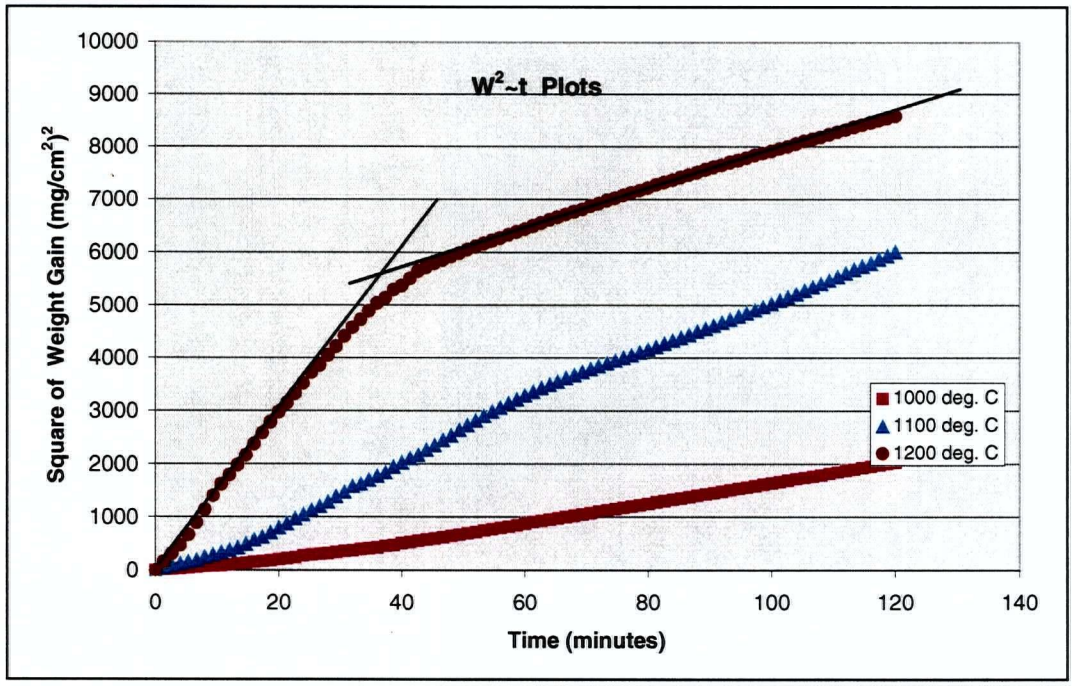

Fig. 18 Effect of Temperature on Oxide Growth for 0.39% Cu Steel

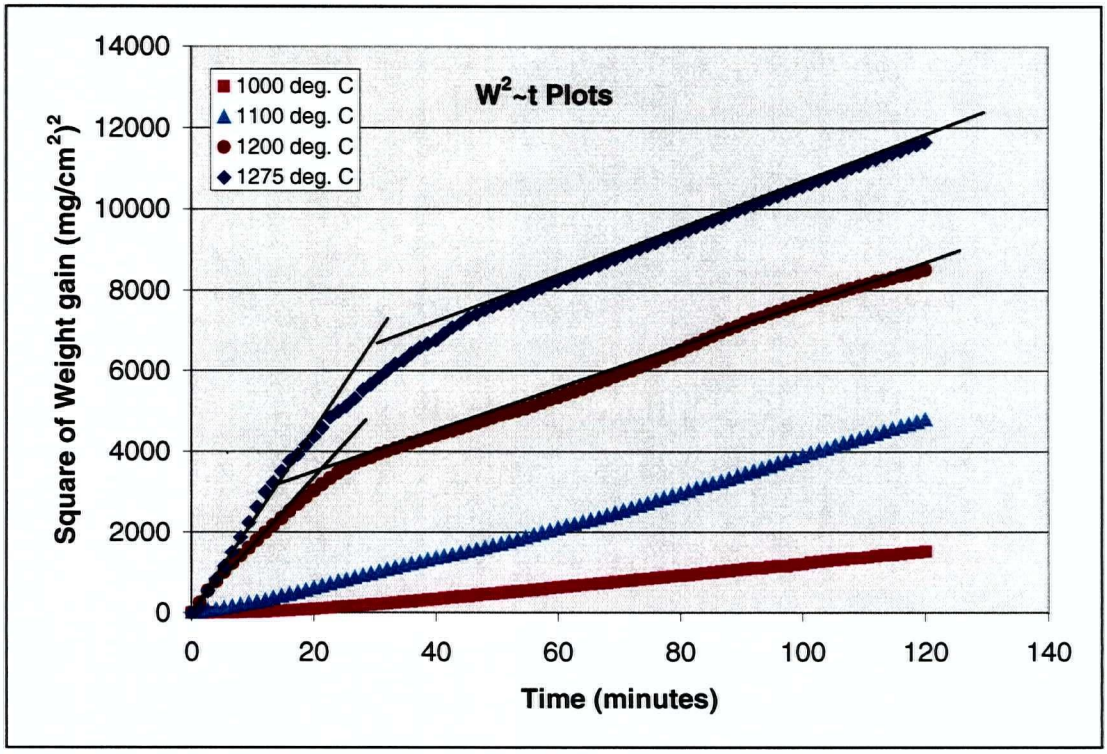

Fig. 19 Effect of Temperature on Oxide Growth for 0.78% Cu Steel

The overall effect of copper was to decrease the rate of oxidation (Fig. 20-23), the sample with the highest copper content (0.78%) showing the lowest oxidation rate. This difference was more pronounced at 1100°C than that at 1000°C (Fig. 20-21). For example, the difference in weight gain after 60 minutes between samples containing 0.22% copper steel and 0.78% copper steel was approximately 20 mg/cm^2 at 1100°C as compared to 10 mg/cm^2 at 1000°C. However, as the temperature was further increased, this difference in oxidation due to copper tended to decrease. As can be observed from Figs. 22-23, the weight gains for all copper levels became close to each other after 80 minutes at 1200°C and after 60 minutes at 1275°C.

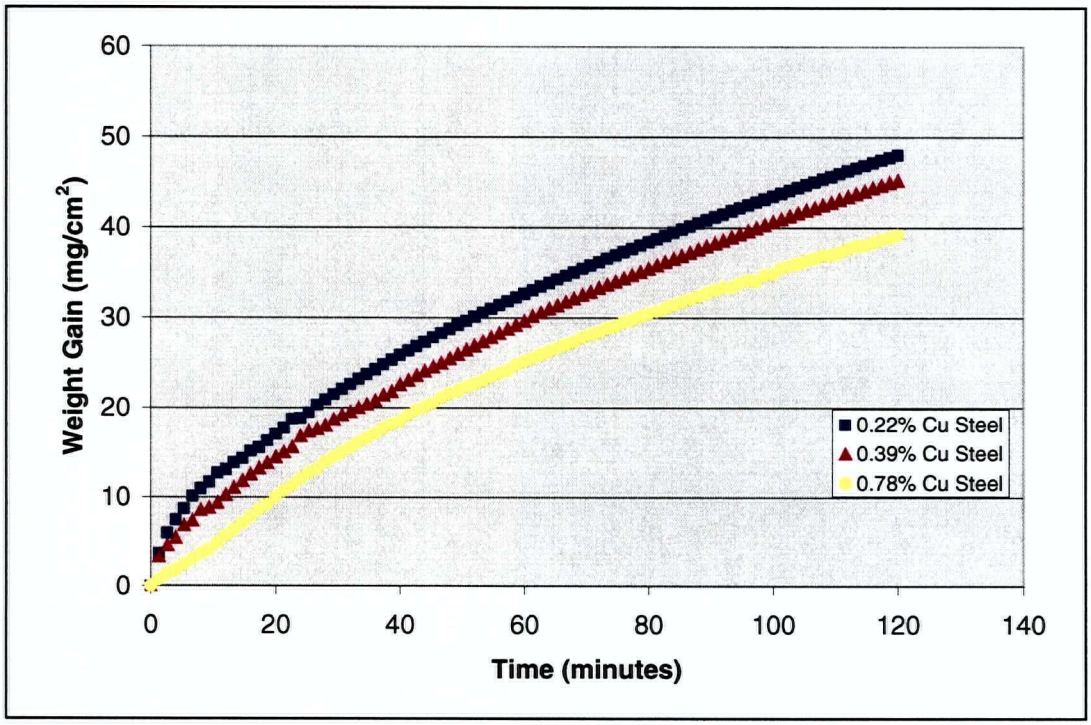

Fig. 20 Effect of Cu Content on Oxide Growth at 1000°C

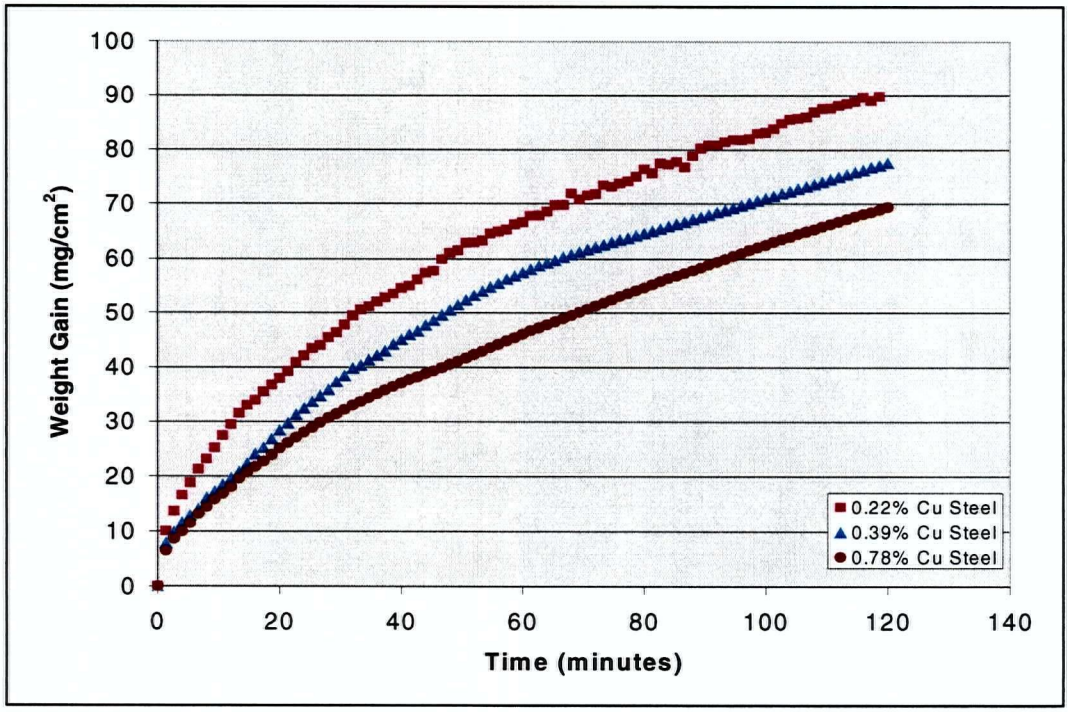

Fig. 21 Effect of Cu Content on Oxide Growth at 1100°C

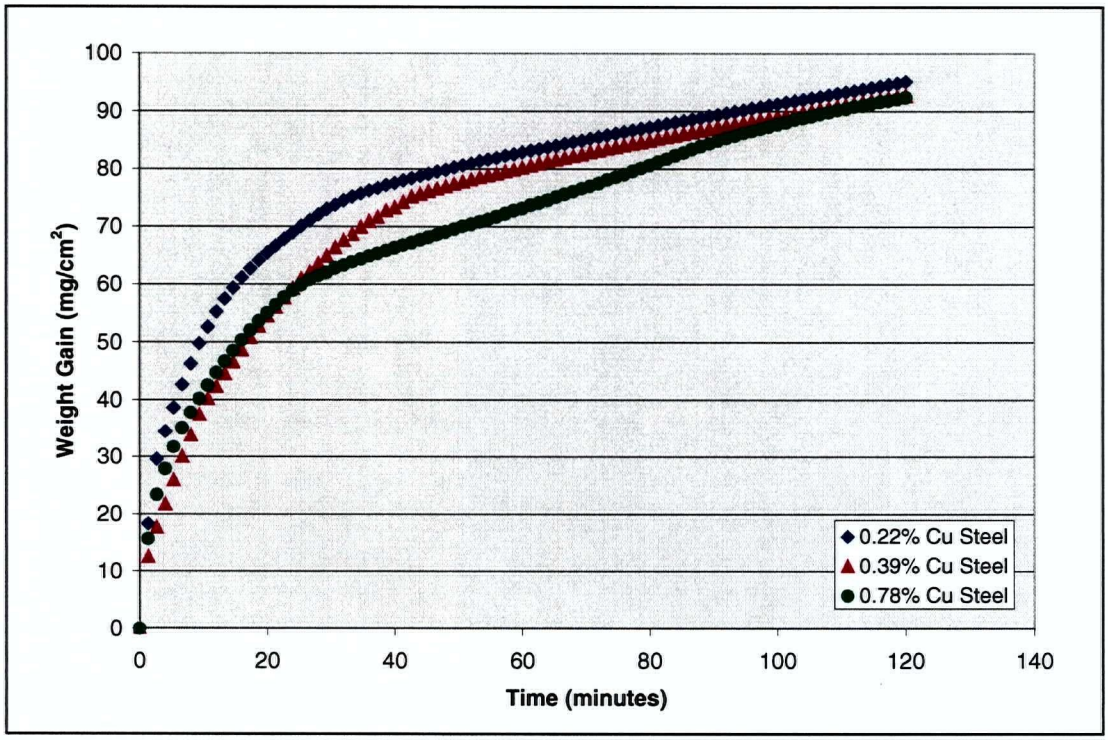

Fig. 22 Effect of Cu Content on Oxide Growth at 1200°C

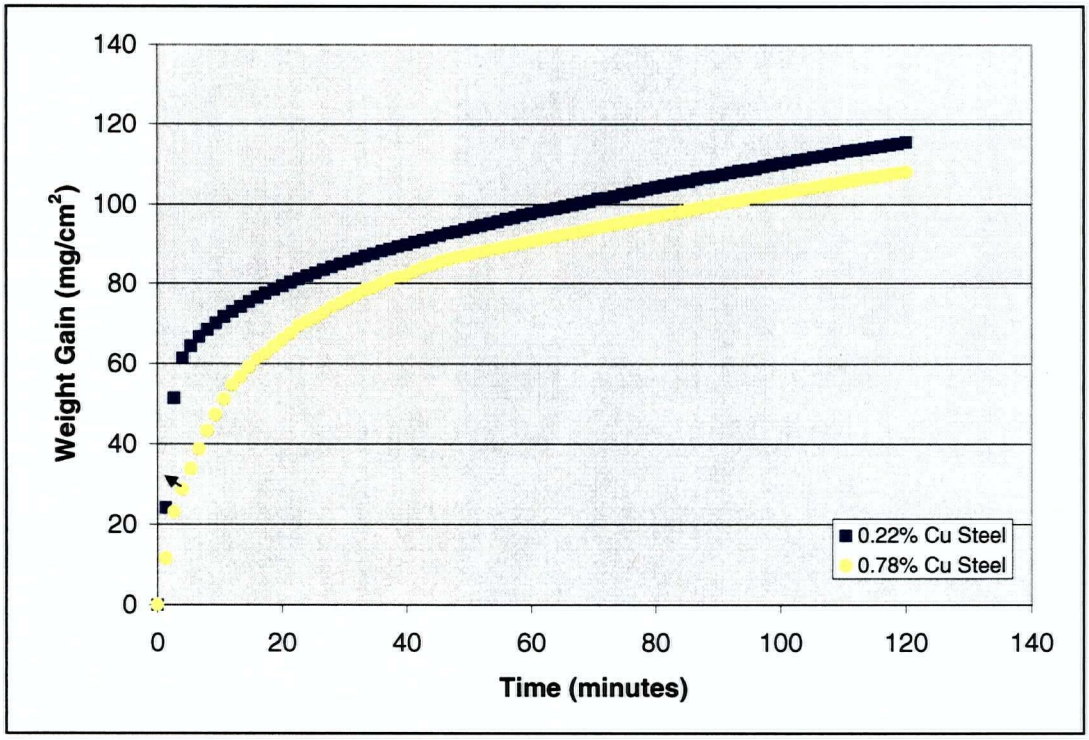

Fig. 23 Effect of Cu Content on Oxide Growth at 1275°C

5.2 Microscopic Studies

5.2.1 Surface Examination

Scale surfaces of all the specimens oxidized for times less than 2 hr. (i.e. 5 min., ½ hr. and 1 hr.) usually revealed dark as well as bright areas when inspected visually or, observed under optical microscope (Fig. 24). The bright areas were detached and lifted from the steel surface whereas the dark areas remained attached. In general, examination of such scale surfaces exhibited velvet-like appearance, particularly in the darker regions (i.e. attached to the substrate). When viewed under SEM (Fig. 25), these consisted of two regions (i) those showing nucleation and growth of oxide whiskers and (ii) those free from whiskers. Further observation at higher magnification depicted the non-uniform nature of whisker growth in regions attached to the substrate (Fig. 26). In general whiskers were 2-18 μm in length and 0.7-2.5 μm in diameter (Fig. 27).

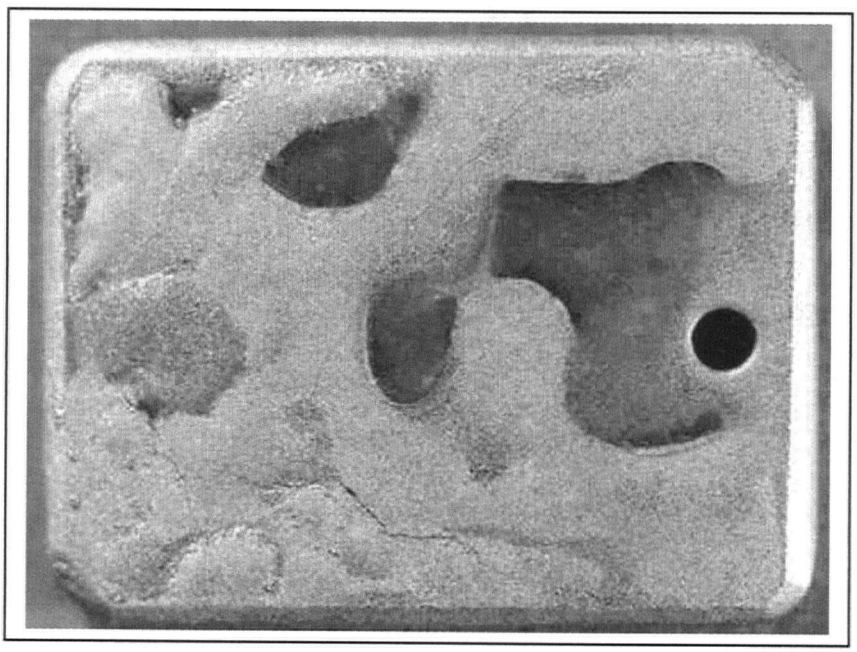

Fig. 24 A typical scale surface showing dark (attached to the substrate) and bright (lifted) regions (Optical Image - X2).

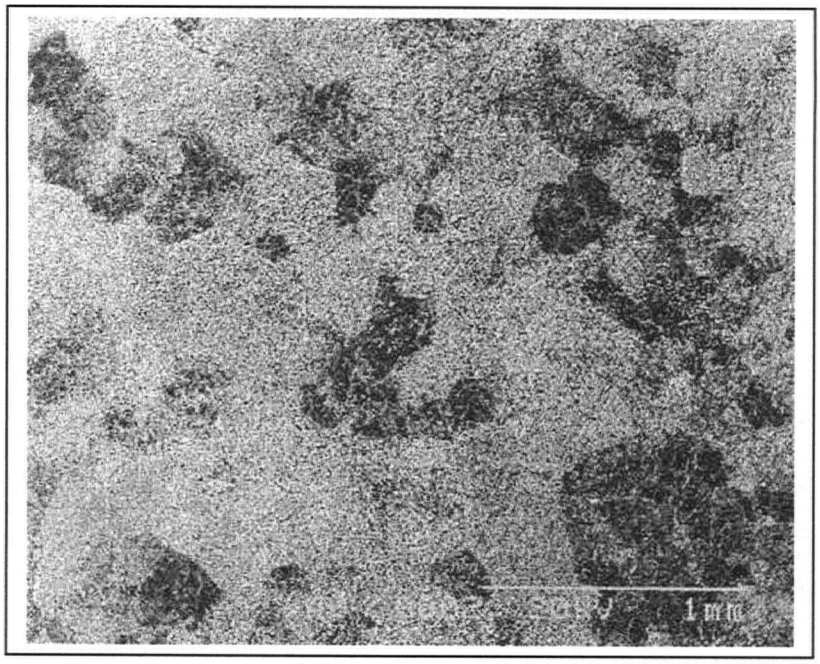

Fig. 25 Nucleation and growth of whisker blades on attached regions of scale surfaces. (SE Image - X40)

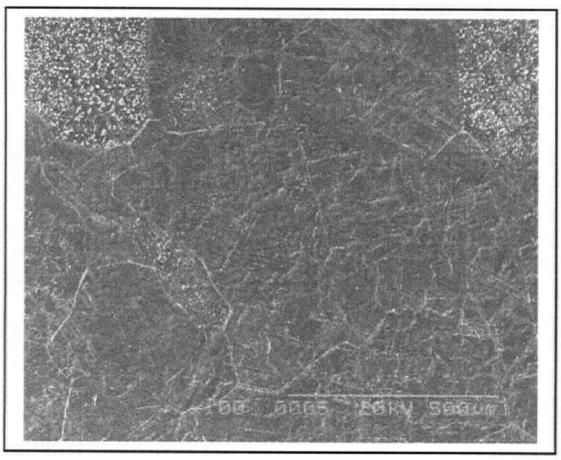

Fig. 26 Non-uniform growth of whiskers on the scale surface (SE image – X100).

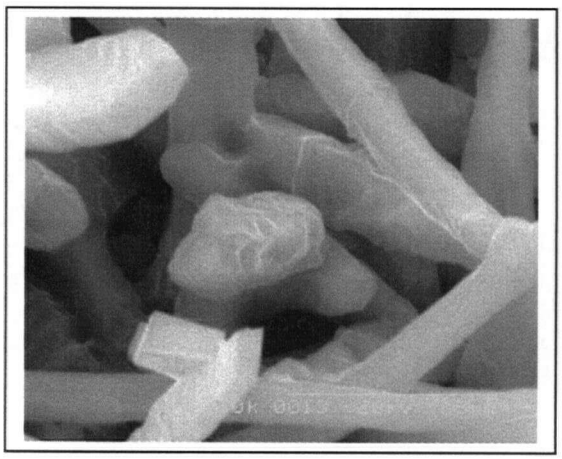

Fig. 27 Whiskers on the scale surface (SE image – X1.0k).

Observation of grains free from whiskers (Fig. 26) under higher magnification on the samples oxidized for 5 minutes (at 1200°C) exhibited formation of regions

having parallel lines with different orientations (Fig. 28), i.e. a substructure within individual grains. Fine cracks were also seen mainly along parallel ridges. However, some cracks did appear to extend across the substructures. Examination of other grains free from whiskers revealed another variant of the sub-structure within individual grains (Fig. 29).

Examination of grains showing whisker growth revealed the presence of small nuclei of blades in certain areas whereas fully developed blades were prevalent in other locations. Figure 30 shows a substructure region with large number of nuclei of whisker blades. It is clearly evident that the parallel lines were disappearing at the positions of nucleation. Moreover, ridges along substructure boundaries were also being eaten away by nucleation and growth of whiskers.

EDX analysis (Fig. 31) over the tips of these nuclei showed enrichment of Cu (28.85%); in many cases this enrichment being more that 30.0% Cu. Strong peaks of

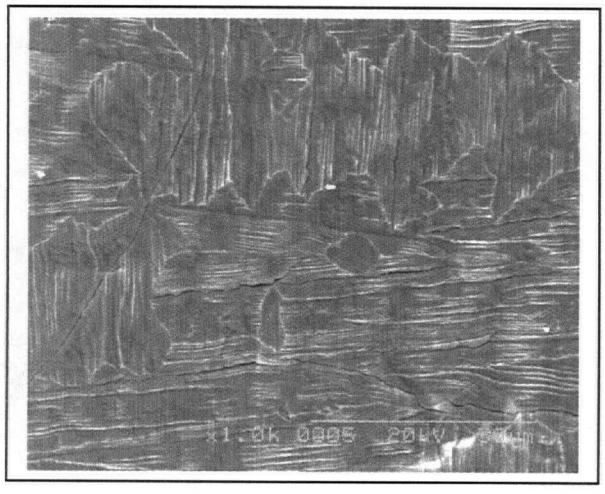

Fig. 28 Substructure formation within individual grains free from whiskers on the scale surface (SE image – X100).

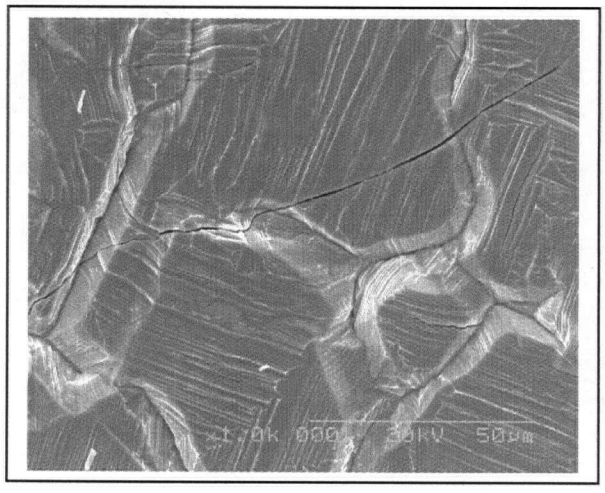

Fig. 29 Another variant of structure within grains free from whiskers on the scale surface (SE image – X1.0k).

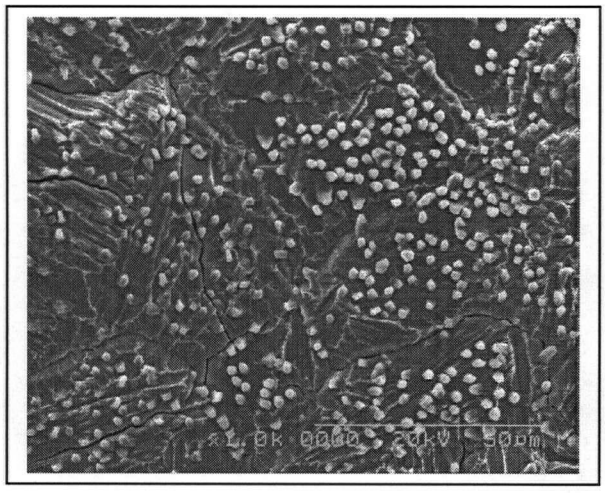

Fig. 30 Nuclei of whisker blades in the grain substructure (SE image – X100).

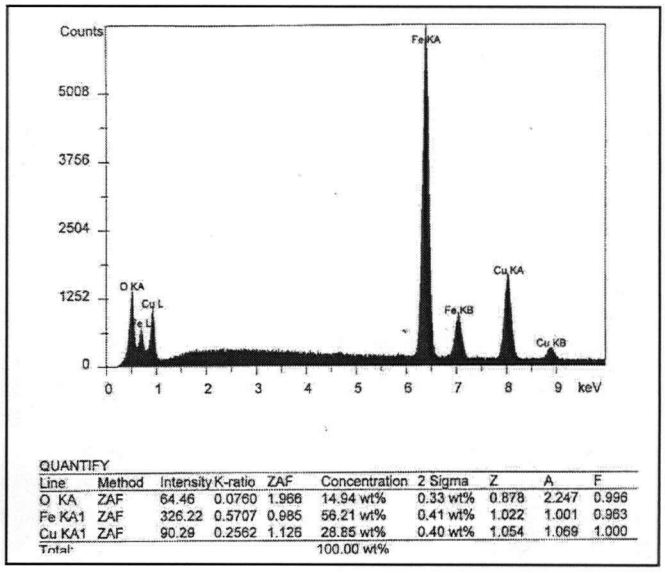

QUANTIFY

Line	Method	Intensity	K-ratio	ZAF	Concentration	2 Sigma	Z	A	F
O KA	ZAF	64.46	0.0760	1.966	14.94 wt%	0.33 wt%	0.878	2.247	0.996
Fe KA1	ZAF	326.22	0.5707	0.985	56.21 wt%	0.41 wt%	1.022	1.001	0.963
Cu KA1	ZAF	90.29	0.2562	1.126	28.85 wt%	0.40 wt%	1.054	1.069	1.000
Total:					100.00 wt%				

Fig. 31 EDX analysis at the tip of a blade nucleus showing enrichment of Cu .

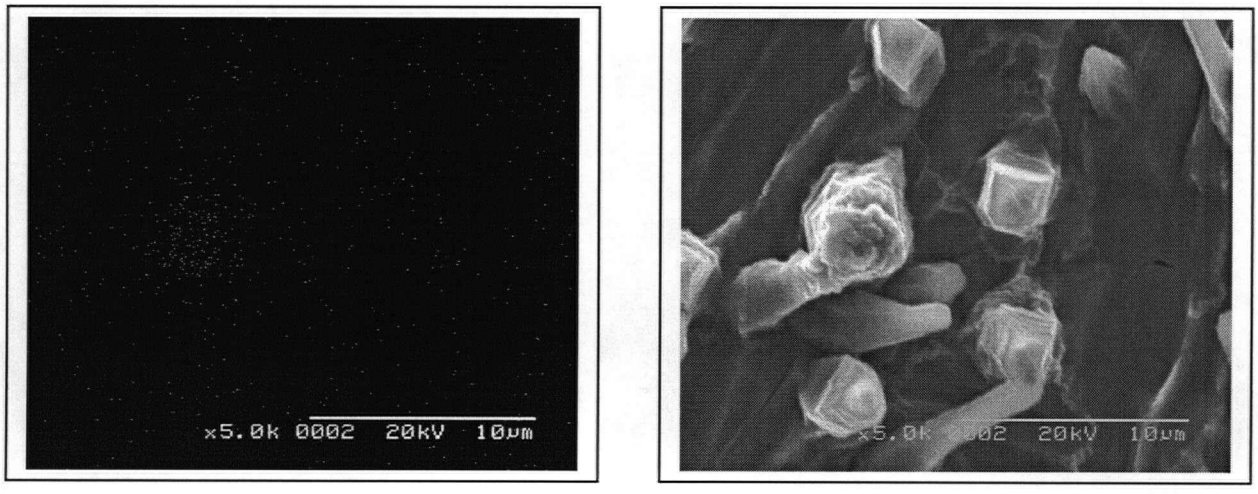

(a) **(b)**

Fig. 32 Enrichment of Cu over a region in the substructure containing nuclei of whisker blades.(a) X-Ray map of Cu (b) SE image – X5.0k).

oxygen as well as iron were also observed. X-ray mapping also revealed enrichment of Cu on these blades as shown in the Figures 32a & b.

Regions with fully developed blades were of two types, i.e. sparsely populated (Fig. 33) and densely populated (Fig. 34). The former showed blades of cross-section 1.5-2.5 μm and length 10-12.5 μm. A few shorter blades (i.e. 3-6 μm length) were also

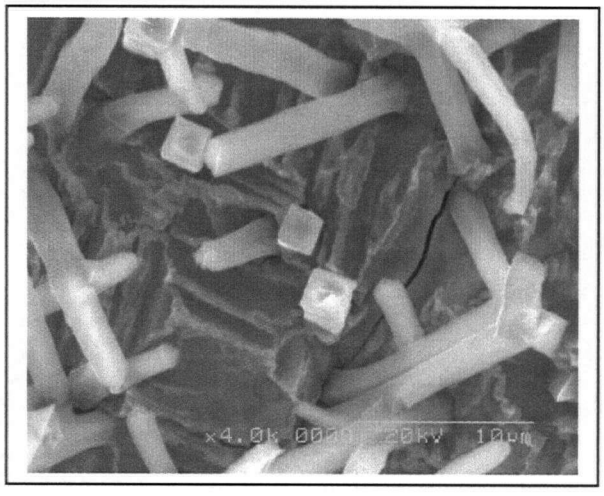

Fig. 33 Sparsely populated blades on the scale surface. (SE image – X4.0k)

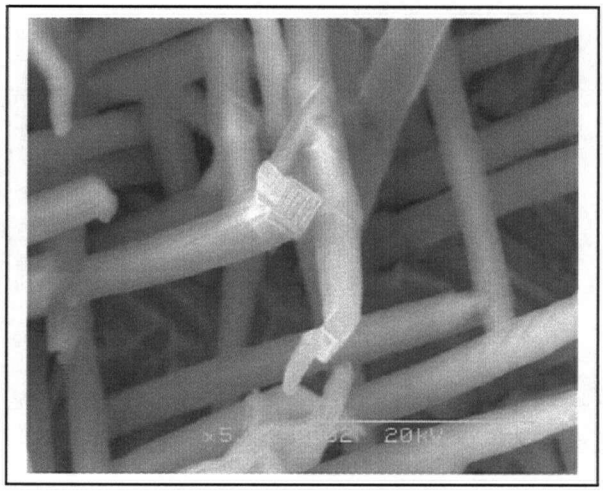

Fig. 34 Densely populated blades on the scale surface (SE image – X5.0k)

The densely populated region showed much longer blades (15-17.5 μm) which were entangled with each other (Fig. 34). However, the cross-sections remained similar to those of blades in sparsely populated regions as mentioned earlier, i.e. 1.5-2.5 μm. EDX analysis over one of these blades indicated very high enrichment (50.62%) of Cu (Fig. 35).

5.2.1.1 Effect of Cu content

Examination of surface microstructures of oxidized steels containing different Cu did not reveal any difference in the enrichment levels of Cu in the whisker blades. However, higher Cu samples revealed in general, shorter and thinner blades (Table II).

5.2.1.2 Effect of Temperature

In general, samples oxidized at lower temperatures exhibited much less adherent scale as compared to those oxidized at higher temperatures. Whisker growth also was affected by temperature. For example, whiskers were almost absent from scales formed at 1000°C except on very tiny isolated areas. Additionally, the steel sample oxidized at lower temperature (e.g. 1100 °C) showed finer and longer blades (Fig.36 & Table III).

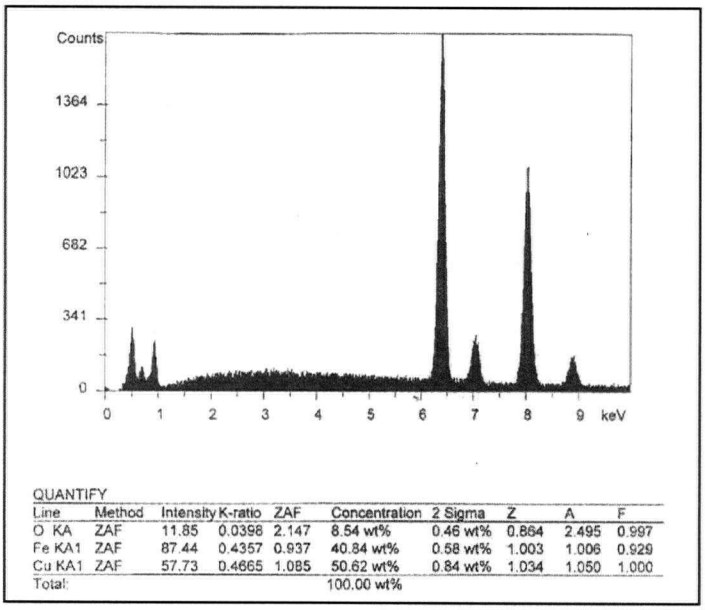

Fig. 35 Result of EDX analysis over the tip of a blade in the centre of Fig. 34.

Table II Effect of Cu content on whisker growth (5 minutes at 1200°C)

Wt % Cu	Nuclei dia. (μm)	Blade length (μm)	Blade dia. (μm)	
			Base	Tip
0.22	1.5-2.5	10.0-17.5	1.5-2.5	
0.39	1.0-1.5	4.0-8.0	1.0-1.5	0.6-0.8
0.78	0.7-1.0	2.0-4.0	0.7-1.0	0.4-0.6

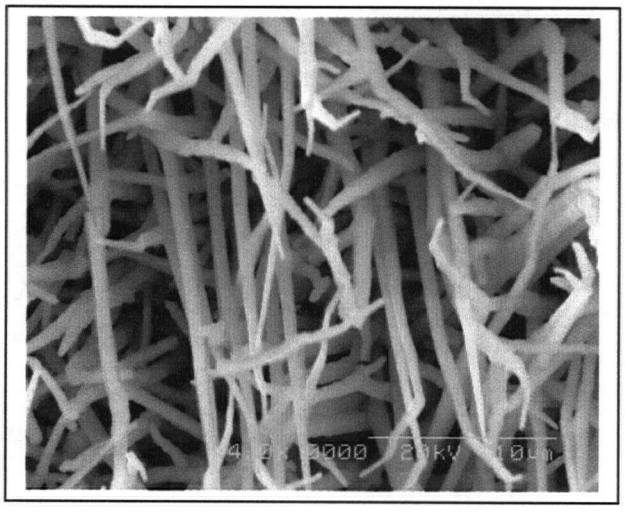

Fig. 36 Finer and longer whisker blades at lower temperature (0.39% Cu oxidized at 1100°C for 5 minutes)
SE image (X4.0k).

Table III Effect of temperature on whisker growth (0.39% Cu; 5 minutes at the given temperature))			
Temperature (°C)	**Blade length (μm)**	**Blade dia. (μm)**	
		Base	**Tip**
1100	12.0-17.0	0.7-1.0	0.25
1200	4.0-8.0	1.0-1.5	0.6-0.8

5.2.1.3 Effect of Oxidation Time

There was no effect of time as such on the enrichment of copper in the whisker blades. The dimensions of the blades also remained unchanged except that the tips of majority of blades got blunted and thickened with the passage of time (Fig. 37 and

Table IV). Additionally, the oxide scale tended to get detached from the metal substrate with time.

Table IV Effect of oxidation time on whisker growth (0.39% Cu at 1100°C)			
Oxidation time (minutes)	**Blade length (μm)**	**Blade dia. (μm)**	
		Base	**Tip**
5	12.0-17.0	0.7-1.0	0.25
60	12.0-17.0	1.0	0.25-0.5

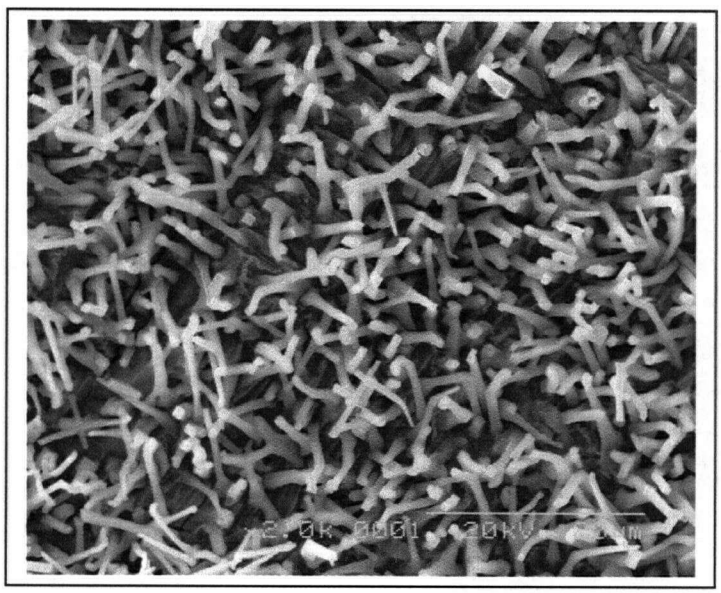

Fig. 37 Blunting and thickening of whisker blades on scales formed after longer oxidation time (0.39% Cu, 1 hour at 1100°C).

5.2.1.4 Effect of Oxide-Metal Adherence

In general, the oxide was largely adherent to the metals surface initially for all the copper levels and all the temperatures studied. This was evident by larger areas of

whisker growth during the initial stages of oxidation. However, with the passage of time, the scale became detached from the metal surface as mentioned earlier. This detachment of the scale was invariably followed by formation of new scale underneath and its subsequent growth. Also, the detachment of the scale occurred after longer times for samples containing higher copper content. For example, the scale was completely detached in the sample with 0.22% Cu steel oxidized at 1100°C when observed after 30 minutes whereas that in 0.78% Cu steel, it remained attached even after 1 hour.

As mentioned previously, all the samples oxidized for times less than 2 hr. at 1100°C and above revealed two different zones (i) those having adherent oxide layer and (ii) those showing detached scale. Almost invariably, these two regions existed side by side with each other on the oxide surface (Fig. 38a & b). It is clear from the surface relief features in these two micrographs that the growth of existing oxide layer somehow stopped in the regions of detachment. This is clearer from Figure. 38c which is showing the two regions at a slightly higher magnification as well as Figure 38d that is depicting the transition region at a much higher magnification. Figure 38e shows the detailed microstructure in the center of the detached region of the scale in Figure 38c. Very similar structure was also observed on the surface of scale formed at 1000°C. It can be noticed from Figures 38d and 38e that whisker blades collapsed slowly on the scale surface after scale detachment and their relief features at the boundaries became faint and disappeared with the passage of time.

At other locations of detachment but side by side with adhered regions, different stages/ features of scale growth were observed (Fig. 39a & b). Surface microstructures on samples oxidized for 2 hours or more invariably showed features like those in

Figures 38e, 39a and 39b. No whisker growth was observed on the surfaces of their scales.

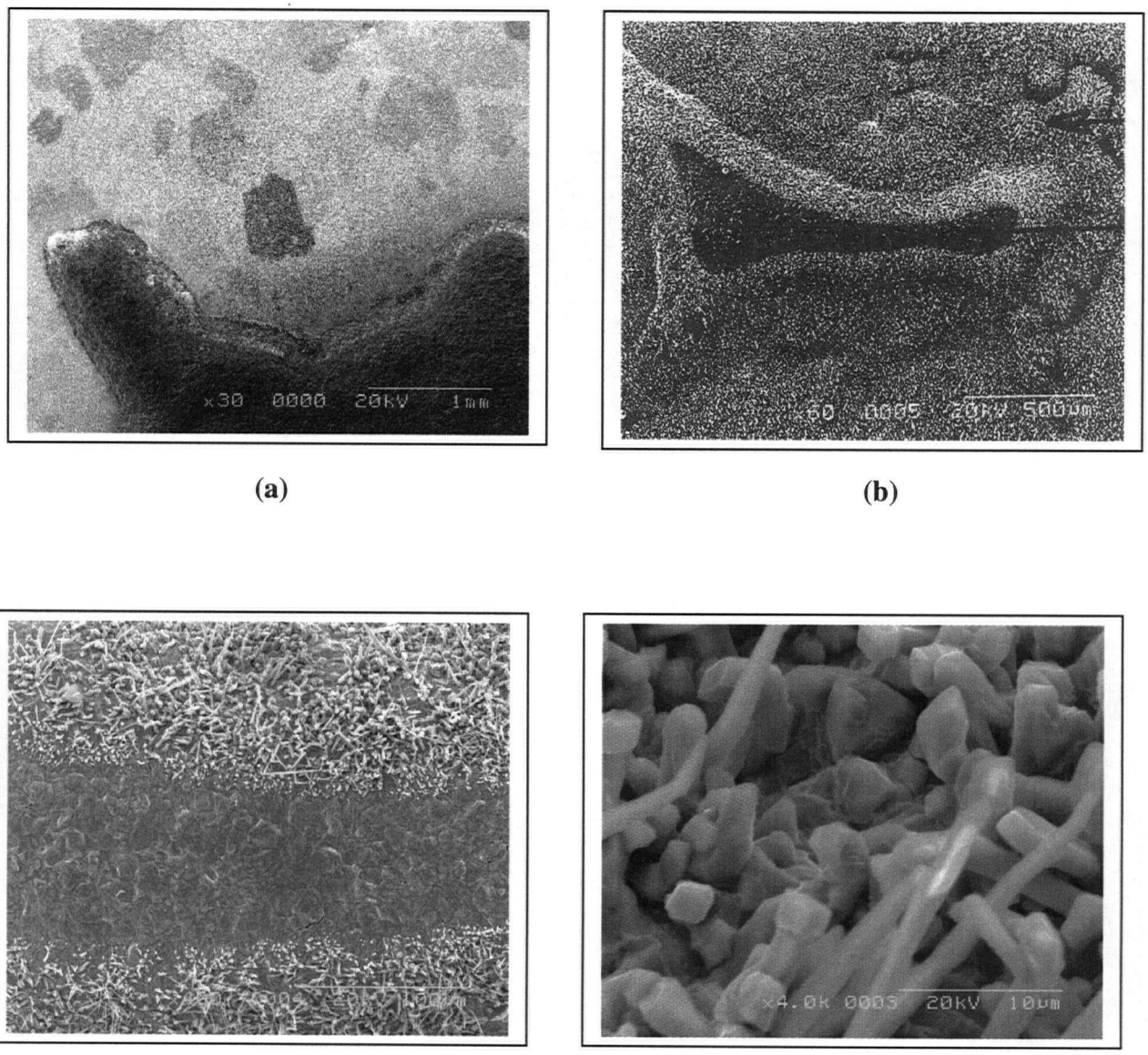

(a) (b)

(c) (d)

Fig. 38 Detached and adhered regions on the scale surface (a) 0.39% Cu oxidized at 1100°C for 30 minutes (SE image – X30). (b) 0.39% Cu oxidized at 1100°C for 5 minutes (SE image – X60). (c) Two regions in the centre of (b) shown at a higher magnification (SE image –X400). (d) Transition region in the centre of (c) at a still higher magnification (SE image – X4.0k). (e) on the next page.

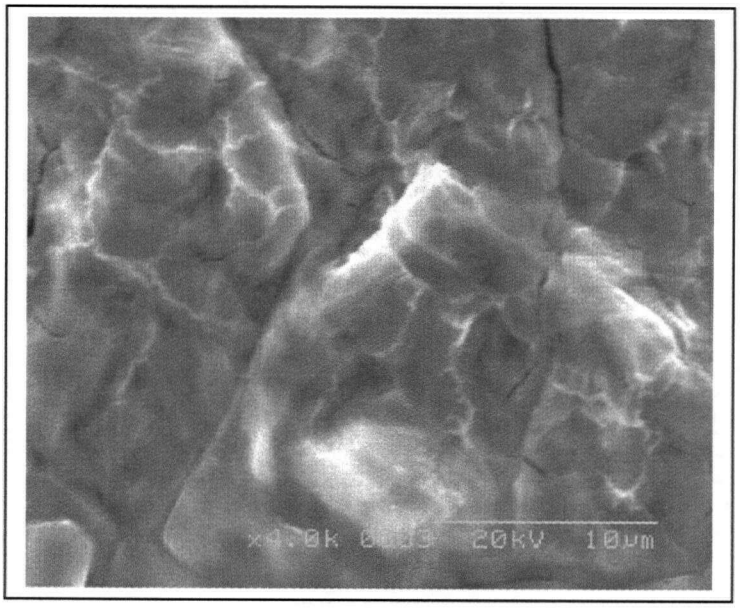

Fig. 38e Microstructure in the centre of the detached region in (c) formed possibly due to collapsed whisker blades (SE image – 4.0k).

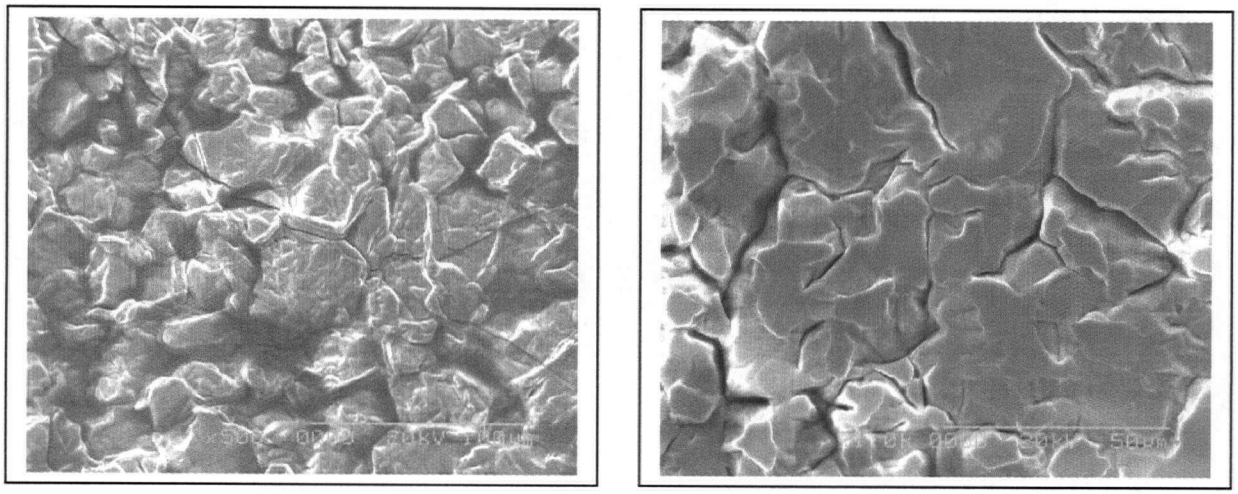

Fig. 39 Different features of scale microstructures formed on detached regions of scales of samples oxidized for times longer than 5 minutes (a) (SE image – X500). (b) (SE image – X1.0k).

5.2.2 Cross-sectional Examination

Examination of cross-sections of the original specimens revealed equi-axed grains of ferrite (Fig. 40). EDX analysis over the grain boundaries as well as inside grains revealed that copper content in the areas within the grains was more or, less matching with the general composition of the alloy. For example, locations within the grains had copper content of 0.64 - 0.90% for the steel with 0.78% Cu. On the other hand, the grain boundaries showed marginally higher Cu levels. For example, in the sample with 0.78% Cu, the grain boundaries indicated 0.90 - 1.10% of Cu. However, Cu content in very few isolated locations on the grain boundaries was 1.2-1.8% Cu. Additionally, no non-uniformity along the cross section as well as on the surface of the steel samples was observed. This means that copper was in general uniformly distributed as solid solution in the alloy and only the grain boundaries were marginally enriched.

5.2.2.1 Oxidized Samples of 0.22% Steel

Examining the microstructures of 0.22% Cu steel oxidized at 1000°C for 5 minutes revealed enrichment of copper along grain boundaries near the surface (Fig. 41). Additionally, copper was also enriched within the grains along the surface. EDX analysis over these enriched grain boundaries showed copper content of ≈2.6%. The depth at which copper enrichment was observed was in general 8-12 μm from the surface.

Increasing the time of oxidation to 2 hours caused a large number of grain boundaries near the surface to be enriched continuously with copper (Fig. 42). Additionally, some of the interior grain boundaries below the surface were also

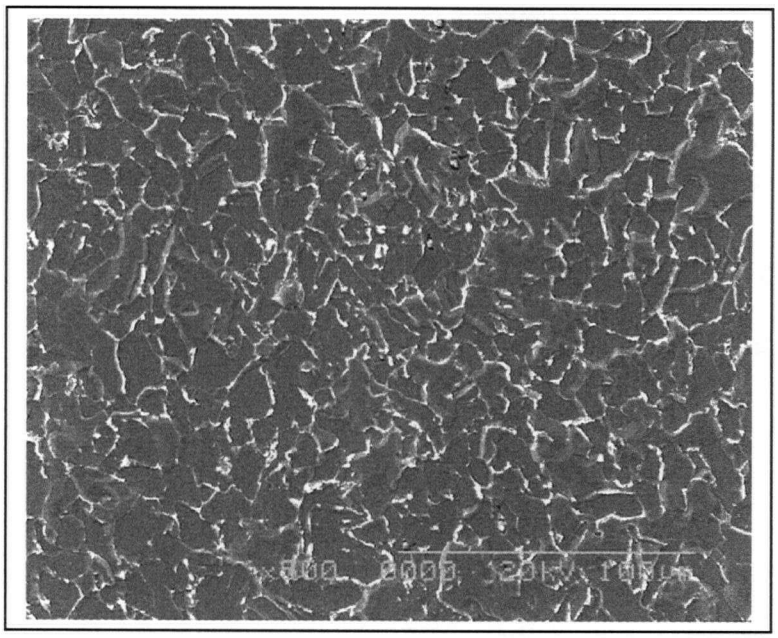

Fig. 40 Equi-axed grains of ferrite in the cross-section of a test specimen (0.39% Cu) (SE Image - X500).

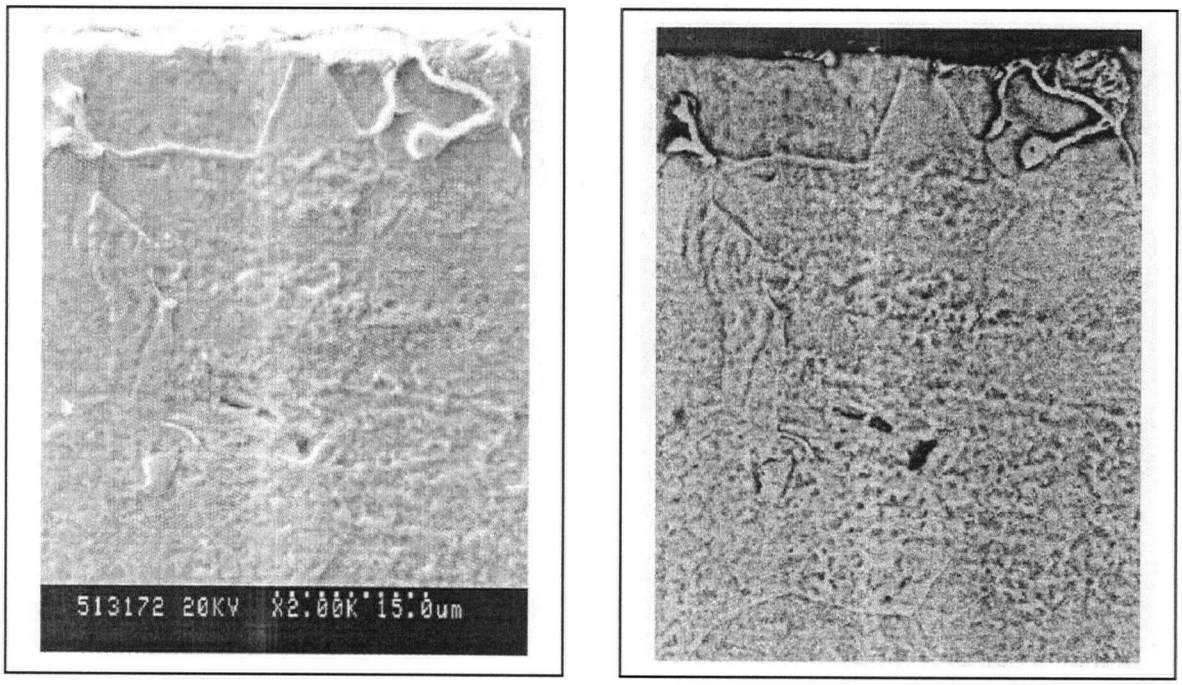

Fig. 41 Cross-section of 0.22% Cu steel oxidized at 1000°C for 5 minutes showing enrichment of Cu along grain boundaries close to the surface (a) SE image (X2.0k). (b) BS image (X2.0k).

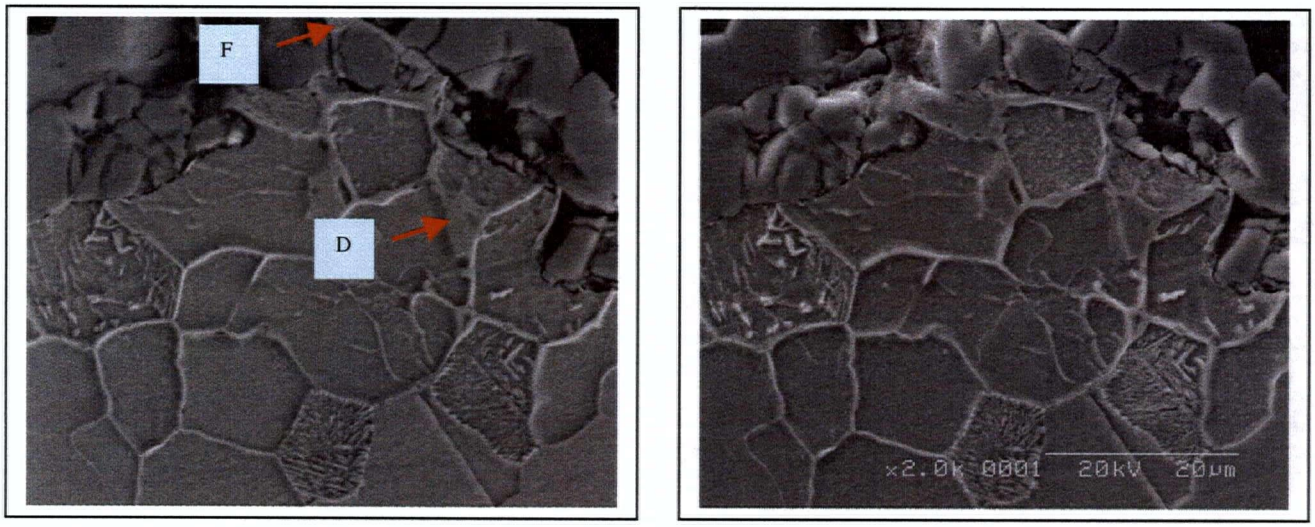

(a) (b)

Fig. 42 Microstructure of the cross-section of 0.22% Cu steel oxidized at 1000°C for 2 hours showing continuous enrichment of Cu along grain boundaries near the surface (a) BS image (X 1.0k) (b) SE image (X 1.0k).

enriched. Copper enrichment was also noticed along certain preferred planes and directions in the interior of some of the near-surface as well as sub-surface grains (Fig. 42). Some of the enriched regions near the surface appeared to be blocky (massive), e.g. region such as D (Fig. 42). The copper enrichment was found to be 5-10% on grain boundaries depending upon distance from the surface, near surface regions showing higher levels. The blocky region showed ~8.5% Cu whereas those embedded in the oxide (region F) showed very high level (e.g. 76.49% Cu) as shown in the EDX spectrum in Figure 43. The enriched region embedded in the oxide also showed the presence of oxygen (3.95%). In addition, other elements such as Si, Sn and Ni were also present increasingly more near the surface. However, there was no continuous film or, enriched layer at the surface of the steel observed as shown in the figures discussed

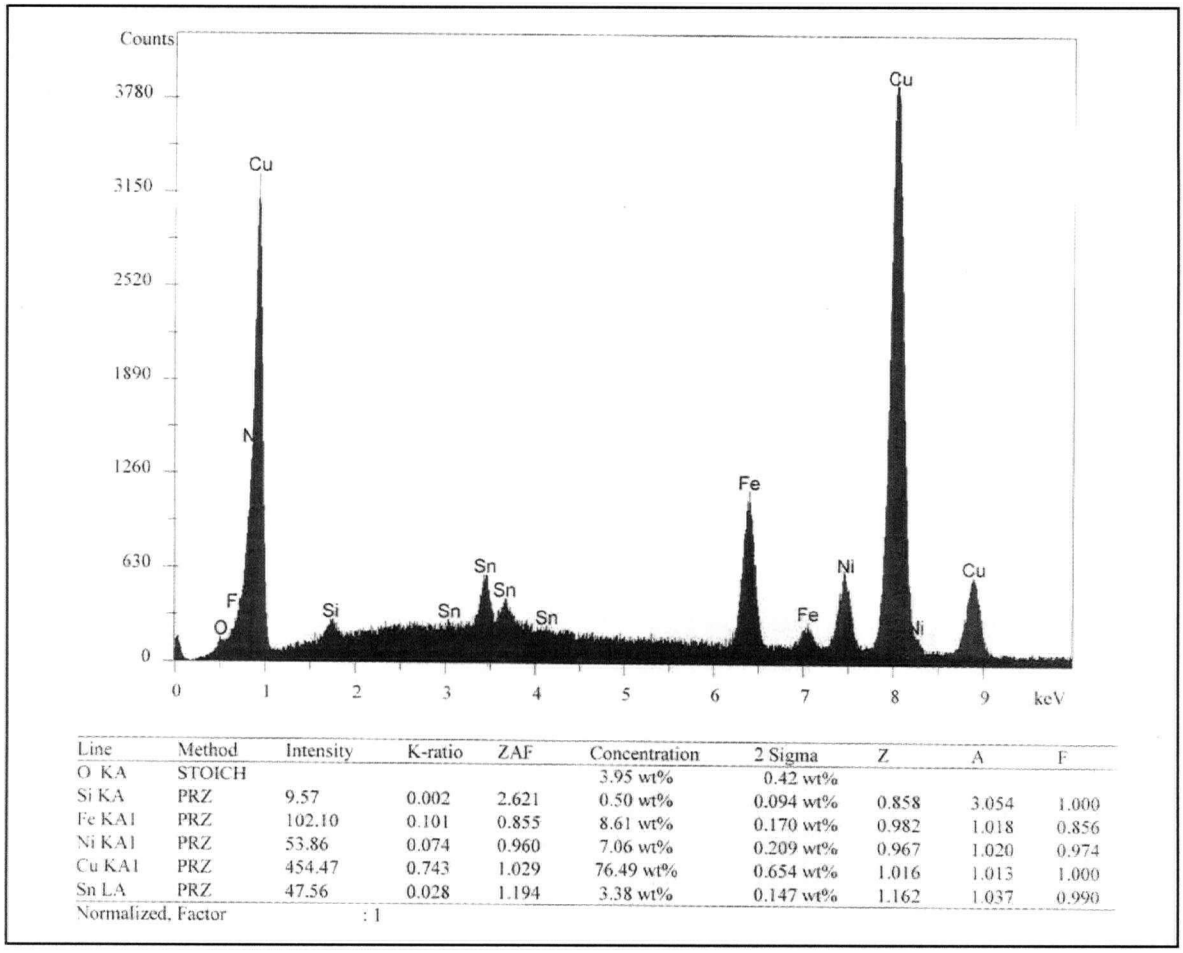

Line	Method	Intensity	K-ratio	ZAF	Concentration	2 Sigma	Z	A	F
O KA	STOICH				3.95 wt%	0.42 wt%			
Si KA	PRZ	9.57	0.002	2.621	0.50 wt%	0.094 wt%	0.858	3.054	1.000
Fe KA1	PRZ	102.10	0.101	0.855	8.61 wt%	0.170 wt%	0.982	1.018	0.856
Ni KA1	PRZ	53.86	0.074	0.960	7.06 wt%	0.209 wt%	0.967	1.020	0.974
Cu KA1	PRZ	454.47	0.743	1.029	76.49 wt%	0.654 wt%	1.016	1.013	1.000
Sn LA	PRZ	47.56	0.028	1.194	3.38 wt%	0.147 wt%	1.162	1.037	0.990
Normalized, Factor			: 1						

Fig. 43 Result of EDX analysis over blocky regions embedded in the scale showing high Cu-enrichment (0.22% Cu steel oxidized at 1000°C for 2 hours).

above. What appeared were discontinuous, isolated enriched regions (~69.36% Cu max.) at the surface (Fig. 44).

Increasing the oxidation temperature to 1100°C (5 minutes) showed more pronounced grain boundary enrichment near the surface clearly. An extremely thin (< 1.0 μm) layer of Cu-enrichment (pointed by an arrow) was clearly visible on the specimen surface (Fig. 45). Increasing the oxidation time at 1100°C to 2 hours caused further enrichment of copper along grain boundaries both near the surface as well as in the substrate region.

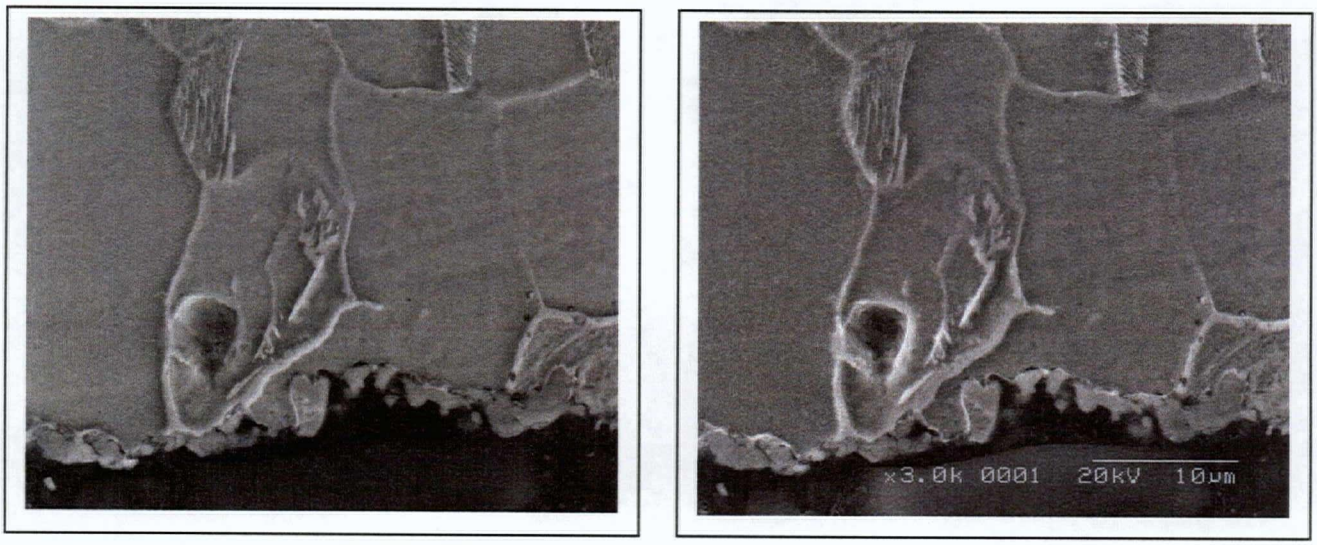

(a) (b)

Fig. 44 Microstructure in the cross-section of 0.22% Cu steel oxidized at 1000°C for 2 hours showing discontinuous isolated regions (at the surface) enriched with Cu (a) BS image (X 3.0k) (b) SE image (X 3.0k).

(a) (b)

Fig. 45 Microstructure in the cross-section of 0.22% Cu steel oxidized at 1100°C for 5 minutes showing pronounced grain boundary enrichment (near the surface) with Cu (a) BS image (X 3.5k) (b) SE image (X 3.5k).

The enriched layer (~1.0 μm thick) at the surface (Fig. 46) showed considerable amount of Cu (i.e. 85.85% Cu – in region G). Massive (blocky) regions also appeared more frequently and also with larger size and enrichment, e.g. 7.72-11.22% Cu. Enriched grain boundaries below the surface (A, B, C & F) had varying amounts of Cu, i.e. 5.96%-66.37% depending upon the distance from the surface. Examining the enriched grain boundaries regions below the surface at higher magnification (Fig. 47) again revealed preferential enrichment along certain directions and locations.

Additionally, there were locations near the surface (Fig. 48) devoid of surface enrichment but accompanied by very high levels of Cu enrichment (75.40-79.75%) at the grain boundaries (regions C and D). The areas within the grains also exhibited high levels of Cu enrichment (A - 16.39%; B - 9.43%). Moreover, a large number of internally oxidized particles some of them enriched with Cu were also seen (Fig. 46- 48) near the oxide metal interface.

5.2.2.2 Oxidized Samples of 0.39% Steel

Increasing the copper content to 0.39% and oxidizing for 2 hours at 1000°C caused again appearance of discontinuous regions of copper enrichment on the surface in addition to enrichment along grain boundaries as well as within the grains (Fig. 49). Comparing this photomicrograph with those for 0.22% Cu steel (Fig. 42-44) oxidized for 2 hours at 1000°C, it was found that enrichment levels were greater and some of the enriched massive regions appeared near the surface (region B). Enriched zones with grains near the surface also appeared separated by pores. Highest enrichment recorded at the surface was 85.03% Cu, however, majority areas were showing Cu levels of 71.0-75.0%.

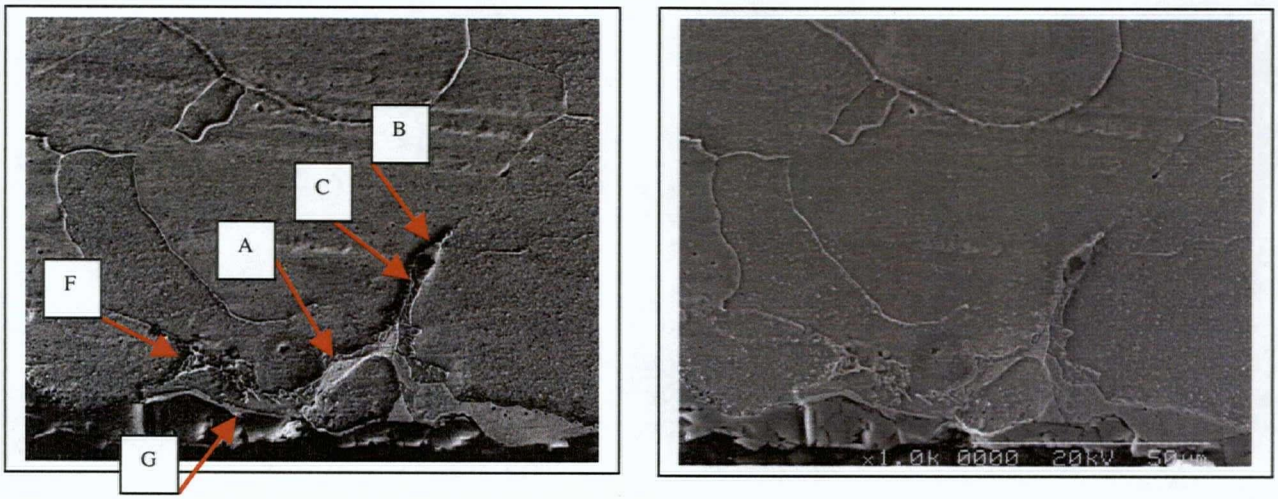

(a) (b)

Fig. 46 Microstructure in the cross-section of 0.22% Cu steel oxidized at 1100°C for 2 hours showing more or less continuous layer enriched with Cu (a) BS image (X 1.0k) (b) SE image (X 1.0k).

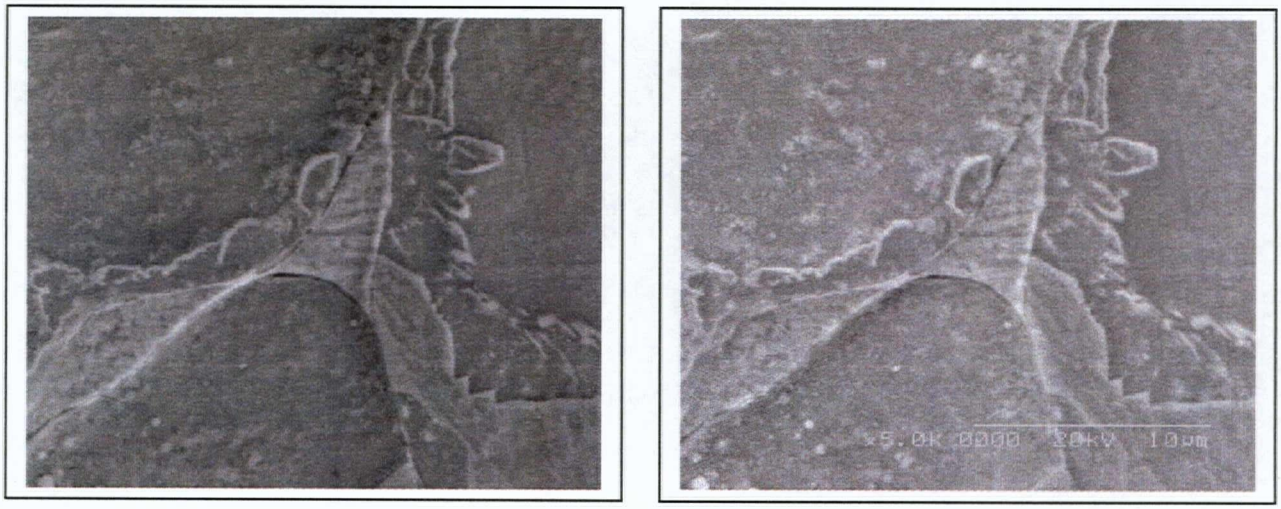

(a) (b)

Fig. 47 Microstructure in the cross-section of 0.22% Cu steel oxidized at 1100°C for 2 hours showing Cu-enriched grain boundaries (region A of Figure 46) in the subsurface region (a) BS image (X 5.0k) (b) SE image (X 5.0k).

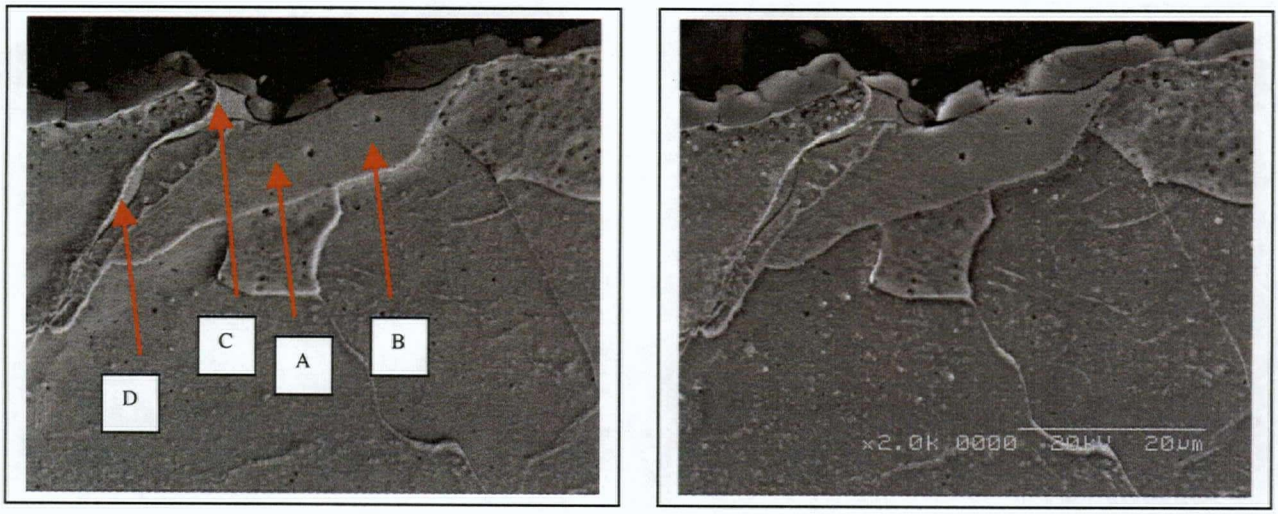

(a) (b)

Fig. 48 Microstructure in the cross-section of 0.22% Cu steel oxidized at 1100°C for 2 hours showing regions devoid of surface enrichment but accompanied by high levels of Cu along grain boundaries .
(a) BS image (X 2.0k) (b) SE image (X 2.0k).

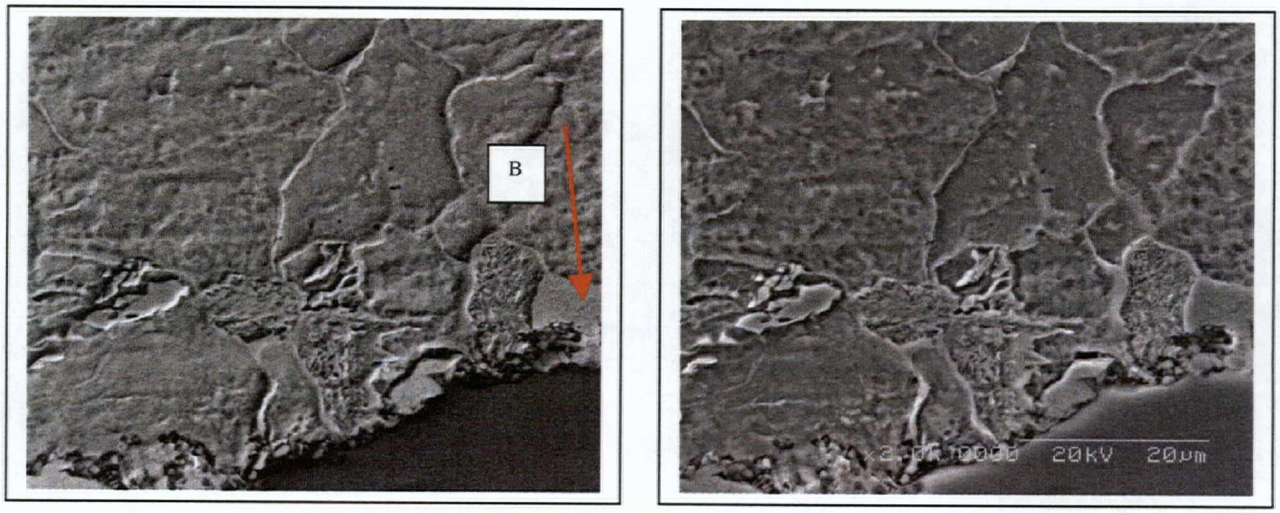

(a) (b)

Fig. 49 Microstructure in the cross-section of 0.39% Cu steel oxidized at 1000°C for 2 hours showing pronounced appearance of discontinuous regions of Cu enrichment at the surface and the grain boundaries (near the surface) .
(a) BS image (X 3.0k) (b) SE image (X 3.0k).

Increasing the oxidation temperature to 1100°C (2 hours) caused thicker (5-8 μm) Cu enriched regions to appear on the steel surface (Fig. 50). These areas appeared to be wavy and gave the appearance as if regions around grain boundaries were getting preferentially enriched as mentioned previously. The Cu enrichment varied from 7.43% at a distance of 20 μm from the surface to 84.45% at the surface. This was clearer by photomicrograph of enrichment at another nearby location (Fig. 51). The Cu content of the region A was 86.88% whereas regions B and C showed only 9.8% and 11.35% respectively. Viewing the location in the above figure at a higher magnification clearly showed that enrichment began occurring at boundaries and also at preferential locations within the grains at regions on the grain boundary (Fig. 52). It is worth noticing that there was extremely thin (0.2-0.5 μm thickness) Cu enriched layer on the steel surface below the oxide layer (Fig. 51 & 52). Also, there were isolated particles in the oxide which were highly enriched in Cu.

5.2.2.3 Oxidized Samples of 0.78% Steel

Oxidizing the highest Cu content steel (under the present study) for 2 hours at 1000°C caused many more large number of Cu enriched massive regions to appear on the surface (Fig. 53). It is worth Comparing Figure 53 with Figures 42 (0.22% Cu steel at 1000°C for 2 hours) and 49 (0.39% Cu at 1000°C for 2 hours). The copper enrichment over massive regions varied from 78.02% to 89.56% in comparison to 71.00 to 75.00% in 0.39% Cu steel samples. Also, Cu enrichment along grain boundaries was much more near the surface (7.37% to 8.14%) as compared to that (1.0-3.5%) for 0.39% steel. Additionally, Cu enrichment became continuous along grain boundaries near the

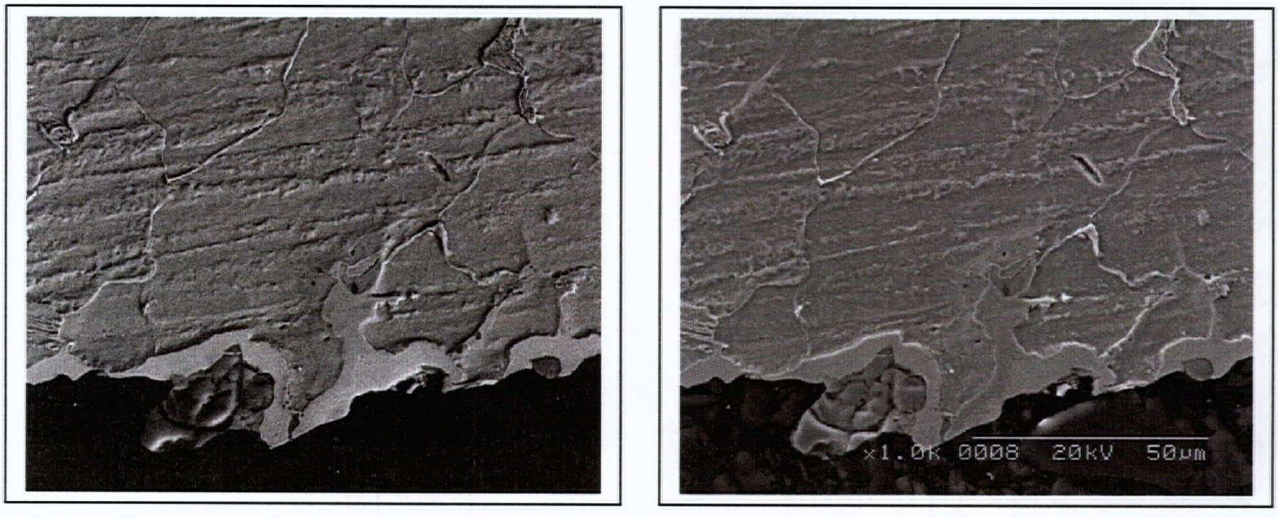

(a) (b)

Fig. 50 Microstructure in the cross-section of 0.39% Cu steel oxidized at 1100°C for 2 hours showing thick and deep regions of Cu enrichment along grain boundaries (a) BS image (X 1.0k) (b) SE image (X 1.0k).

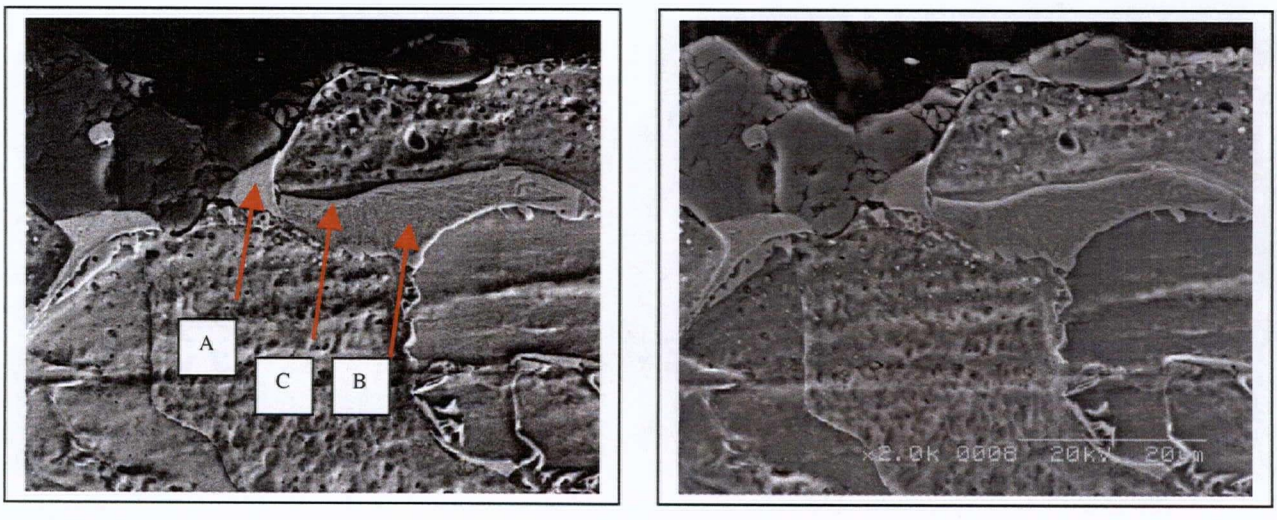

(a) (b)

Fig. 51 Microstructure in the cross-section of 0.39% Cu steel oxidized at 1100°C for 2 hours showing clear penetration of Cu enriched layer along grain boundaries (near the surface) and very thin or, no enriched deposit on the specimen surface (a) BS image (X 2.0k) (b) SE image (X 2.0k).

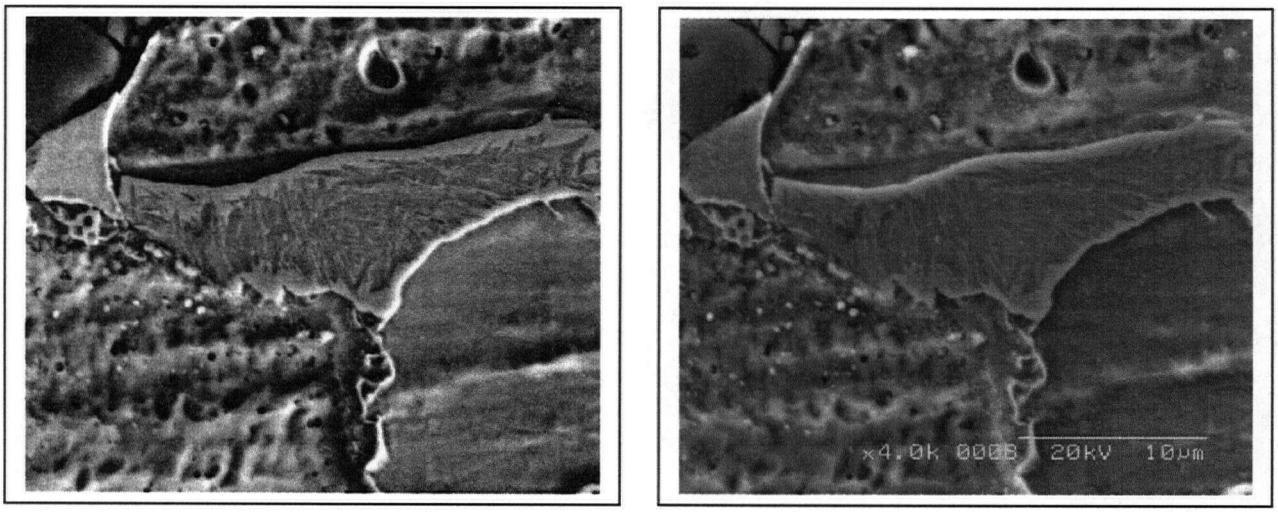

(a) (b)

Fig. 52 Microstructure in the cross-section of 0.39% Cu steel oxidized at 1100°C for 2 hours showing enrichment of Cu along grain boundaries and at preferential locations within the grains.
(a) BS image (X 4.0k) (b) SE image (X 4.0k).

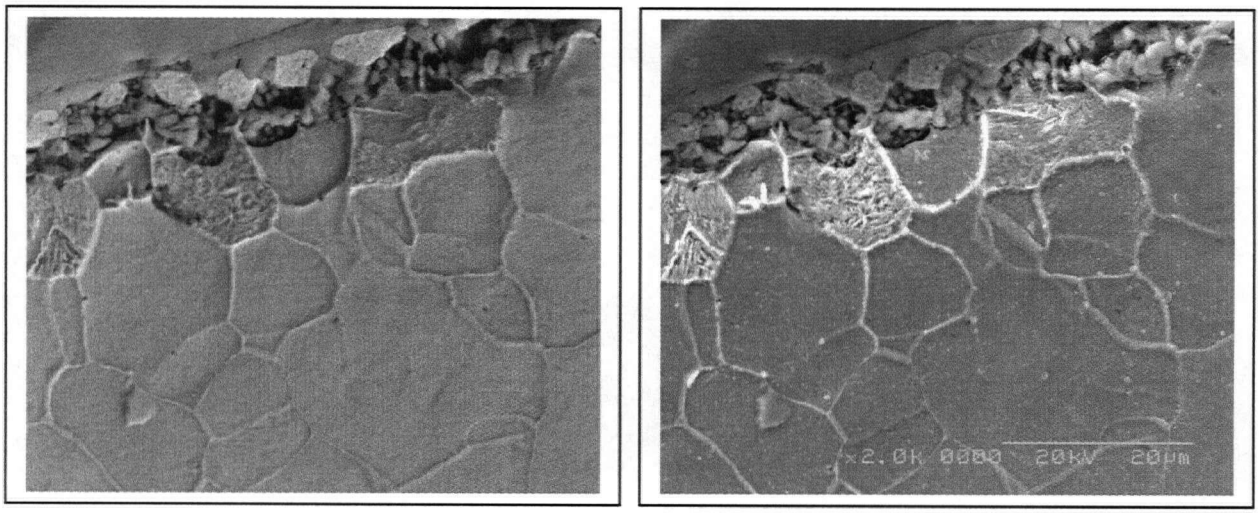

(a) (b)

Fig. 53 Microstructure in the cross-section of 0.78% Cu steel oxidized at 1000°C for 2 hours showing large number of Cu enriched massive regions disjointed and separated from the substrate .
(a) BS image (X 2.0k) (b) SE image (X 2.0k).

surface covering them completely all along individual grains. Enrichment was also present within the grains below the steel surface as mentioned previously, however it was much more pronounced. It is also worth noticing that Cu enriched massive regions at the surface were disjointed and separated from the substrate by pores, voids as well as particles (Fig. 53) as observed for lower Cu content steel previously.

Oxidizing 0.78% Cu steel at 1100°C for 5 minutes revealed the existence of continuous Cu rich layer (1-5 μm thick) for the first time (Fig. 54) with Cu content varying from 86.15% to 91.25%. Thin lines of Cu enrichment (2.69-5.42%) along grain boundaries were also observed near the surface. At certain locations, however there was no presence of enriched phase at the surface (Fig. 55), but the grain boundaries were enriched (6.53-17.72%) as mentioned before. Additionally, a large number of extremely fine voids (a few as big as 50 μm average size) were also noticed (Fig. 56).

Increasing the oxidation time to 1 hour caused 3-8 μm thick layer of Cu enrichment to appear in general everywhere on the surface (Fig.57). However, the enriched layer was extremely thin and was barely seen at certain locations on the surface (Fig. 58) as noted previously (Fig. 55). However, the Cu enrichment along grain boundaries at these regions was very significant (~67.78%). At most of the locations (Fig. 59), the surface showed 82.35-93.10% Cu (e.g. location A) whereas grain boundaries showed 15.92% Cu (locations B and C). The areas within the grains also showed 12.60% Cu. There were also signs of Cu enriched zones getting engulfed into the oxide layer (Fig. 59).

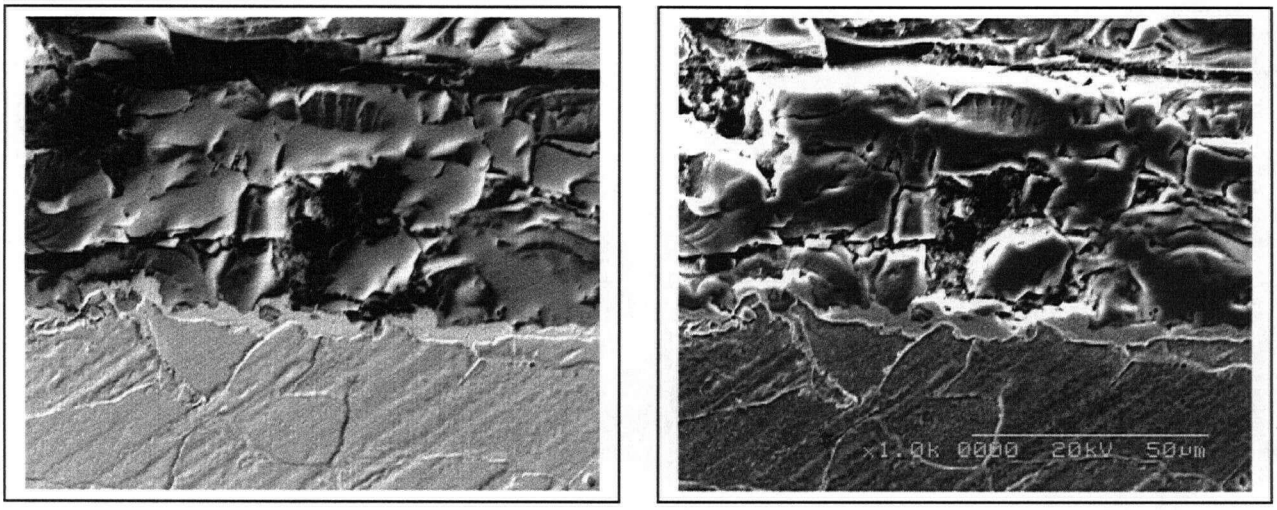

(a) (b)

Fig. 54 Microstructure in the cross-section of 0.78% Cu steel oxidized at 1100°C for 5 minutes showing continuous layer of Cu enrichment at the surface. (a) BS image (X 1.0k) (b) SE image (X 1.0k).

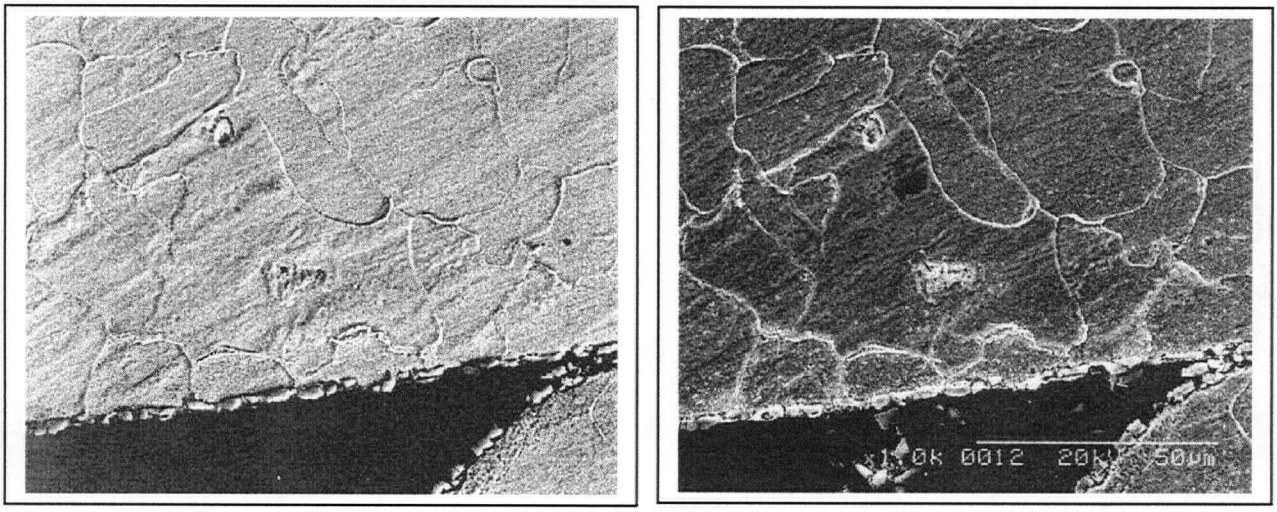

(a) (b)

Fig. 55 Microstructure in the cross-section of 0.78% Cu steel oxidized at 1100°C for 5 minutes showing grain boundaries enriched with Cu and the steel surface devoid of any enrichment. (a) BS image (X 1.0k) (b) SE image (X 1.0k).

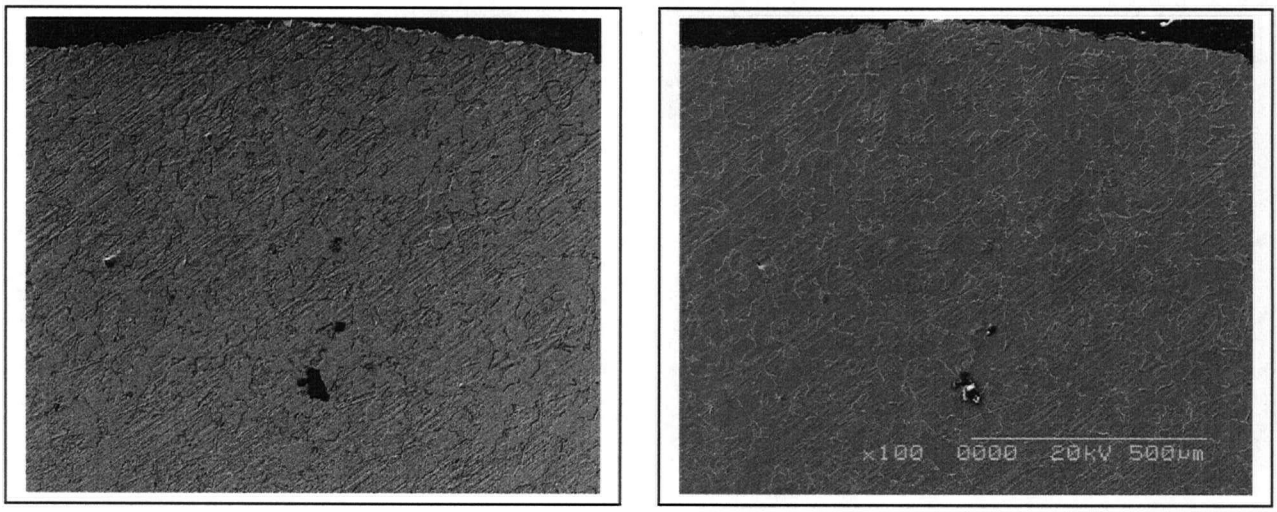

(a) (b)

Fig. 56 Microstructure in the cross-section of 0.78% Cu steel oxidized at 1100°C for 5 minutes showing the presence of voids below the surface. (a) BS image (X 100) (b) SE image (X 100).

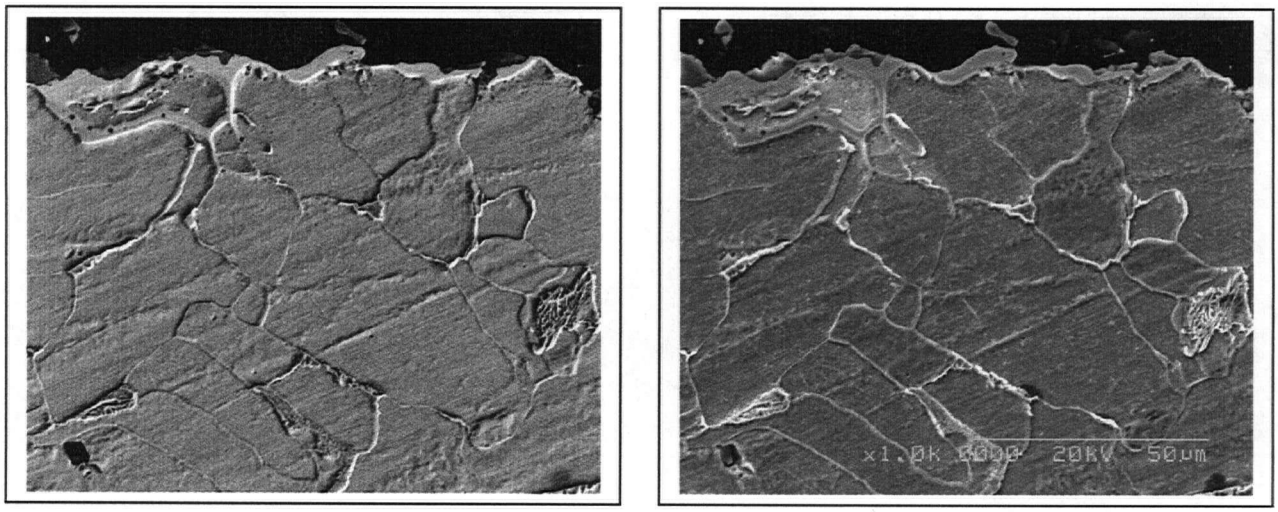

(a) (b)

Fig. 57 Microstructure in the cross-section of 0.78% Cu steel oxidized at 1100°C for 1 hour showing thick continuous layer of Cu enrichment at the surface. (a) BS image (X 800) (b) SE image (X 800).

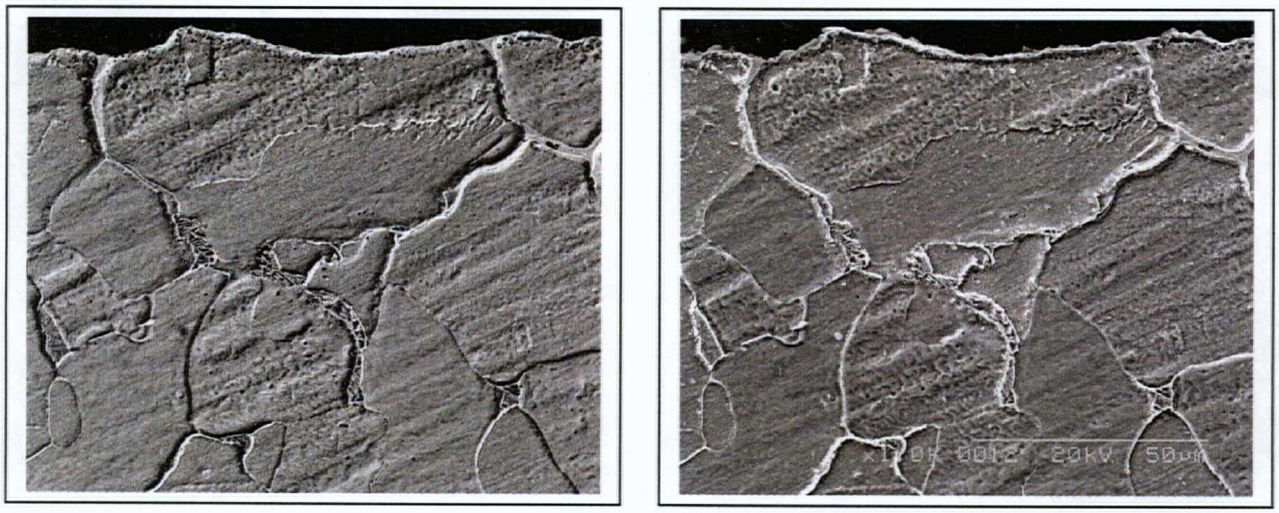

(a) (b)

Fig. 58 Microstructure in the cross-section of 0.78% Cu steel oxidized at 1100°C for 1 hour showing deep penetration of grain boundaries by Cu enriched phase and very thin layer at the surface..
(a) BS image (X 1.0k) (b) SE image (X 1.0k).

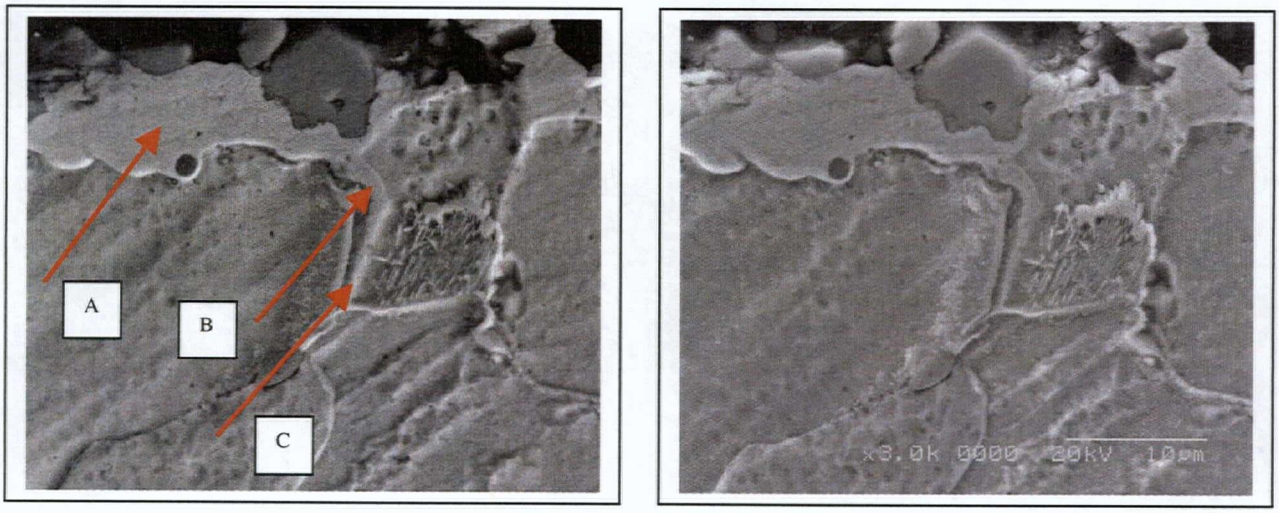

(a) (b)

Fig. 59 Microstructure in the cross-section of 0.78% Cu steel oxidized at 1100°C for 1 hour showing thick continuous layer of Cu enrichment at the surface at a higher magnification. (a) BS image (X 3.0k) (b) SE image (X 3.0k).

Increasing the oxidation time at 1100°C further to 2 hours resulted into larger number of voids. This also caused highly enriched Cu layer to have penetrated more deeply along grain boundaries near the surface (Fig. 60). Additionally, highly enriched continuous layer of Cu was markedly absent from the surface. What was noticed instead were isolated patches of 4-8 μm thick regions highly enriched with Cu (Fig. 61). The Cu content along grain boundaries (Fig. 61) varied between 23.95-87.01% (locations A & C). Presence of tin and oxygen was also noticed from the EDX spectrum (Fig. 62). The regions on grain boundaries adjoining these Cu rich phase (location B) showed Cu content of 9.57%, whereas the isolated highly enriched regions (location D) at the surface had a Cu content of 98.50%. Additionally, voids and pores were prominent along grain boundaries as within grains near the surface at many places (Fig. 63).

A few internally oxidized particles were also seen particularly, near the surface (Fig. 60 & 61). Analysis by EDX over these particles showed them to be of two types, one containing some Cu (~4.02%), e.g. the bright particle (in the back-scattered electron image) in Figure 61 and the other (dark particle) with almost no Cu at all. These particles of the latter type were found to be consisting mainly of oxides of Fe along with Mn (11.88%) and Si (11.47%). However, the particle containing Cu showed very small amounts of Si (1.16%) and Mn (0.92%). Traces of Al, P and S were also seen (Fig. 64).

Oxidizing this steel (i.e. 0.78% Cu) at 1200°C for 5 minutes caused again Cu-rich layer (7 to 10 μm thick) to appear continuously on the surface. Enrichment accompanied by considerable internal oxidation as well as formation of pores (Fig. 65). Enrichment along grain boundaries near the surface was also observed. At these

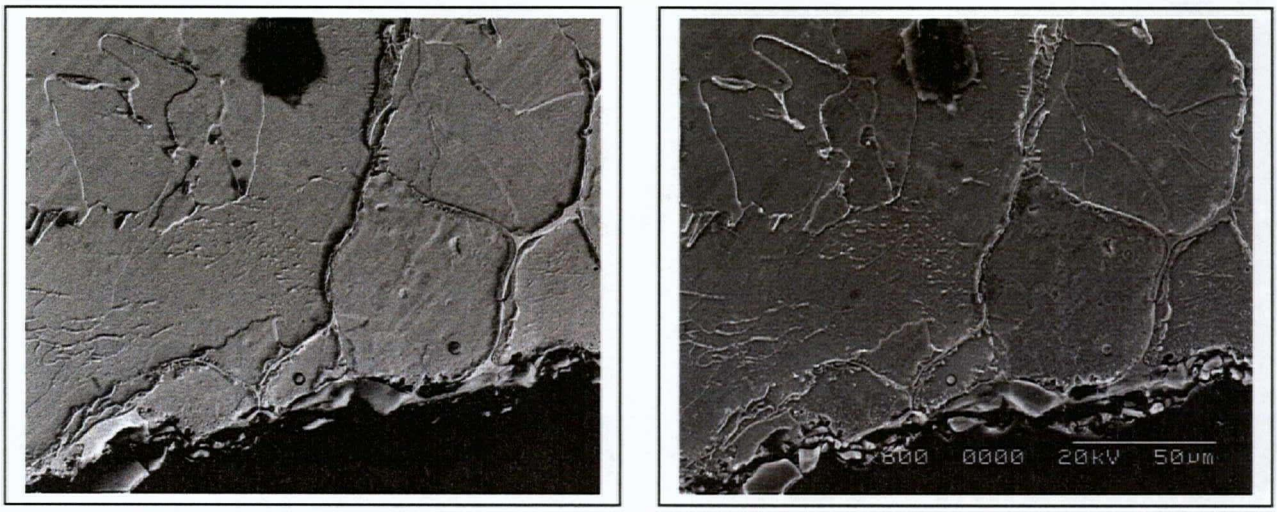

(a) (b)

Fig. 60 Microstructure in the cross-section of 0.78% Cu steel oxidized at 1100°C for 2 hours showing deeper penetration of Cu enriched phase along grain boundaries and internally oxidized particles near the surface. (a) BS image (X 600) (b) SE image (X 600).

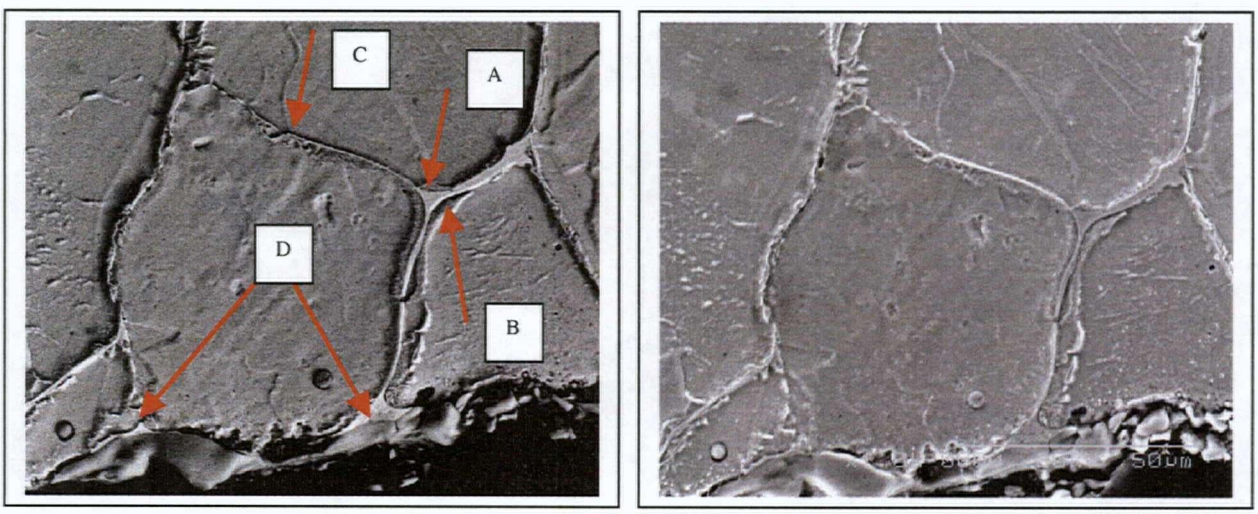

(a) (b)

Fig. 61 Microstructure in the cross-section of 0.78% Cu steel oxidized at 1100°C for 2 hours showing Cu enriched phase along grain boundaries and internally oxidized particles near the surface in the above Figure at a higher magnification (a) BS image (X 1.0k) (b) SE image (X 1.0k).

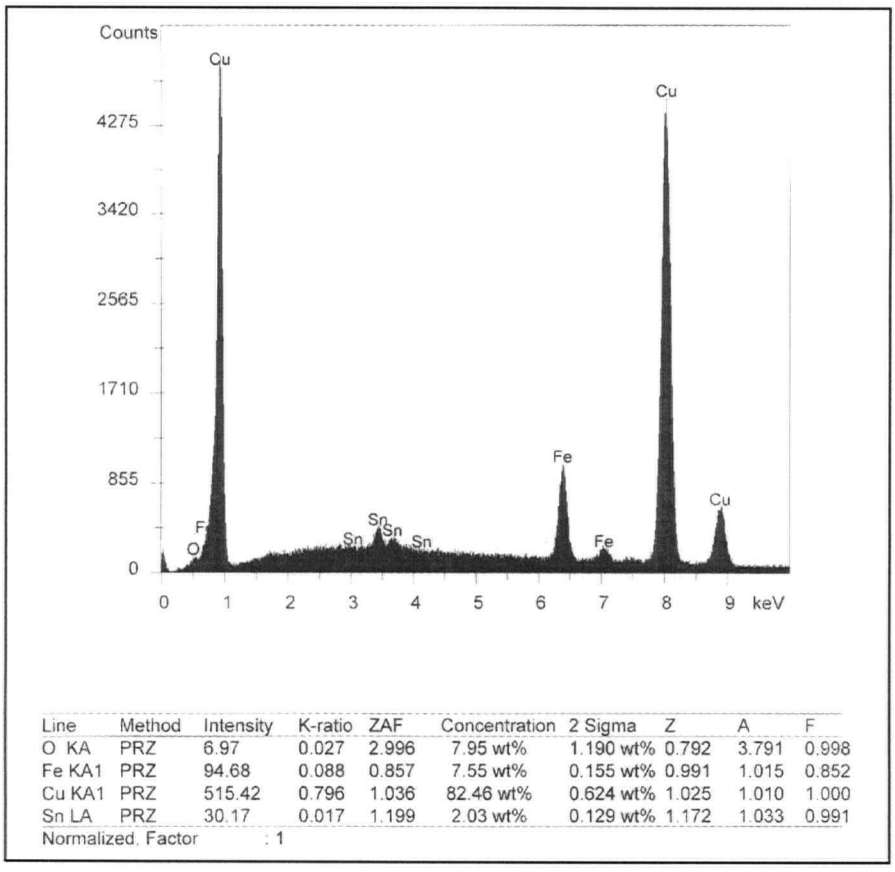

Line	Method	Intensity	K-ratio	ZAF	Concentration	2 Sigma	Z	A	F
O KA	PRZ	6.97	0.027	2.996	7.95 wt%	1.190 wt%	0.792	3.791	0.998
Fe KA1	PRZ	94.68	0.088	0.857	7.55 wt%	0.155 wt%	0.991	1.015	0.852
Cu KA1	PRZ	515.42	0.796	1.036	82.46 wt%	0.624 wt%	1.025	1.010	1.000
Sn LA	PRZ	30.17	0.017	1.199	2.03 wt%	0.129 wt%	1.172	1.033	0.991

Normalized. Factor : 1

Fig. 62 Result of EDX analysis over Cu enriched phase along grain boundaries (region A in Figure 61) in the cross-section of 0.78% Cu steel oxidized at 1100°C for 2 hours.

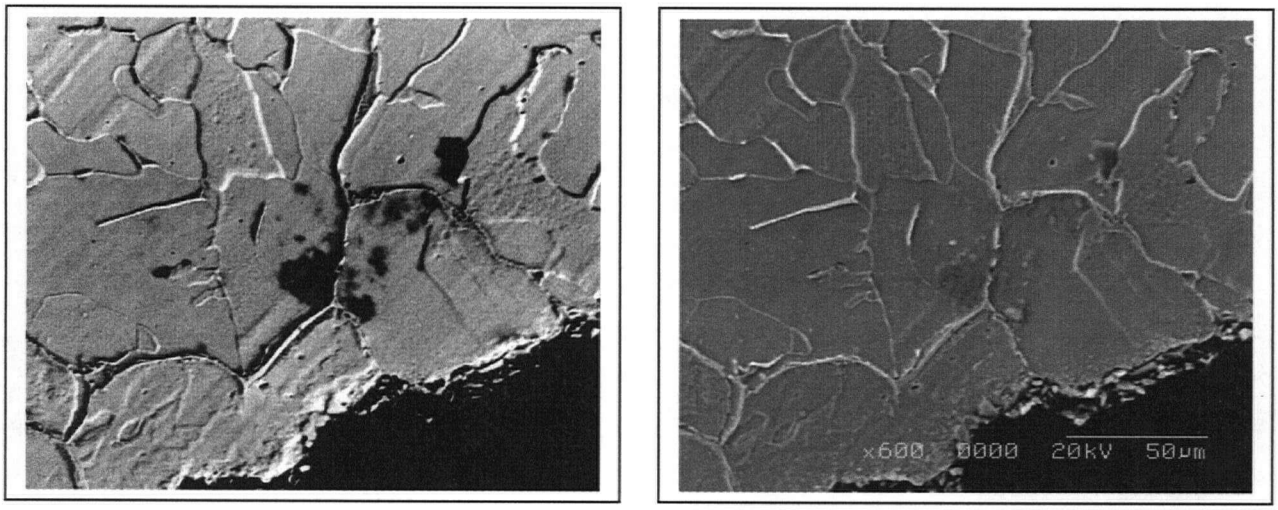

(a) (b)

Fig. 63 Microstructure in the cross-section of 0.78% Cu steel oxidized at 1100°C for 2 hours showing voids along grain boundaries as well as within grains near the surface. (a) BS image (X 600) (b) SE image (X 600).

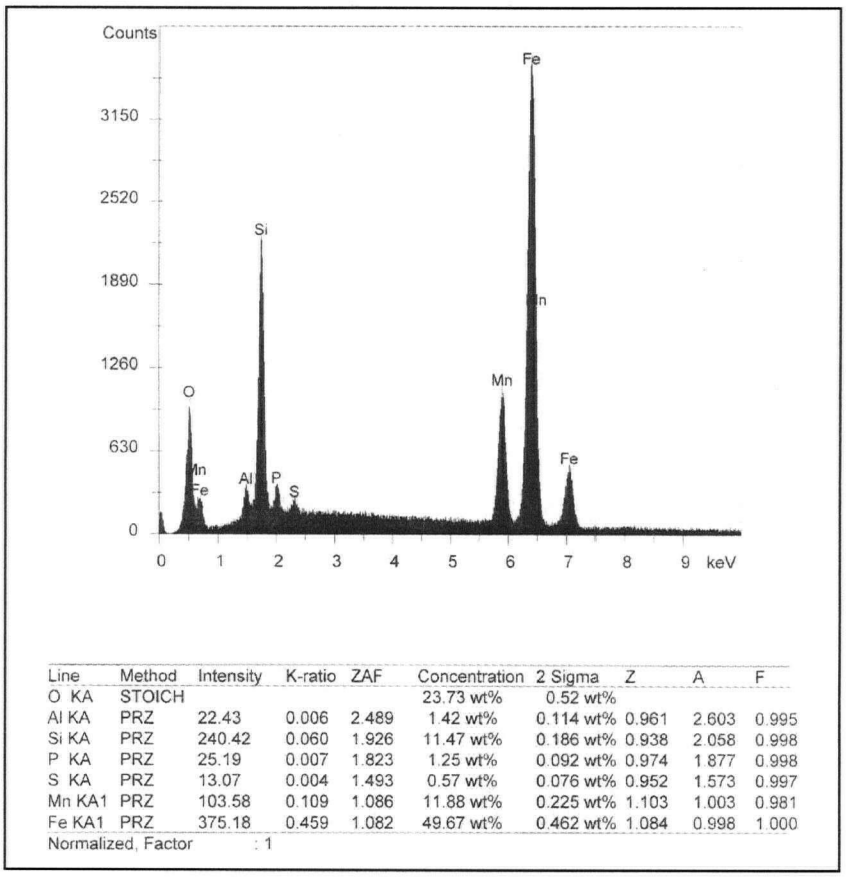

Line	Method	Intensity	K-ratio	ZAF	Concentration	2 Sigma	Z	A	F
O KA	STOICH				23.73 wt%	0.52 wt%			
Al KA	PRZ	22.43	0.006	2.489	1.42 wt%	0.114 wt%	0.961	2.603	0.995
Si KA	PRZ	240.42	0.060	1.926	11.47 wt%	0.186 wt%	0.938	2.058	0.998
P KA	PRZ	25.19	0.007	1.823	1.25 wt%	0.092 wt%	0.974	1.877	0.998
S KA	PRZ	13.07	0.004	1.493	0.57 wt%	0.076 wt%	0.952	1.573	0.997
Mn KA1	PRZ	103.58	0.109	1.086	11.88 wt%	0.225 wt%	1.103	1.003	0.981
Fe KA1	PRZ	375.18	0.459	1.082	49.67 wt%	0.462 wt%	1.084	0.998	1.000

Normalized, Factor : 1

Fig. 64 Result of EDX analysis over dark internally oxidized particle in Figure 61 in the cross-section of 0.78% Cu steel oxidized at 1100°C for 2 hours.

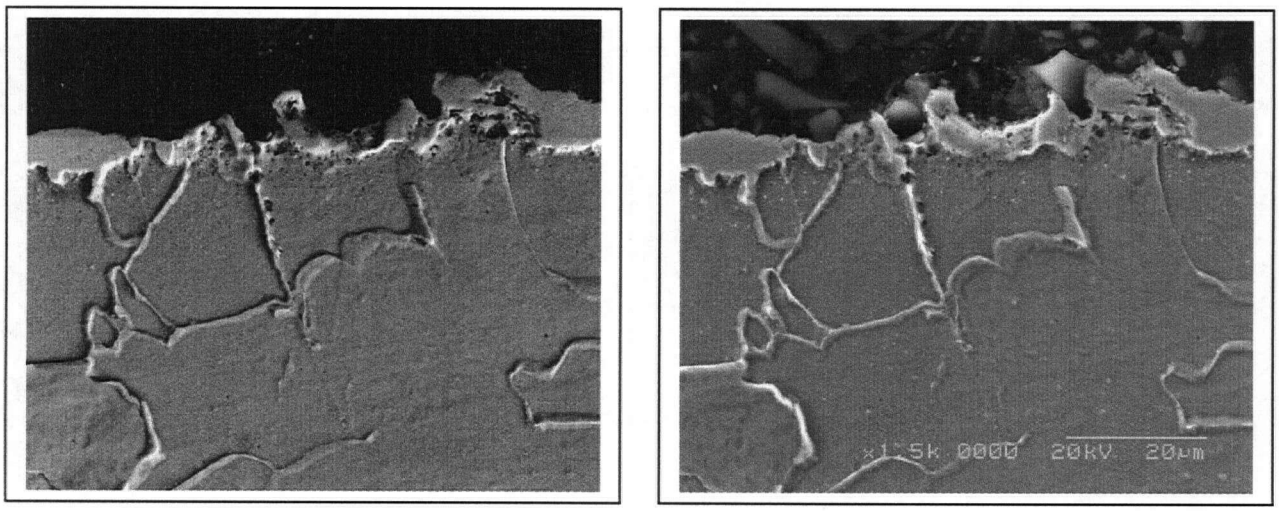

(a) (b)

Fig. 65 Microstructure in the cross-section of 0.78% Cu steel oxidized at 1200°C for 5 minutes showing Cu enriched layer at the surface as well as internally oxidized particles. (a) BS image - X 1.5k. (b) BS image - X 1.5k.

locations, the enriched layer tended to remain in contact with the substrate. However, the enriched region appeared to have begun to separate from the steel in some other areas (Fig. 66) due to formation of large voids and internally oxidized particles at the interface between the enriched layer and the metal surface. EDX analysis revealed very high levels of Cu on the enriched layer (Fig. 67) varying from 88.41% (region C) at the extreme end of the surface to 4.3% (region F) at the grain boundaries. These were lower than that for steel oxidized at 1100°C for 5 minutes. Some Ni, Sn, Si as well as Al were also observed. (Fig. 68). Most of the locations at grain boundaries below the surface indicated much lower levels of enrichment (< 2.0% Cu).

Increasing the oxidation time at this temperature to 1 hour at 1200°C caused further separation of Cu enriched layer. The thickness of enriched layer also increased marginally to 10-15 μm. Enrichment along the grain boundaries also continued. At other locations however, the thickness of enriched layer was less, i.e. 2-10 μm (Fig. 69). In these locations, a lot of internal oxidation was observed due to which the enriched layer appeared to have broken contact with the steel surface significantly. A lot of oxide and Cu enriched particles were also seen everywhere near the surface. In some of the locations, the high Cu regions (e.g. 88.5% at locations A and B) appeared to have existed side by side with low Cu (7.76% at locations C and D) regions (Fig. 70). In addition, Cu rich phase appeared to be surrounding some of the oxide precipitates inside the metal close to the surface (Fig. 70). The grain boundary area near the surface (region E) indicated a lot of Cu, e.g. 20.83%. Presence of oxygen was also detected over the highly enriched regions on the surface.

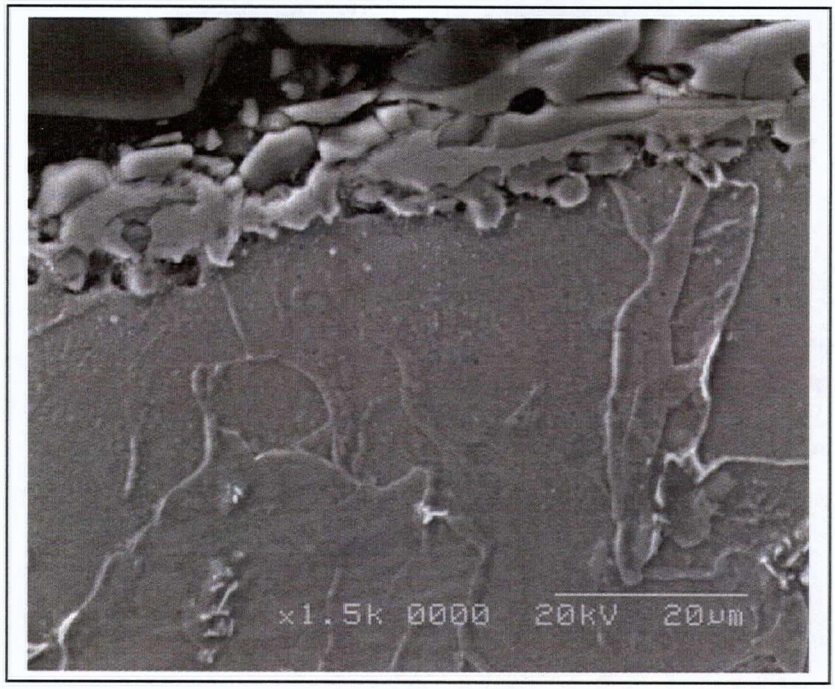

Fig. 66 Microstructure in the cross-section of 0.78% Cu steel oxidized at 1200°C for 5 minutes showing the beginning of separation of Cu enriched phase at the surface from the substrate (SE Image – X 1.5k).

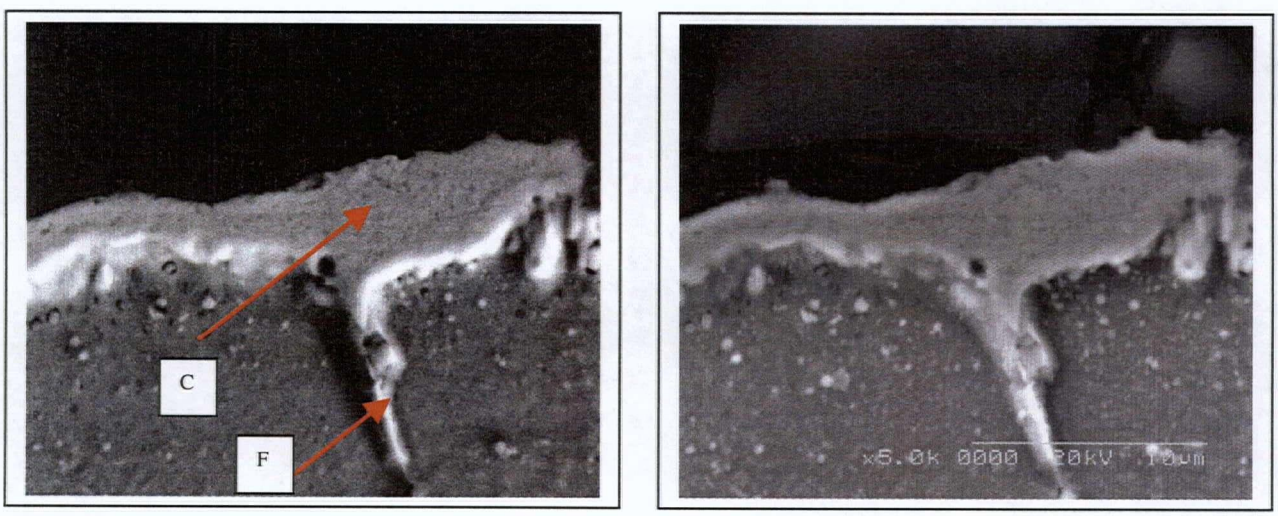

(a) (b)

Fig. 67 Microstructure in the cross-section of 0.78% Cu steel oxidized at 1200°C for 5 minutes showing Cu enriched layer at the surface as well as internally oxidized particles. (a) (BS image - X 5.0k. (b) SE image – X 5.0k.

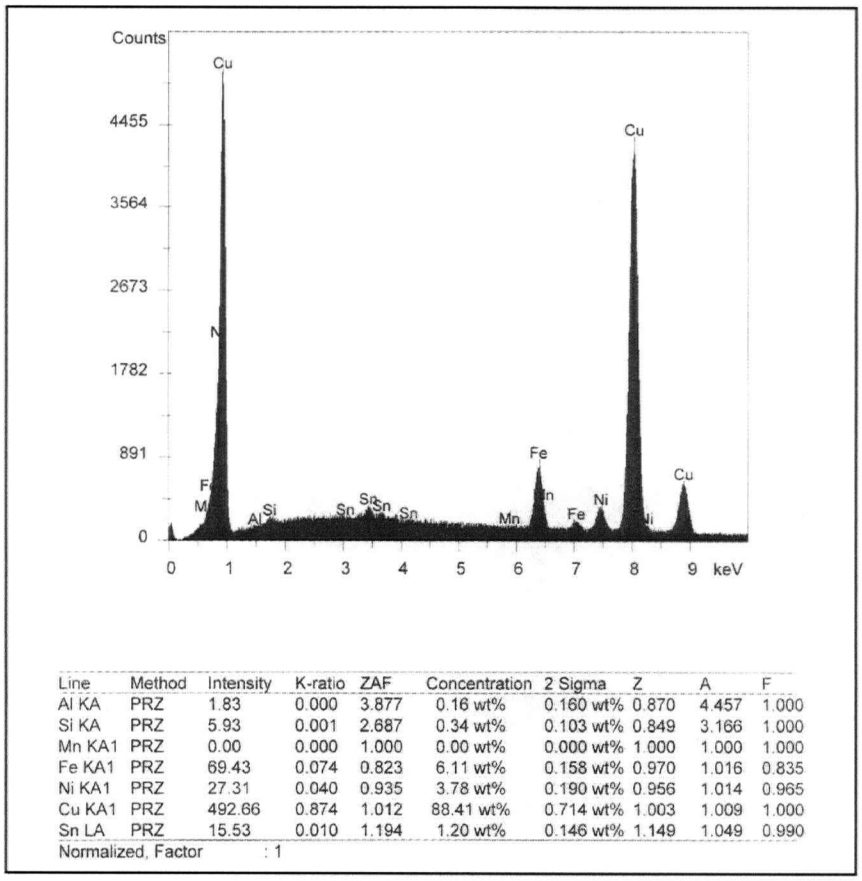

Line	Method	Intensity	K-ratio	ZAF	Concentration	2 Sigma	Z	A	F
Al KA	PRZ	1.83	0.000	3.877	0.16 wt%	0.160 wt%	0.870	4.457	1.000
Si KA	PRZ	5.93	0.001	2.687	0.34 wt%	0.103 wt%	0.849	3.166	1.000
Mn KA1	PRZ	0.00	0.000	1.000	0.00 wt%	0.000 wt%	1.000	1.000	1.000
Fe KA1	PRZ	69.43	0.074	0.823	6.11 wt%	0.158 wt%	0.970	1.016	0.835
Ni KA1	PRZ	27.31	0.040	0.935	3.78 wt%	0.190 wt%	0.956	1.014	0.965
Cu KA1	PRZ	492.66	0.874	1.012	88.41 wt%	0.714 wt%	1.003	1.009	1.000
Sn LA	PRZ	15.53	0.010	1.194	1.20 wt%	0.146 wt%	1.149	1.049	0.990

Normalized, Factor : 1

Fig. 68 Result of EDX analysis over the region C of Cu enriched phase in Figure 67.

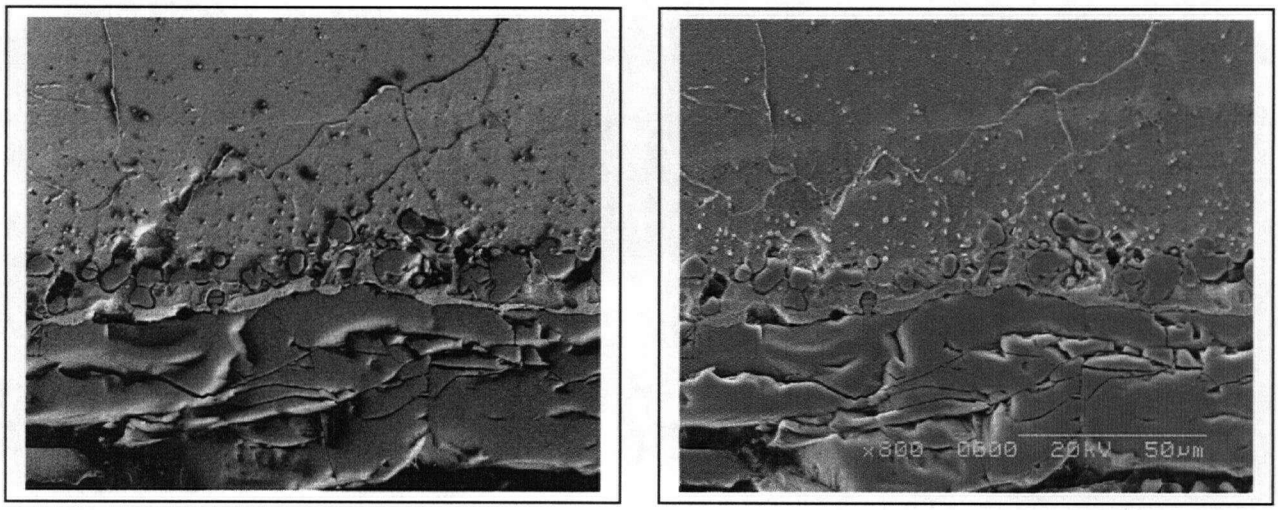

(a) (b)

Fig. 69 Microstructure in the cross-section of 0.78% Cu steel oxidized at 1200°C for 1 hour showing reduced thickness of Cu enriched layer at the surface. Also prominent is significant separation of Cu enriched phase from the substrate. (a)BS image - X 800. (b) SE image - X 800.

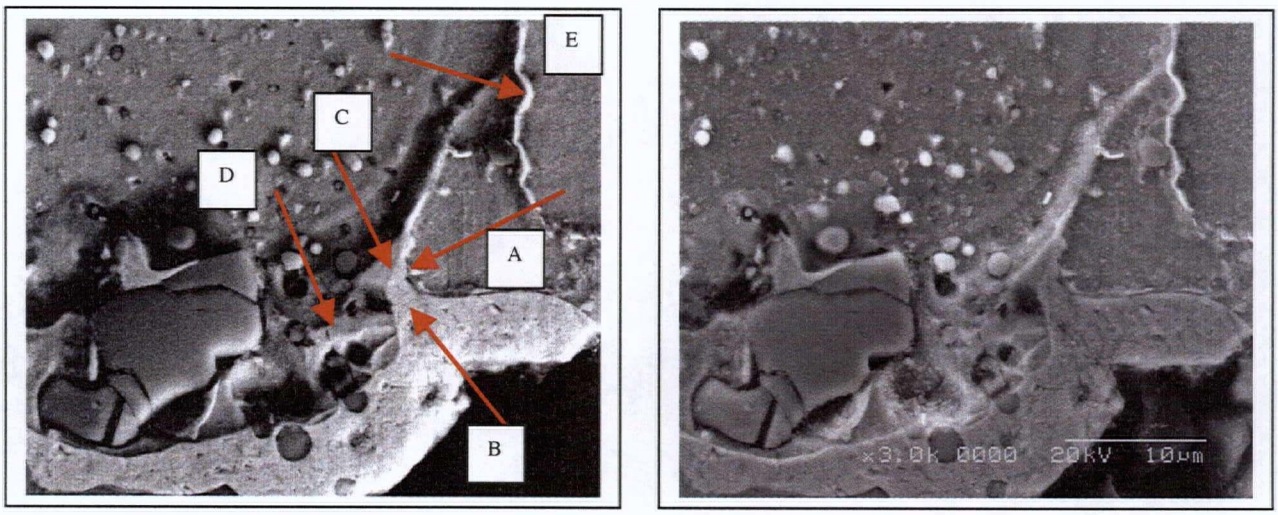

(a) (b)

Fig. 70 Microstructure in the cross-section of 0.78% Cu steel oxidized at 1200°C for 1 hour showing existence of high Cu region side by side with low Cu region and surrounding of internally oxidized particles by Cu enriched phase. (a)BS image - X 800. (b) SE image - X 800.

At some rare locations, Cu-rich phase did appear to form along grain boundaries (Fig. 71), but it appeared to be broken and disjointed due to presence of voids and possibly oxide particles. At few other locations, internal oxidation occurred quite deep along the grain boundaries (Fig. 72). EDX analysis at the edge of this internally oxidized grain boundary showed 26.88%Cu, 14.91% O and other elements such as Al, Si, P and Mn (Fig. 73). On the other hand, it showed much less copper (7.25%), higher oxygen (27.99%) and higher amounts of other elements such as Al, Si, S, P, Cr ad Mn (Fig. 74) at the centre.

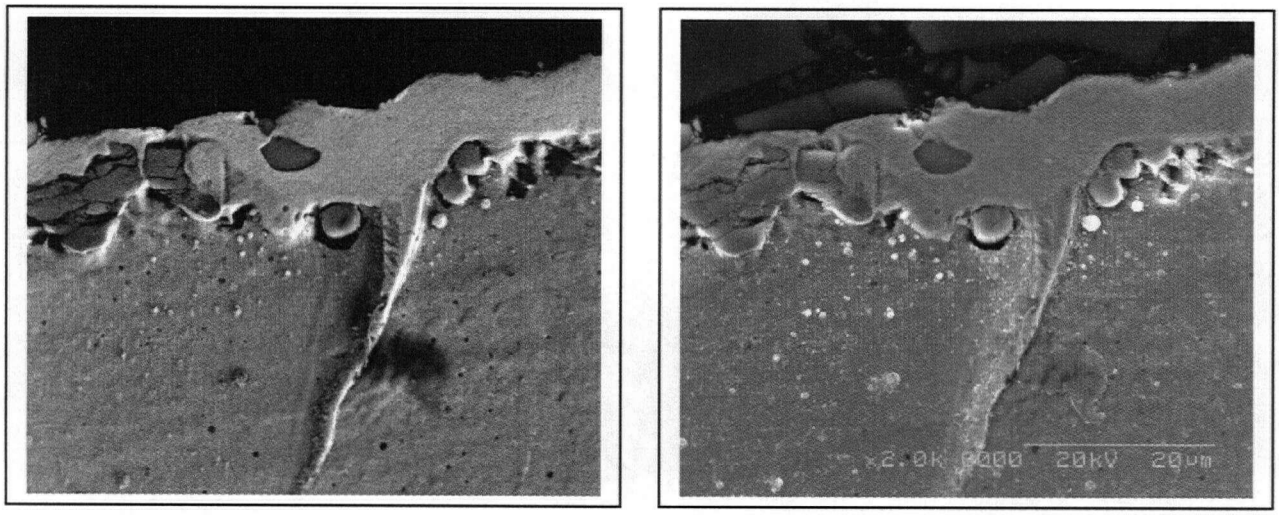

(a) (b)

Fig. 71 Microstructure in the cross-section of 0.78% Cu steel oxidized at 1200°C for 1 hour showing Cu enriched phase penetrated along grain boundaries but broken and disjointed due to presence of oxide particles and voids. (a) BS image - X 2.0k. (b) SE image - X 2.0k.

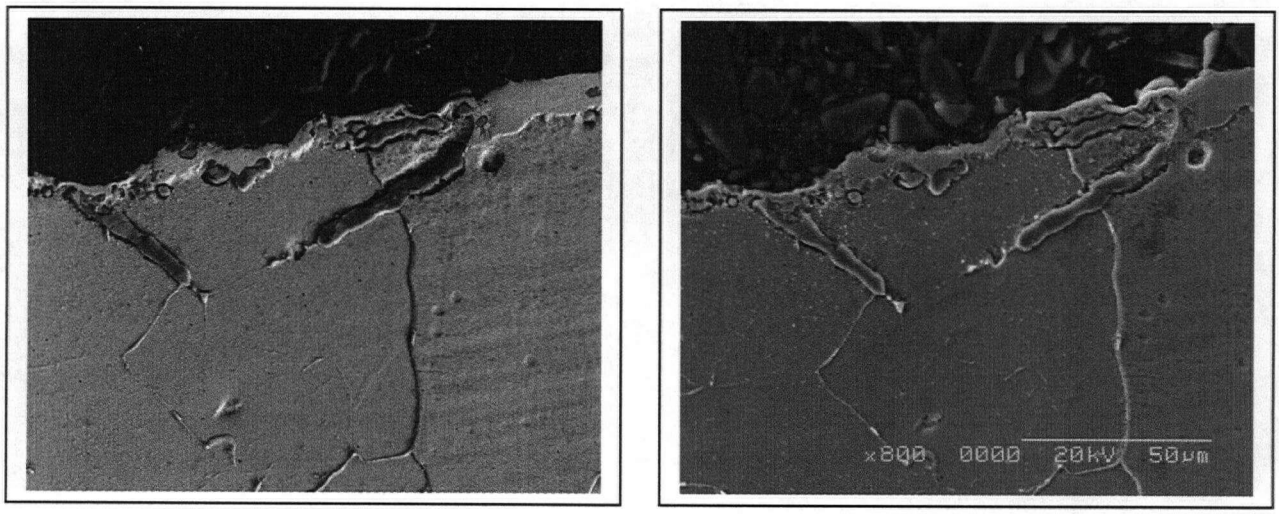

(a) (b)

Fig. 72 Microstructure in the cross-section of 0.78% Cu steel oxidized at 1200°C for 1 hour showing internal oxidation along grain boundaries near the surface(a) BS image - X 800. (b) SE image - X 800.

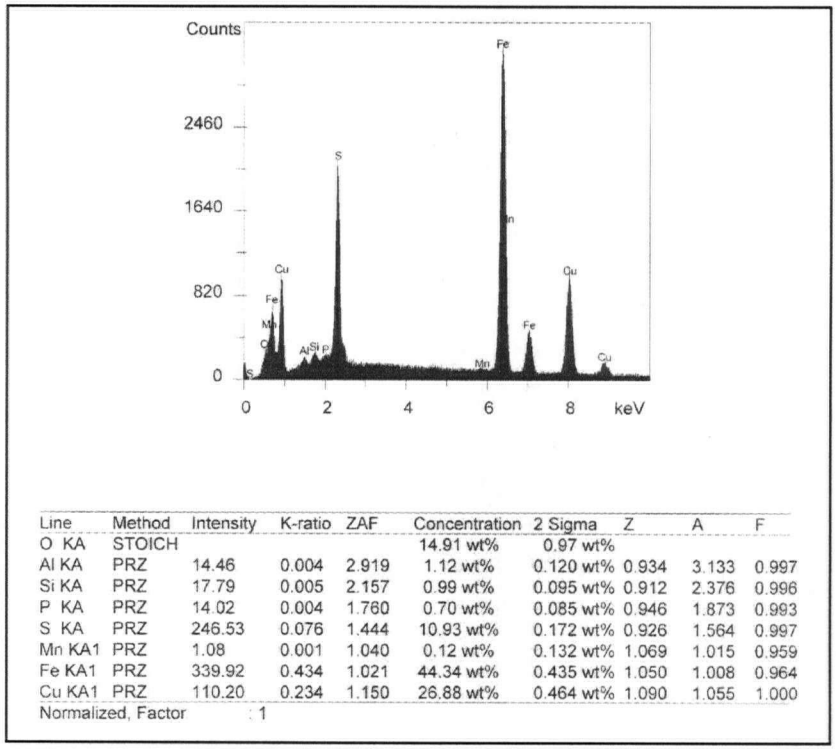

Line	Method	Intensity	K-ratio	ZAF	Concentration	2 Sigma	Z	A	F
O KA	STOICH				14.91 wt%	0.97 wt%			
Al KA	PRZ	14.46	0.004	2.919	1.12 wt%	0.120 wt%	0.934	3.133	0.997
Si KA	PRZ	17.79	0.005	2.157	0.99 wt%	0.095 wt%	0.912	2.376	0.996
P KA	PRZ	14.02	0.004	1.760	0.70 wt%	0.085 wt%	0.946	1.873	0.993
S KA	PRZ	246.53	0.076	1.444	10.93 wt%	0.172 wt%	0.926	1.564	0.997
Mn KA1	PRZ	1.08	0.001	1.040	0.12 wt%	0.132 wt%	1.069	1.015	0.959
Fe KA1	PRZ	339.92	0.434	1.021	44.34 wt%	0.435 wt%	1.050	1.008	0.964
Cu KA1	PRZ	110.20	0.234	1.150	26.88 wt%	0.464 wt%	1.090	1.055	1.000

Normalized, Factor : 1

Fig. 73 Result of EDX analysis over the edge of internally oxidized grain boundary in Figure 72.

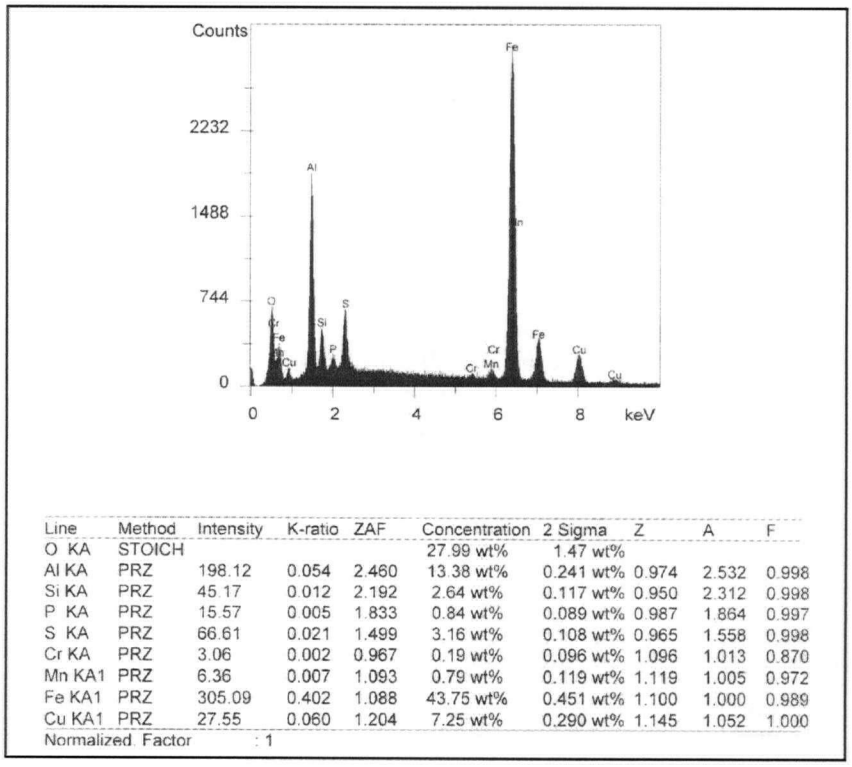

Line	Method	Intensity	K-ratio	ZAF	Concentration	2 Sigma	Z	A	F
O KA	STOICH				27.99 wt%	1.47 wt%			
Al KA	PRZ	198.12	0.054	2.460	13.38 wt%	0.241 wt%	0.974	2.532	0.998
Si KA	PRZ	45.17	0.012	2.192	2.64 wt%	0.117 wt%	0.950	2.312	0.998
P KA	PRZ	15.57	0.005	1.833	0.84 wt%	0.089 wt%	0.987	1.864	0.997
S KA	PRZ	66.61	0.021	1.499	3.16 wt%	0.108 wt%	0.965	1.558	0.998
Cr KA	PRZ	3.06	0.002	0.967	0.19 wt%	0.096 wt%	1.096	1.013	0.870
Mn KA1	PRZ	6.36	0.007	1.093	0.79 wt%	0.119 wt%	1.119	1.005	0.972
Fe KA1	PRZ	305.09	0.402	1.088	43.75 wt%	0.451 wt%	1.100	1.000	0.989
Cu KA1	PRZ	27.55	0.060	1.204	7.25 wt%	0.290 wt%	1.145	1.052	1.000

Normalized Factor : 1

Fig. 74 Result of EDX analysis over the centre of internally oxidized grain boundary in Figure 72.

Increasing the time of oxidation to 2 hours (at 1200°C) caused further separation of Cu enriched phase from grain boundaries due to enhanced internal oxidation (Fig.75). The internally oxidized particles became much bigger in size especially close to the steel surface. There appeared to be progressively less enrichment along grain boundaries. The thickness of the enriched layer on the surface also tended to decrease (e.g. to 3-5 μm). At locations in between, it appeared as a thin line. Enrichment of Cu at the surface (Fig. 76) was found to be 82.12-88.71% (locations A and B). Some O, Sn and Ni were also present. However, the enrichment along the thin layer (region C) and at the grain boundaries (region D) was 14.97% Cu and 3.16% Cu respectively.

The internally oxidized particles appeared to be coated with a highly enriched Cu layer (Fig. 77) containing 78.29% Cu, some Ni (1.44%), Mn (1.98%) and oxygen (4.49%) (location A). The centre of these particles (location B) consisted mainly of iron oxide with trace of Cu and Mn (< 1.0%) and significant amounts of oxygen (22.17%). Considerable Si (i.e. 8.5%) was present near the edges (i.e. at the interface between Cu rich phase and Fe-oxide). Particles farther from the steel surface contained smaller amount of Cu in the enriched layer around them (e.g. at a a distance of 50 μm they contained less than 1.0% Cu).

Increasing the oxidation temperature to 1275°C (2 hours) caused the depth of internally oxidized zone to increase further, voids and internally oxidized particles to become more numerous and Cu enriched layer to become thinner (1-3 μm) as well as more separated into the scale (Fig. 78).

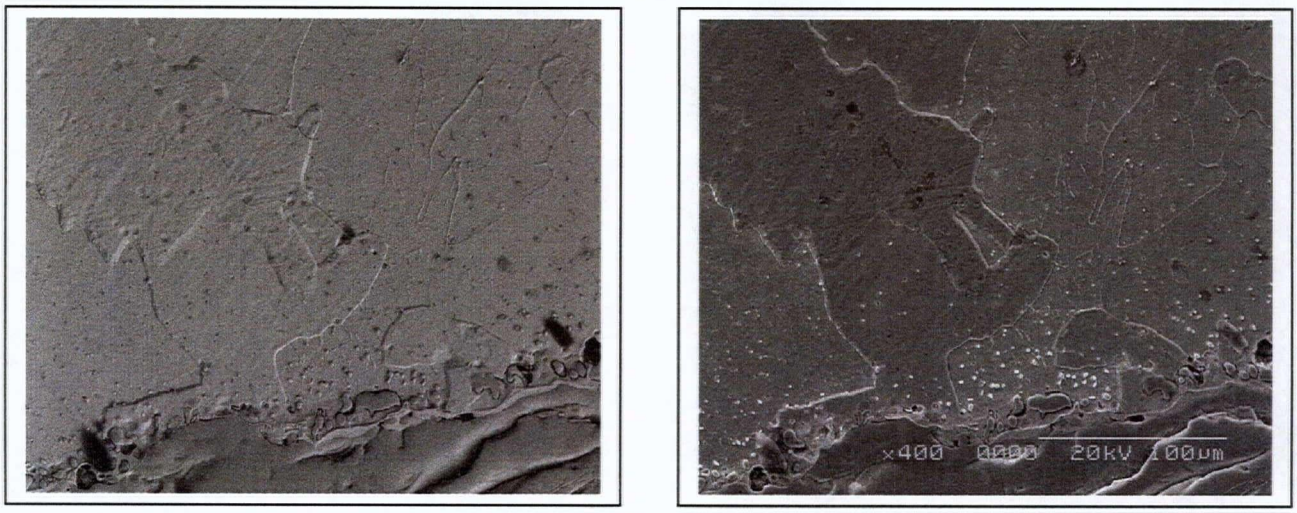

(a) (b)

Fig. 75 Microstructure in the cross-section of 0.78% Cu steel oxidized at 1200°C for 2 hours showing thin Cu enriched phase at the surface and numerous internally oxidized particles (a) BS image - X 400k. (b) SE image - X 400k.

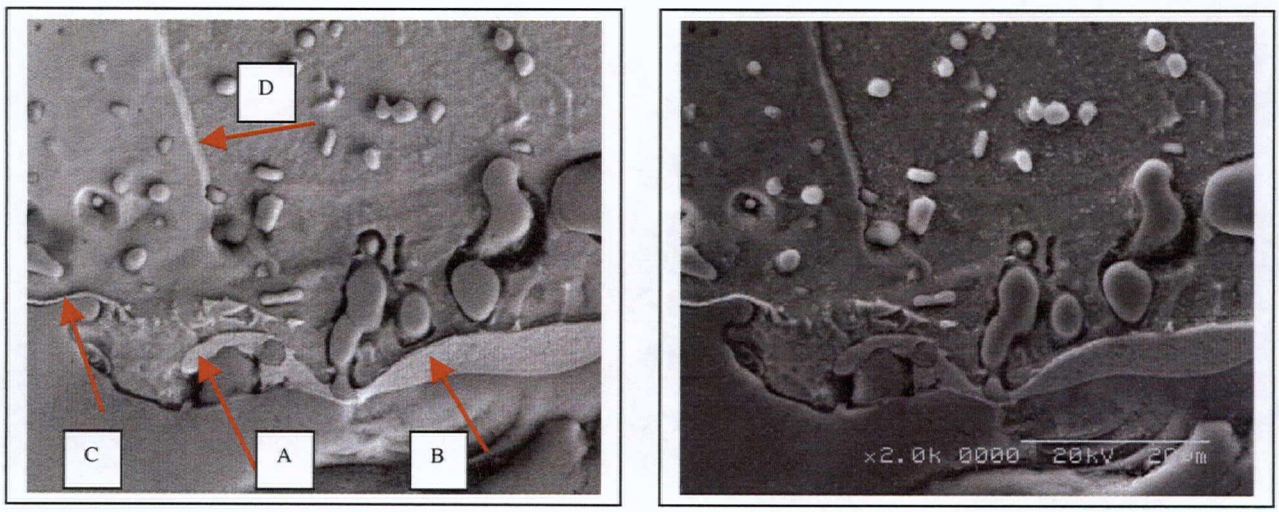

(a) (b)

Fig. 76 Same as above at a higher magnification (a) BS image - X 2.0k. (b) SE image - X 2.0k.

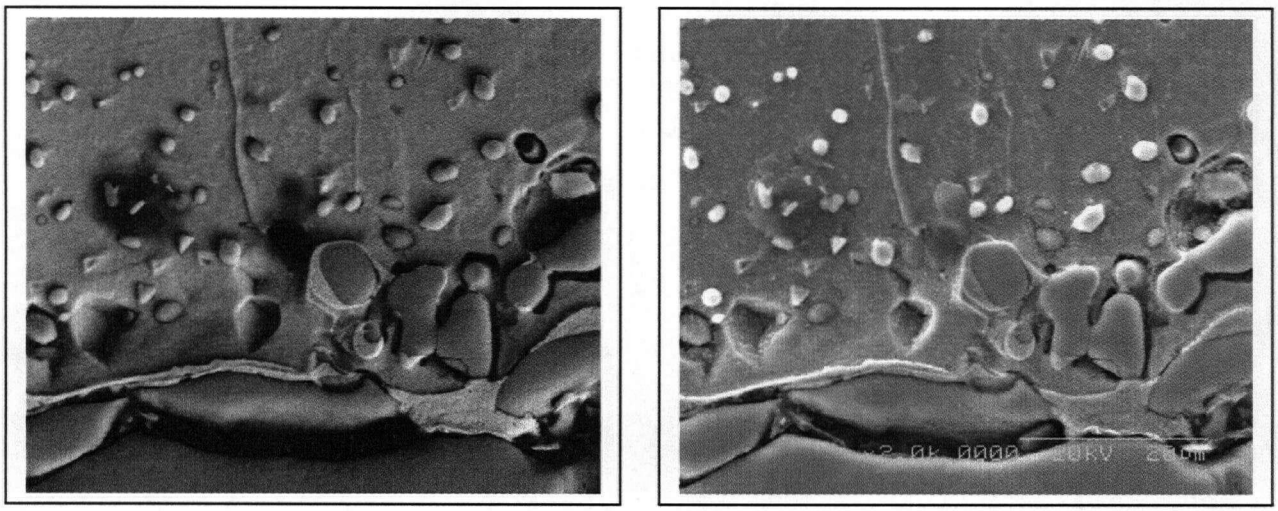

(a) (b)

Fig. 77 Microstructure in the cross-section of 0.78% Cu steel oxidized at 1200°C for 2 hours showing internally oxidized particles surrounded with Cu enriched phase (a) BS image - X 2.0k. (b) SE image - X 2.0k.

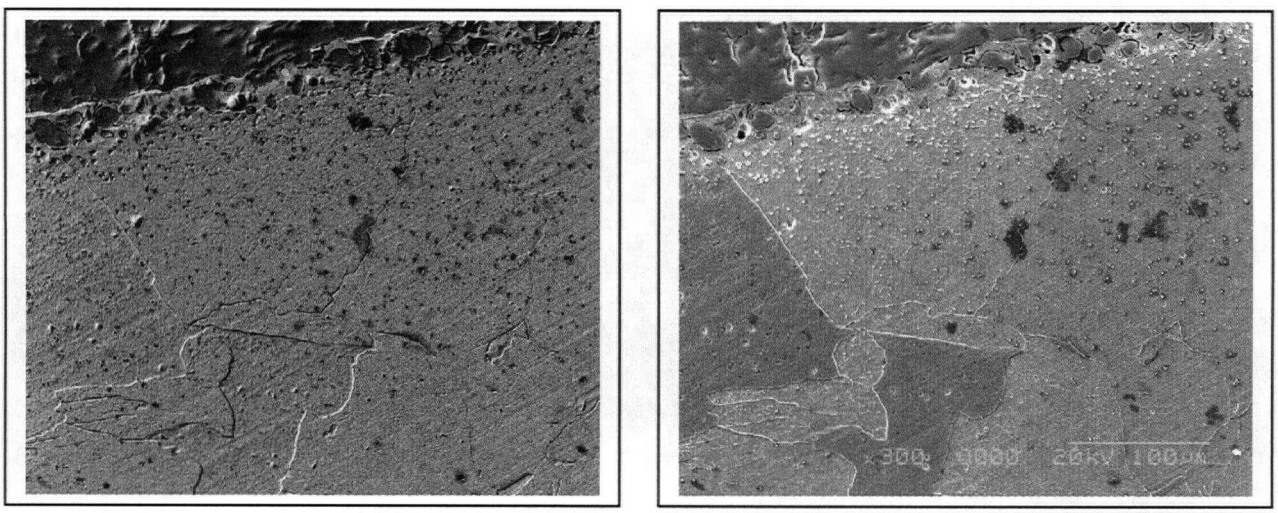

(a) (b)

Fig. 78 Microstructure in the cross-section of 0.78% Cu steel oxidized at 1275°C for 2 hours showing thin Cu enriched phase at the surface and numerous internally oxidized particles (a) BS image - X 300k. (b) SE image - X 300k.

Additionally, existence of regions mildly enriched with Cu (7.97% Cu and 1.88% Ni) just below the highly enriched regions (Fig. 79) became more pronounced and spread over much longer distance (15-20 μm). The surface enriched layer contained 83.70% Cu; 1.45% Ni and 2.96% Sn. It also exhibited distinct oxygen (3.3%) peaks. The surface enriched layer was further separated by large oxide particles (Fig. 80).

Oxidation at higher temperatures (e.g. 1200-1275°C) of lower Cu content (e.g. 0.39%) steels for 2 hours did not show the presence of any highly enriched continuous layer (Fig. 81). Rather, the Cu enriched layer was broken, discontinuous and getting engulfed into the oxide scale very markedly (Fig. 81 and 82). Also, Cu content of the enriched layer was ~6.09% at the surface and it decreased gradually to less than 1.0% at a distance of 15 μm from the surface. Again, a lot of internally oxidized particles were observed. At 1200°C, the features were similar except that Cu content was lower at the surface.

5.3 XPS Studies

XPS studies on a sample (0.78% Cu steel oxidized at 1200°C for 5 minutes) carried over an area with dark appearance (e.g. in Figure 24). indicated distinct 2p peaks of CuO (Fig. 83) as well as those of Fe_2O_3 (Fig. 84). It could be noticed from the spectra in these figures that the peaks of CuO (particularly, $2p_{3/2}$) were much sharper whereas those of Fe_2O_3 were broadened. A broader peak of Fe_2O_3 was indicative of presence of FeO too, as the binding energies for $2p_{3/2}$ peaks of these two oxides are very close

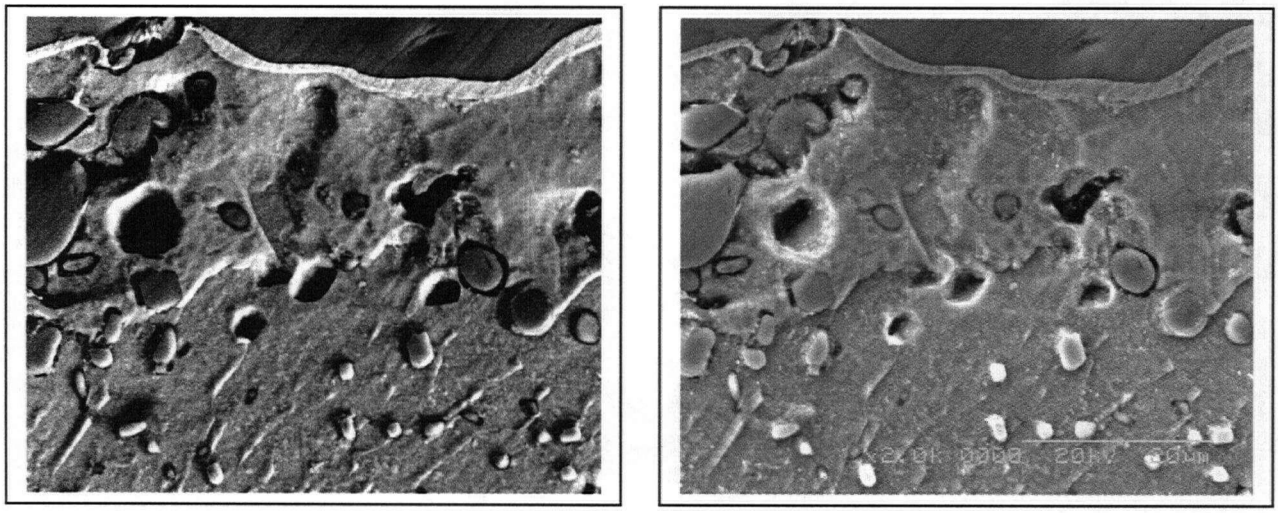

(a) (b)

Fig. 79 Microstructure in the cross-section of 0.78% Cu steel oxidized at 1275°C for 2 hours showing side by side existence of regions mildly as well as severely enriched with Cu (a) BS image - X 2.0k. (b) SE image - X 2.0k.

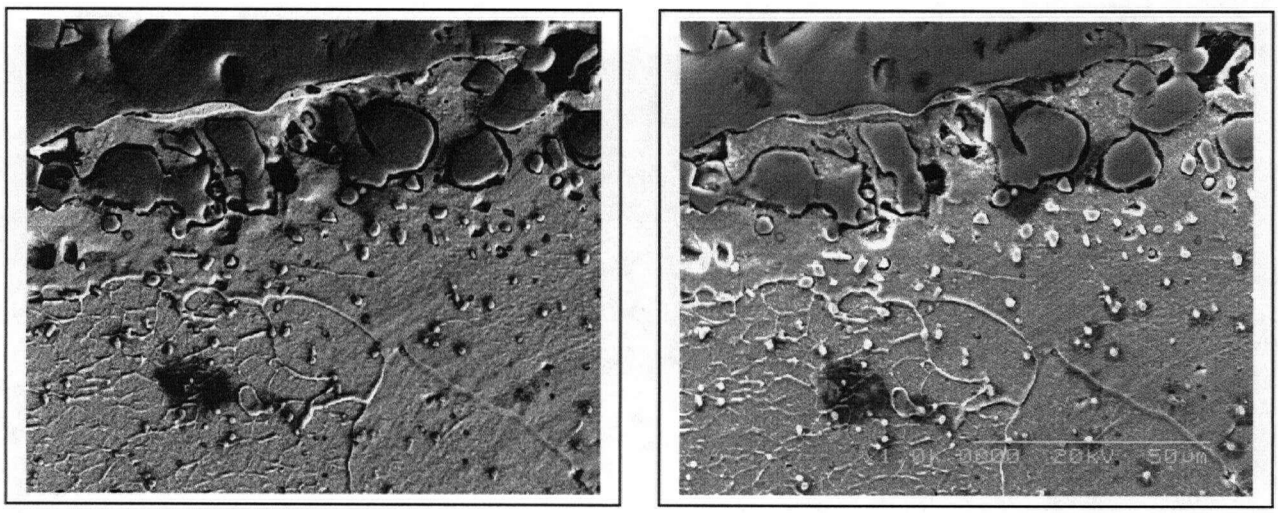

(a) (b)

Fig. 80 Microstructure in the cross-section of 0.78% Cu steel oxidized at 1275°C for 2 hours showing separation of thin Cu enriched phase at the surface by large internally oxidized particles.
(a) BS image - X 1.0k. (b) SE image - X 1.0k.

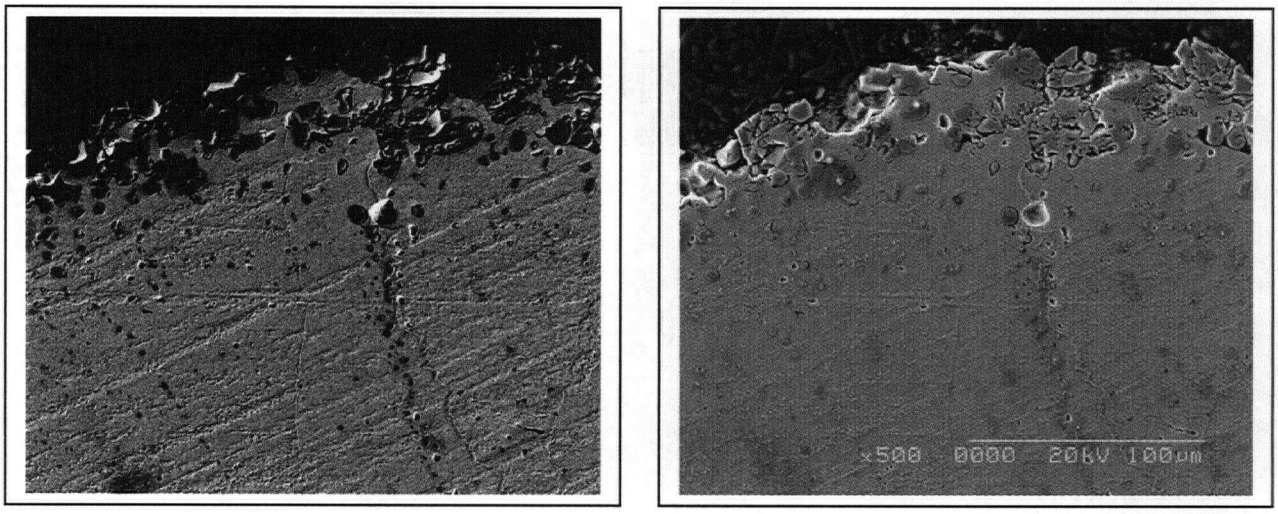

(a) (b)

Fig. 81 Microstructure in the cross-section of 0.39% Cu steel oxidized at 1275°C for 2 hours showing absence of continuous layer of Cu enriched phase at the surface and presence of internally oxidized particles.
(a) BS image - X 500. (b) SE image - X 500.

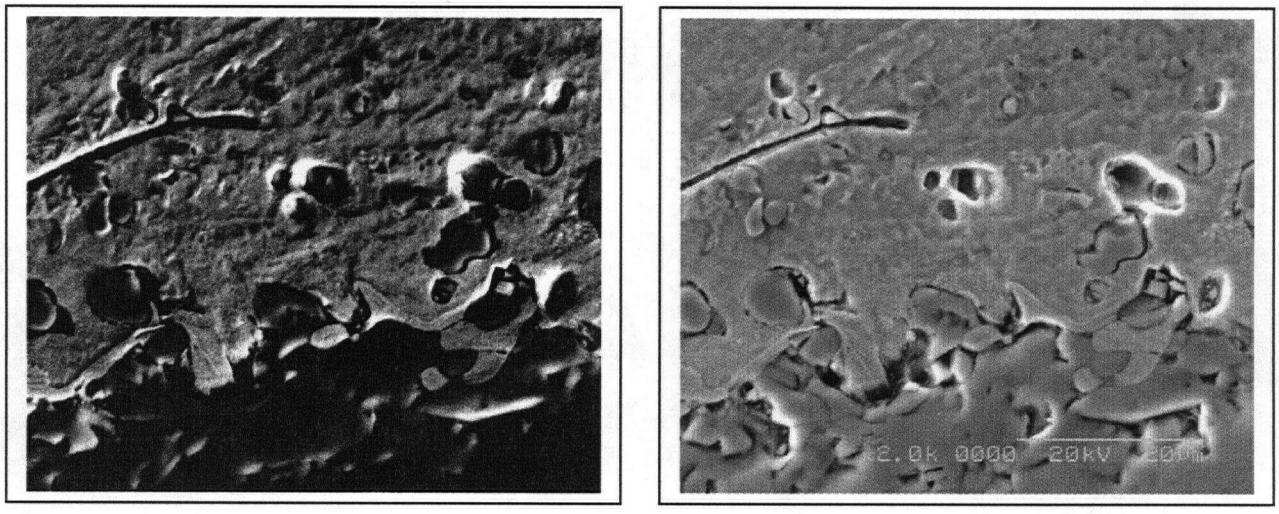

(a) (b)

Fig. 82 Same as above at a higher magnification.
(a) BS image - X 2.0k. (b) SE image - X 2.0k.

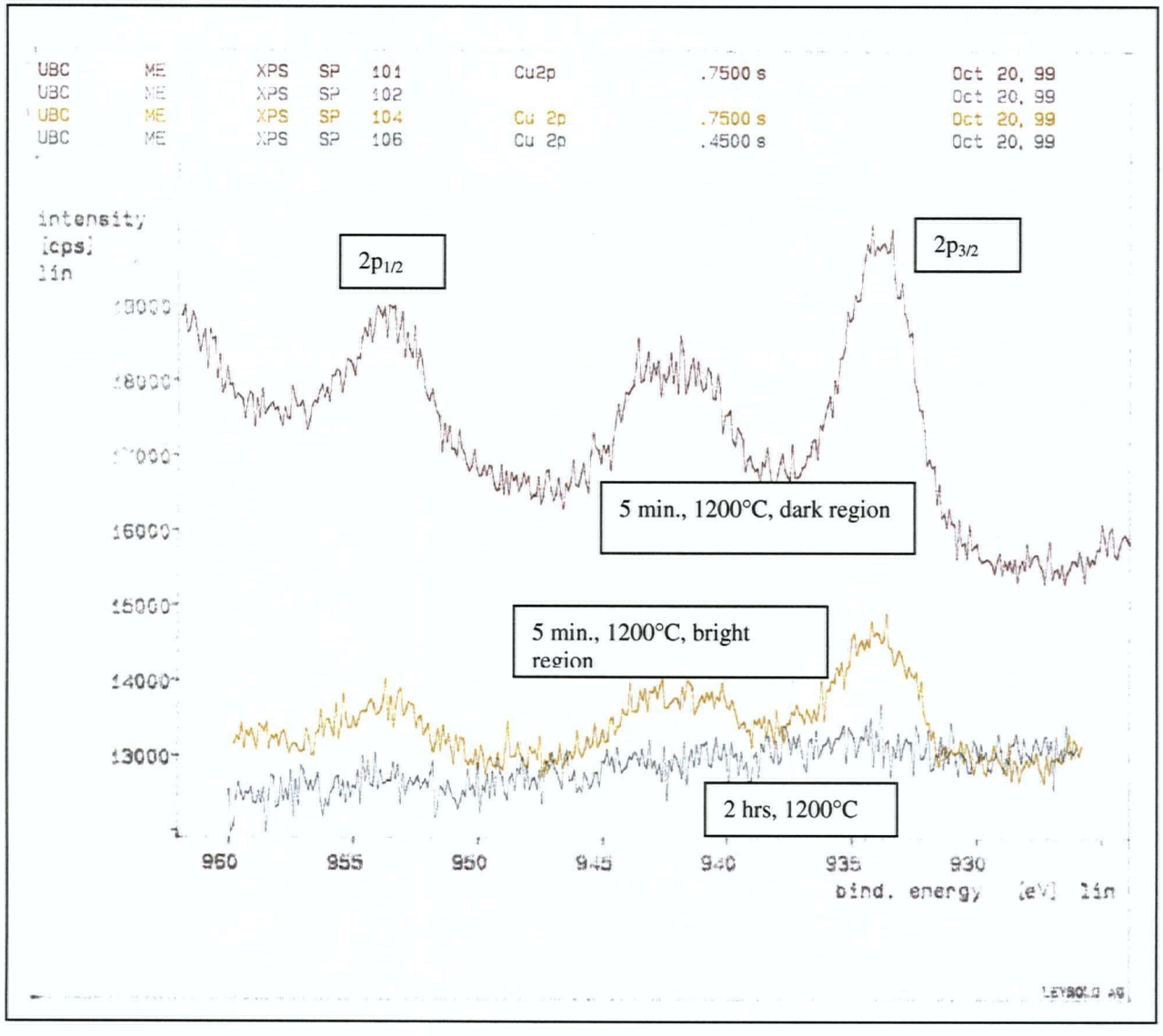

Fig. 83 CuO spectra from XPS studies performed over the scales of 0.78% Cu steel.

(i.e. ~711 and ~709 eV respectively). Similar results were obtained when XPS spectra were taken over an area (on the same sample) with bright appearance. However, the peaks of both CuO as well as Fe_2O_3 showed less intensity indicating qualitatively that these were present in smaller amounts.

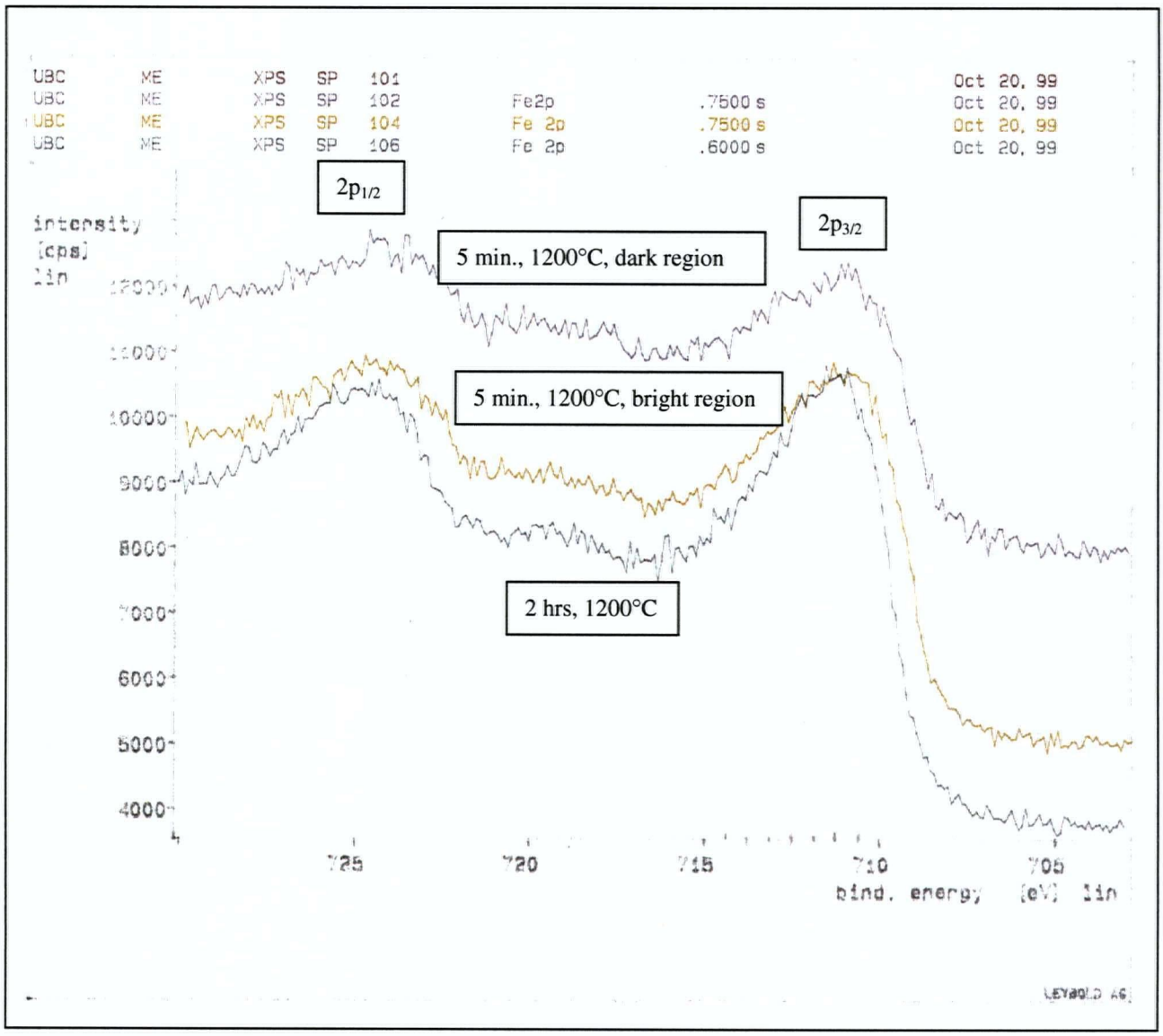

Fig. 84 Fe_2O_3/FeO spectra from XPS studies performed over the scales of 0.78% Cu steel.

Finally, XPS spectra for a sample of 0.78% Cu steel oxidized for 2 hours at 1200°C did not indicate any peaks of CuO (Fig. 83). Additionally, the peaks of Fe_2O_3 were sharper than those for the sample oxidized for 5 minutes (Fig. 84). This indicated that possibly little or, no FeO was present on the surface of the oxide scale formed over this sample.

5.4 X-Ray Diffraction Studies

X-ray diffraction studies carried out on the surfaces of oxide layers revealed strong peaks of spinels, i.e. $CuFe_2O_4$ / $CuFeMnO_4$ in the case of steels oxidized for times less than two hours. The samples oxidized for 5 min. also revealed strong peaks of wustite, i.e. FeO (Fig. 85). In addition, peaks of hematite, i.e. Fe_2O_3 also were observed.

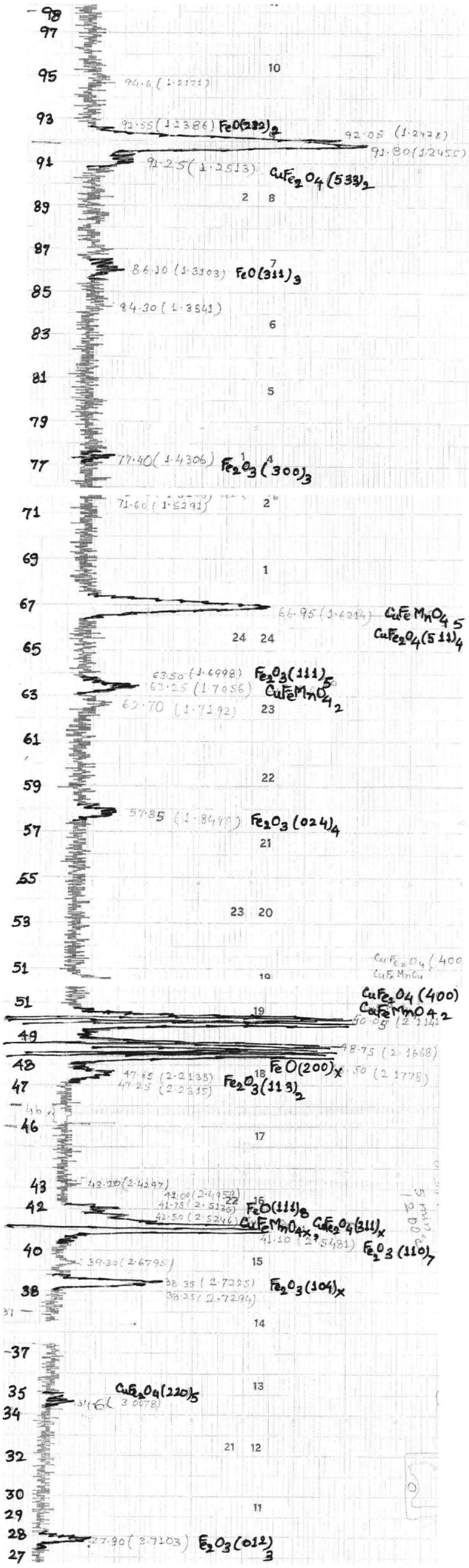

Fig. 85 X-Ray diffraction pattern showing peaks of $CuFe_2O_4$ / $CuFeMnO_4$, FeO and Fe_2O_3 on the scale surface of 0.39% Cu steel oxidized for 5 minutes at 1200°C.

6. Discussion

From oxide growth curves (W^2~t plots), it can be observed that they exhibited distinct parabolic behavior even during the early stages of oxidation (e.g. for times less than 5 minutes). In fact, it could be argued after seeing the plots that if at all, the linear stage existed, it was during very early stages of oxidation, i.e. for times less than 80 seconds. This is similar to what Abuluwefa et al[27] reported. They observed a linear stage of 2 minutes or, less during the oxidation of mild steel in an environment with high oxygen potential. Sheasby et al[44] also observed parabolic rate curve from the beginning during oxidation of low alloy steels in pure oxygen. It is expected that for an atmosphere of high oxygen activity such as air, the reaction processes at the scale-gas interface are rapid enough so as not to be rate limiting[7]. As a result, the scale formed becomes sufficiently thick and the transport of ions across the scale becomes the rate controlling process. This causes the oxidation rate to decrease with time as per the parabolic law under such conditions.

Increasing Cu in steels caused a reduction in the rate of oxidation because a greater thickness of Cu-rich layer appeared on the surface of the substrate with higher Cu. Although the layer appeared to be thin in the beginning, it might be still acting as a barrier to the diffusion of ions across it. Additionally, increasing Cu content also caused more adherent oxide scale to form causing the scale to have smaller tendency to detach from the substrate. This resulted into scale being more protective. Reduction in oxidation rate due to increase in Cu content was found by previous investigators[9, 45]. However, Olson et al[46] did not observe any variation in rates of oxidation of Fe-Cu alloys at high temperatures. This is possibly because they studied the oxidation behavior

in H_2O/H_2 mixture. Increasing adherence of scale in steels with higher copper levels observed during present investigations was noticed by steel plant operators who had been hot rolling these steels[45]. This was also observed by previous investigators[9]. The observed increase in scale adherence due to Cu in steel is possibly because the scale-metal interface became very uneven due to occlusion of Cu-enriched layer into the oxide as well as localized inward advancement of the oxides into the metal. This resulted into good interlocking bond between the oxide and the metal substrate. This was even more prominent for greater Cu levels and at higher temperatures. Vannerberg and Hammer[46] reported interlocked tenacious scales during oxidation of Fe-Cu alloys at 625°C. Nicholson and Murray[10] also argued that increased surface roughening at the interface caused more adherent scales in higher Ni steels. However, Olson et al[47] did not observe any variation in rates of oxidation of Fe-Cu alloys at high temperatures. This is possibly because they studied the oxidation behavior in H_2O/H_2 mixture.

The change in the slope of W^2~t plots at higher temperatures (i.e. 1200 and 1275°C) was indicative of reduced oxidation rate after a certain time. This was probably due to precipitation of Cu-enriched layer at the surface. The enriched layer (including both high Cu as well as low Cu regions (Fig. 79) was much thicker (e.g. 10–20 μm) after a certain time at higher temperatures, acting as the second effective barrier that impeded the diffusion of ions in addition to the first one, i.e the oxide scale.

At lower temperatures (e.g. 1000°C) diffusivities were smaller causing lesser rate of oxidation. This resulted into smaller tendency to formation of copper-rich phase on the substrate. This was obvious from the micro-structural examination of cross-sections as Cu layer was in the form of massive, discontinuous regions (Fig. 49, 53) at

1000°C. The maximum thickness of the Cu layer was only 3-4 μm at 1000°C and it was much less at most of the locations in general. For 0.22% Cu sample, it was not even noticed in the cross section (Fig. 42) and was barely seen on the surface. Hence, the difference in oxidation due to variation in copper content was small at 1000°C. As the temperature was increased, continuous copper layer began to form/increase in thickness resulting into larger difference in oxidation behavior at 1100°C. However, this was still not thick enough so as to cause any appreciable change in the rate constant with time and hence the oxidation rate.

At higher temperatures (i.e. 1200° and 1275°C), the differences in weight gain due to Cu content decreased particularly after longer times because highly enriched Cu regions were getting occluded into the scale (Fig. 76-81). Accordingly, the thickness of the highly enriched layer decreased at the surface. This made it less effective as a barrier to diffusion. However, a region (10-20 μm thick) mildly enriched with Cu was always present below the surface irrespective of Cu content in the steel. Whatever little difference in scaling due to variation in Cu content was observed at higher temperatures, it could be attributed to the difference in Cu content of the mildly enriched region as well as to the presence of a very thin layer of highly enriched region at the surface (Fig. 79).

Formation of whiskers on the scale surface during the present investigations was very surprising as most of the previous workers reported that whiskers formed at much lower temperatures. For example, Voss et al[48] reported the growth of hematite whiskers during oxidation of iron and mentioned that they formed at temperatures from 400° to 850°C. Earlier, Gulbransen and Copan[49] also reported growth of oxide

whiskers on Armco iron at 500°C in dry oxygen. Kofstaad[13] mentioned in his comprehensive review on high temperature oxidation that whisker growth never occurred during the initial stage of oxidation but was always associated with thicker films or, scales. However, Gulbransen and Copan[49] found in their study that whiskers were only present during the first few hours of reaction. The present investigation supports the work done by Gulbransen and Copan[49] as growth of blades was observed on the scale surface during oxidation for times less than two hours. Additionally, whiskers were found to be hollow from within and their growth used to get stopped after blunting of their tips (Fig. 33-37). Voss et al[48] also observed hollow tunnel in α-Fe_2O_3 whiskers. Based upon their results as well as review of previous work, they argued that the whiskers grew at their tips and the primary mechanism for their growth was surface diffusion along the central tunnel. In addition, diffusion along twin boundary along the blade axis also played a minor role. Preferential growth along the axis was also evident during the present studies as the blade cross-sections rarely differed from those of the nuclei formed during the early stages. It was reported in the literature[50] that whisker blades nucleated at the sites of emerging dislocations on the oxide surface and that the hollow tunnel along the blade-axis developed due to existence of the dislocation core[48, 50].

It was found that the length as well as width of whiskers did not alter very much with the passage of time. Similar results were also found by Voss et al[48]. It is possible that although primary mechanism was growth along the hollow tunnel, marginal sidewise growth also occurred due to lattice diffusion in the lateral direction. Due to this lateral growth, the tunnel eventually became clogged, most likely at the tip that stopped

its further growth. Reduced growth of whiskers in higher Cu samples might be because of decreased rate of oxidation due to greater enrichment of Cu at the surfaces. Increasing the temperature of oxidation shortened the length of whisker blades and increased their diameter marginally. This is because at lower temperatures, volume diffusion was less prominent and sidewise growth of blades took place to a lesser extent. Hence, chances of blocking up of the hollow tunnel were less likely resulting into unhindered growth along the length.

Formation of parallel lines (Fig. 28, 29) within a substructure in the oxide grains was possibly due to plastic deformation of the oxide scale as it collapsed on the receding metal. Plastic deformation of scales is known to be caused by growth stresses during the early stages of oxidation, i.e. when the scale is relatively thin[7, 13, 50]. Ridge-like appearance along parallel lines as well as along substructure boundaries indicated the possibility of preferential oxidation. Lee and Rapp[51] observed formation of substructures under hot-stage SEM during high temperature oxidation of iron in oxygen. Ridge like appearance on the scale surface was observed by Raman et al[52] during oxidation of 9Cr-1Mo steel and by Prescott et al[53] during high temperature oxidation of β-NiAl.

Presence of FeO in the X-Ray and XPS spectra indicated that the regions showing parallel lines and substructure formation that inhabited the whisker colonies were possibly made of FeO. Stronger peaks of CuO and Fe_2O_3 in dark regions (Fig 24) indicated that they were densely populated with whiskers of $CuFe_2O_4$ spinels whereas bright regions were sparsely populated with them as indicated by weaker peaks of CuO and Fe_2O_3. This was confirmed by observing these regions under SEM. The absence of

CuO from XPS spectra for the samples oxidized for two hours indicated that $CuFe_2O_4$ whiskers vanished from the surface during later stages. What remained on the surface after 2 hrs, was only Fe_2O_3 as confirmed by sharpness of its peaks in these samples. How this happened, is still not clear at this stage. It is possible that due to detachment of the scale, the whisker blades collapsed on the oxide surface and got further oxidized. Additionally, it is also probable that crystals of Fe_2O_3 nucleated everywhere on the surface and covered the entire surface (Fig. 39). Ren[43] also observed similar Fe_2O_3 structures on the surface of low carbon steels oxidized for times more than 2 hrs.

Detachment of scales with the passage of time observed during oxidation occurred in order to relieve the growth stresses. It has been widely discussed in the literature[13, 50, 54-56] that there are multiple sources of growth stresses during oxidation reactions of metals and alloys, e.g. oxide growth mechanisms, differences in volumes of oxide and substrate, changes in the scale, specimen geometry, scale-metal epitaxial relationship, etc. These growth stresses may be relieved through various mechanisms, e.g. plastic deformation of scales, scale detachment at the scale/metal interface, etc. As long as the scale is thin, its plastic deformation by dislocation glide and vacancy insertion into the metal with annihilation at grain boundaries, dislocations and second phases should permit the inherent chemical bonds to maintain intimate contacts at the metal/scale interface[50]. However, as the scale grows in thickness it may not be able to deform sufficiently rapidly to maintain adherence to the receding metal. This might cause development of voids and cavities as well as cause detachment at the interface. It is also possible that under the severe compressive stresses the oxide film buckles in order to release the strain energy[57].

The observation that grain boundaries were getting enriched in the beginning of oxidation at lower temperatures (e.g. 1000°C) was notable. It is highly probable that at lower temperatures (e.g. 1000°C) diffusion was occurring predominantly along grain boundaries. Hence copper diffused along grain boundaries due to concentration gradient near the surface. As the temperature was low and copper content was below 80.0% wt, the enriched phase remained solid. This was observed by Zou and Langer[57] as well as Imai et al[41]. The voids observed along grain boundaries must have been created due to condensation of vacancies[13] .

Massive regions enriched with Cu at the surface were disjointed and separated from the substrate by pores at 1000°C because the scale was unable to deform at this temperature. Condensation of vacancies also must have played an important role[13, 50]. It is also possible that as the enriched region was solid at this temperature, there was high interfacial energy between this and the solid substrate. Kajitani et al[39] also observed Cu-enriched regions at the surface disjointed and separated from the interface. They argued that it was possibly due to higher interfacial energy between Cu-phase and steel in comparison to that between Cu-phase and scale.

It is possible that once the grain boundaries at the surface region were enriched enough in Cu and also Sn, the enriched layer became molten. The presence of Sn accentuated this process as it is well known to lower the melting point of Cu-rich phase[36]. Once molten, this easily penetrated the grain boundaries very deep inside the surface as they had the lowest dihedral angle at 1100°C[34]. At lower temperatures (e.g. 1000°C), however this did not happen as the Cu enriched region was not molten due to smaller amounts of Cu (<90.0%) as well as Sn (<3.0%). A Fe-Cu-Ni (<5%) phase at

this temperature with the prevailing composition should be solid[41]. Presence of isolated highly enriched (with Cu) particles at 1100°C (Fig. 51) in the scale indicated the beginning of occlusion of enriched regions into the oxide layer. However, this was barely perceivable at 1100°C and was very prominent at higher temperatures.

Increasing the temperature, particularly above 1100°C caused very enhanced internal oxidation of Si, Mn and Fe. This was more so with increasing times of oxidation. This was because Cu-rich phase that was liquid at 1200°C and above had a much higher solubility and mobility of oxygen atoms[59]. Due to this, more and more oxygen atoms could dissolve into the liquid Cu-enriched phase and diffuse into the substrate rapidly. In addition, greater diffusivities at higher temperatures also must have contributed to this.

Increasing the time of oxidation resulted into enhanced thickness of Cu rich layer due to more oxidation. Increasing temperature in general caused the thickness of the Cu-rich layer on the surface to increase because higher temperature increased the diffusion coefficients causing enhanced migration as well as selective oxidation of Fe. However, increasing the time to 2 hrs at 1200°C as well as 1275°C caused the Cu rich layer (highly enriched) thickness to decrease because (i) a lot of Cu-rich phase was getting occluded into the scale due to enhanced intrusion of oxide into the metal substrate. (ii) more and more Cu rich phase was precipitating at internally oxidized particles. Several authors reported occlusion of Cu rich layer into the scale with increasing time and at higher temperatures. For example, Fisher[35] reported entrapment of Cu-rich phase into the oxide due to internal oxidation of iron brought forth by the presence of Ni in the steel. Kajitani et al[39] also observed occlusion of Cu-rich phase

into the scale due to heavy internal oxidation. However, the observation that Cu rich layer was getting precipitated at internally oxidized particles was not reported earlier in the literature.

There were significant amounts of Si (and also Al, Mn, etc.) near the edges of the many internally oxidized particles and Fe everywhere on them. It is possible that FeO and SiO_2 combined after internal oxidation to form $2FeO.SiO_2$ (i.e. Fayalite) which then combined again with FeO to form a low melting eutectic with a melting point of 1177°C. As this phase was liquid at 1200° as well as 1275°C, liquid Cu-rich phase precipitated at the boundaries of this molten eutectic phase due to lower interfacial energy. Kajitani et al[39] used similar arguments in explaining the precipitation and entrapment of Cu-rich phase along grain boundaries in the scale formed at 1300°C in low carbon steel containing residual Cu. Increasing oxidation time as well as temperature (e.g. from 1200°C to 1275°C) enlarged the size of the internally oxidized particles and also increased the copper content of the enriched phase around them, as it allowed further oxidation causing more copper to diffuse and arrive at the interface due to favorable interfacial energy as discussed above.

Increasing temperature also caused a large number of pores to form all over the cross-section. However, they were more numerous near the surface. This was a confirmation that mass transport occurred by vacancy diffusion and pores formed because of condensation of vacancies[13]. Formation of pores near grain boundaries at lower temperatures again confirmed that primary mechanism of transport was grain boundary diffusion, whereas pores were formed everywhere at higher temperatures indicating that lattice diffusion was becoming important at elevated temperatures.

The existence of mildly enriched regions below highly enriched zones (Fig. 79) can be explained by internal oxidation as well as lattice diffusion back into the substrate. It is possible that internal oxidation at numerous locations within the surface (below the liquid Cu-rich region) caused the formation of low melting eutectic at the interface between internally oxidized particle and the substrate and consequently Cu-enriched region precipitated there due to smaller interfacial energy as explained in the previous paragraphs.

7. Conclusions

(i) The oxide growth curves displayed parabolic behavior in general, even during the early stages of oxidation. However, the parabolic rate constants dropped to lower values after a certain time at 1200°C as well as 1275°C. This was possibly due to precipitation of sufficiently thick Cu enriched layer at the steel surface.

(ii) The oxide scale was mainly adherent to the substrate surface initially for all Cu levels and temperatures studied. However, the scale became detached from the metal surface after passage of time in order to relieve the growth stresses. The scale adherence increased with increasing Cu content as well as increasing temperature because of greater occlusion of Cu enriched phase into the scale as well as localized inward advancement of scale into the metal resulting into interlocking bond between oxide and the substrate.

(iii) Oxide surfaces in the steels oxidized for times 1 hour or, less exhibited growth of whiskers of $CuFe_2O_4$ spinels over the scale comprising mainly of FeO. Increasing temperature increased the diameters of whiskers marginally and decreased their lengths due to greater extent of volume diffusion. Higher Cu steels exhibited

reduced growth of whisker blades due to reduction in the oxidation rate. These blades disappeared from the scale surface when the steel was oxidized for 2 hours and what remained on the surface was only Fe_2O_3.

(iv) Enrichment of Cu was observed at the oxide-metal interface and the grain boundaries close to the steel surface even in the early stages of oxidation at all temperatures. However, the enriched phase at the surface was discontinuous and separated from the substrate at 1000°C. This happened because the interfacial energy between Cu phase and the steel was greater than that between enriched layer and the scale at this temperature. Grain boundary enrichment of Cu was very marginal at 1000°C as this phase was solid and separated from substrate. At 1100°C, the size of Cu rich phase increased for lower Cu levels (e.g. 0.22% and 0.39%). However, this phase remained discontinuous and separated from substrate for these steels. A continuous layer of Cu was observed at the surface at most of the locations for 0.78% Cu steel. Additionally, there were locations near the interface devoid of any surface enrichment but accompanied by penetration of grain boundaries by the enriched layer. This occurred because Cu rich phase became molten as it contained high concentration of Cu and then penetrated the grain boundaries because of the lowest dihedral angle at 1100°C.

(v) Increasing the temperature above 1100°C caused enhanced internal oxidation of Si, Mn and Fe. Increasing the time of oxidation accentuated this process. This was due to enhanced solubility of oxygen in Cu rich phase as well as higher diffusivities at 1200°C and above.

(vi) Increasing time increased the Cu content of the enriched layer at both 1000°C as well as 1100°C. The thickness of the enriched phase also increased. Increasing temperature also had a similar effect. This was due to enhanced diffusion coefficients. However, increasing the time to 2 hours at 1200°C and 1275°C caused the thickness of highly enriched layer to decrease due to occlusion of Cu rich phase into the scale as well as its precipitation at internally oxidized particles.

(vii) No penetration of grain boundaries by the enriched phase was observed at 1200°C and 1275°C as it got separated from the substrate by internally oxidized particles and pores.

8. Further work

It was observed during the present investigation that precipitation of Cu along grain boundaries near the surface did not occur at temperatures 1200°C and above because of separation of enriched phase from the substrate due to enhanced internal oxidation as well as precipitation around internally oxidized particles. It is possible that similar phenomenon might happen at 1100°C in an atmosphere with higher oxidizing power than air. Hence it would be interesting to undertake work on oxidation of steels at 1100C using a gas mixture with oxygen content more than that in air.

It also will be interesting to explore the precipitation of Cu enriched phase after oxidation for times much less than 5 minutes. This might bring greater insights into the mechanism of precipitation of the Cu rich phase at the surface as well as grain boundaries near the surface of steel.

Additionally, it will be worthwhile to study the precipitation of Cu phase during high temperature oxidation of binary Fe-Cu alloys (<1.0% Cu), particularly at

temperatures 1200°C and above as fayalite will not be present to facilitate the precipitation around internally oxidized particles.

Further, as very little work was reported in the literature on the modeling of Cu enrichment it will be useful to model the processes of enrichment in the oxide-metal interfacial zone as well as precipitation around internally oxidized particles.

9. References

1. R.C. Ormerod IV, H.A. Becker. E.W. Grandmaison, A. Pollard and A. Sobiesiak, Canad. J. of Chem. Engg. **75** 402-413 (1997).

2. C. Skagen and D.C. Gilbert, Iron and Steel Engineer **72** No. 5, 42-44 (1995).

3. K. Noro, M. Takeuchi and Y. Mizukami, "Necessity of scrap reclamation technologies and present conditions of technical development in steel and problems of removing it", ISIJ International **37** No. 3 (1997).

4. I.N. Zigalo, V.I. Baptizmanskii, Y.F. Vyatkin, A.G. Velichko, E.K. Shakhpazov and Y. Grishchenko, "Copper in steel and problems of removing it", Steel USSR (UK), **21** No.7, 299-302 (1991).

5. C. Bodsworth, "Technological means for removal of tramp elements", Ironmaking and Steelmaking **12** No. 6, 290-292 (1985).

6. D.T. Llewellyn, "Copper in steels", Ironmaking and Steelmaking **22** No. 1, 25-34 (1995).

7. N. Birks and G.H. Meier, "Introduction to High Temperature Oxidation of Metals", Edward Arnold (Publishers) Ltd., 1983.

8. A.Bergman and R. West, Scripta Metallurgica **22** No. 5, 659-663 (1988).

9. L. Habraken and J. Lecomte-Beckers, Hot shortness and scaling of copper-containing steels", Copper in Iron and Steels, John Wiley and Sons Inc., New York, 1982, 45-81.

10. A. Nicholson and J.D. Murray, Journal of the Iron and Steel Institute **203** 1007-1018 (1965).

11. K. Mayland, R.W. Welburn and A. Nicholson, "Influence of microstructural and compositional variables on hot working of steel", Met. Technol., August 1976, 350-357.

12. E.T. Stephenson, "Effect of recycling on residuals, processing and properties of carbon and low-alloy steels", Metall. Trans. **14A** 343-353 (1983).

13. Per Kofstad, "High temperature corrosion", Elsevier Applied Science Publishers Ltd., London (1988).

14. A. Rahmel and J. Tobolski, "Effect of water vapour and carbon dioxide on the oxidation of iron at high temperature", Corrosion Sc. **5**, 333-346 (1965).

15. K. Sacks and C.W. Tuck, "Surface oxidation of steel in industrial furnaces", Publication no. 111, Iron and Steel Institute (1968).

16. E.A. Cook and K.E. Rasmussen, "Scale-free heating of slabs and billets", Iron and Steel Engineer **47** (3), 63-69 (1970).

17. E.A. Cook, and K.E. Rasmussen, Iron and Steel year Book, 175-182. (1970).

18. K. Sacks and C.W. Tuck "Scale growth during reheating cycles", Werk. und Korr. **21**, 945-954 (1970).

19. K.H. Hemsath and F.J. Vereecke, "Method of minimum scale in reheating", Proc. Conf. Mechanical working and Steel processing XII, Dalton, Illinois, Met. Society/AIME, 217-235 (1974).

20. M. Kuhn and F. Oeters, "On the scaling of steel in gases with several oxidizing components", Arch. Eisenhuttenwes. **46** 515-520 (1975).

21. H.J. Selenz and F. Oeters, "A contribution to the scaling of steel in technical flue gases", Arch. Eisenhuttenwes. **55**, 201-208 (1984).

22. A.N. Mianev, V.M. Ol'Shanskii, M.M. Volkova and N.I. Iprova,"Scale formation of steels exposed to gaseous fuel combustion products", Steel in the USSR **13** 576-577 (1983).

23. D. Caplan and M. Cohen, "Scaling of iron at 500 C", Corrosion Sc. **6** 321-335 (1966).

24. D. Caplan, G.I. Sproule and R.J. Hussey, "Comparison of the kinetics of high temperature oxidation of Fe as influenced by metal purity and cold work", Corrosion Sc. **10** 9-17 (1970).

25. M. Jarl and B. Leden, "Oxide scale formation in steel in fuel fired reheating furnaces", Scanheating : Proceedings of the International Conf. on Process Control and Energy savings in Reheating Furnaces, Lulea, Sweden, 22.1-22.18 (1985).

26. H.T. Abuluwefa, G. Carayannis, F. Dallaire, R.I.L. Guthrie, J.A. Kozinski, V. Lee and F. Mucciardi, "Oxidation and decarburization in the reheating of steel slabs", Proc. International Conf. on Steel reheat Furnace Technology, Hamilton, Ontario, 243-267 (1990).

27. H.T. Abuluwefa, R.I.L. Guthrie and F. Ajersch, "The effect of oxygen concentration on the oxidation of low carbon steel in the temperature range 100 to 1250 C", Oxidation of Metals **46** 424-440 (1996).

28. H.T. Abuluwefa, R.I.L. Guthrie and F. Ajersch, "Oxidation of low carbon steel in multicomponent gases:Part I. Reaction mechanisms during isothermal oxidation", Metallurgical and Materials Transactions **28A** 1633-1641 (1997).

29. H.T. Abuluwefa, R.I.L. Guthrie and F. Ajersch, "Oxidation of low carbon steel in multicomponent gases:Part II. Reaction mechanisms during reheating", Metallurgical and Materials Transactions **28A** 1643-1651 (1997).

30. D.A. Melford, "Surface hot shortness in mild steel", J. of the Iron and Steel Institute **200** 290-299 (1962).

31. J.A. Nicholson, "Discussion on surface hot shortness of mild steel", J. of the Iron and Steel Institute **200** 748-749 (1962).

32. W.J.M. Salter, "Discussion on surface hot shortness of mild steel", J. of the Iron and Steel Institute **200** 750-751 (1962).

33. A.R. Cox and J.M. Winn, "Scaling of plain and complex copper steels", ", J. of the Iron and Steel Institute **203** 175-179 (1965).

34. W.J.M. Salter, "Effects of alloying elements on solubility and surface energy of copper in mild steel", J. of the Iron and Steel Institute **204** 498-488, (1966).

35. G.L. Fisher, "The effect of Ni on the high temperature oxidation characteristics of Cu bearing steels", J. of the Iron and Steel Institute **207** 1010-1016 (1969).

36. W.J.M. Salter, "Effect of mutual additions of Sn and Ni on the solubility and surface energy of Cu in mild steel", J. of the Iron and Steel Institute **207** 1619-1623 (1969).

37. B.S.C., "Reheating and residual element enrichment", Steel Research 77, Info serv dept. B.S.C. 151 Gower Street, London.

38. Y. Kohsaka, C. Ouchi, "Hot shortness of copper bearing high strength low alloy steels", Proc. Conf. Copper in Steels, Luxembourg, ATB Metall. **23** 9.1-9.29 (1983).

39. T. Kajitani, M. Wakoh, N. Tokumitsu, S. Ogibayashi and S. Mizoguchi, "Influence of temperature and strain of surface crack due to residual copper in carbon steel", Steelmaking Conference Proceedings, 621-626 (1996).

40. N. Imai, N. Komatsubara and K. Kunishige, "Effect of Cu, Sn and Ni on hot workability of hot rolled mild steel", ISIJ International **37** No. 3, 217-223 (1997).

41. N. Imai, N. Komatsubara and K. Kunishige, "Effect of Cu and Ni on hot workability of hot rolled mild steel", ISIJ International **37** No. 3, 224-231 (1997).

42. D. Geneve, M. Confente, D. Rouxel, P. Pigeat and B. Weber, "Distribution around the oxide-substrate interface of alloying elements in low carbon steel", Oxidation of Metals **51** Nos. 5/6, 527-537 (1999).

43. Xuzhan Ren, Experimental study and modeling of IF steel oxidation process in air", M.A.Sc. Thesis, The University of British Columbia, Vancouver (1999).

44. J.S. Sheasby, W.E. Boggs and E.T. Turkdogan, "Scale growth on steels at 1200°C : rationale of rate and morphology", Metal Science **18** 127-136 (1984).

45. G. Dallin, Stelco - Private communication 2000.

46. N.G. Vannerberg and A.B. Hammer, Scand. J.Metall. **3** 123 (1974).

47. R.G. Olson, B.B. Rice and E.T. Turkdogan, "Rate of oxidation of Fe-Cu and Fe-Sn alloys to wustite" J. Iron and Steel Institute, December, 1607 - 1611 (1969).

48. D.A. Voss, E.P. Butler and T.E. Mitchell, "The growth of hematite blades during the high temperature oxidation of iron", Metall. Trans. **13A** 929-935 (1982).

49. E.A. Gulbransen and T.P. Copan, "Effect of stress and environment on the microtopology of the corrosion product", 155 - 179.

50. R.A. Rapp, "The high temperature oxidation of metals forming cation-diffusing scales", Metall. Trans. **15A** 765 - 782 (1984).

51. Moonyong Lee and R.A. Rapp, "Coalescence of wustite grain during iron oxidation in a hot-stage environment SEM", Oxidation of Metals **27** No. 3/4, 187 - 197 (1987).

52. R.K. Singh Raman, J.B. Gnanamoorthy and S.K. Roy, "Synergistic influence of alloy grain size and Si content on the oxidation behaviour of 9Cr-1Mo steel", Oxidation of Metals **42** Nos. 5/6, 335-355 (1994).

53. R. Prescott, D.F. Mitchell, and M.J. Graham, "A SIMS study of the effect of Y and Zr on the growth of oxide on β-NiAl", Microscopy of Oxidation, (Eds.)S.B. Newcomb and M.J. Bennet, The Institute of Materials, London, 455-462 (1993).

54. D.L. Doughlass, Oxidation of Metals, Vol. 1, (1969), 127.

55. J. Stringer, Corrosion Science, Vol. 10, (1970), 513.

56. P. Hanock and R.C. Hurst, Advances in Corrosion Science and Technology, Vol. 4, Eds. Fontana, M. G. and Staehle, R.W., Plenum Press, New York, (1974), 1.

57. A.G. Evans and R.M. Cannon, "Stresses in oxide films and relationships with cracking and spalling", Proc. Symp. Oxidation of Metals and Assiciated Mass Transport, Ed. M.A. Dayananda, S.J. Rothman and W.E. King, Orlando, Florida, Publ. The Metallurgical Society, Warrendale, Pennsylvania, 135-160 (1986).

58. Y. Zou and E.W. Langer, "A study of the formation and penetration of the molten Cu-rich phase in Fe with addition of Ni and Sn", Materials Sc. And Engg. **A110** 203-208 (1989).

59. H. Baker (ed.), "Alloy Phase Diagrams", ASM Handbook Vol. 3, ASM International, Materials Park, Ohio, USA 2.174 (1992).